LIFE CYCLES IN THE METHANOGENIC ARCHAEBACTERIUM *METHANOSARCINA MAZEI*

By

RALPH WENDELL ROBINSON

A DISSERTATION PRESENTED TO THE GRADUATE SCHOOL OF
THE UNIVERSITY OF FLORIDA
IN PARTIAL FULFILLMENT OF THE REQUIREMENTS FOR THE
DEGREE OF DOCTOR OF PHILOSOPHY

UNIVERSITY OF FLORIDA

1985

ACKNOWLEDGMENTS

This dissertation is dedicated to my parents, for without their help and encouragement someone else's name would be on the cover.

I would like to thank my fellow graduate students Debbie Akin and Donna Williams for their help on this project. Also, special thanks to my committee and to Drs. Greg Erdos and Howard Berg.

An unsigned pastel drawing of a thin section of *Methanosarcina mazei* by the late Doris Murray 1982 (compare with Fig. 51).

TABLE OF CONTENTS

ACKNOWLEDGEMENTS....................................ii

ABSTRACT..iii

CHAPTER

1. INTRODUCTION.......................................1

2. LITERATURE REVIEW..................................5
   - Early Descriptions and Taxonomy..................5
   - Isolated Strains and Ultrastructure..............6

3. MATERIALS AND METHODS.............................13
   - Cultures and Growth Conditions..................13
   - Light Microscopy................................15
   - Sample Preparation for Electron Microscopy.......15
     - Method 1. For General Morphology using TEM.....15
     - Method 2. For Gold Labelling and X-ray Microanaysis..................16
     - Method 3. For Silver Staining and UV Fluorescence Analysis...................17
     - Method 4. For Scanning Electron Microscopy.....17
     - Method 5. For Freeze-Fracture..................18
     - Method 6. For Negative Staining................18
     - Changes in Cytoplasmic Fluorescence............19
   - Cytochemical Analysis of the Cell Surface........19
     - Silver Stain...................................19
     - Fluorescein-Labelled Lectins...................20
     - Gold-Labelled Lectins..........................21
     - Enzyme Extraction..............................22
     - Cytochemical Analysis of the Granules and Polyphosphate Bodies.............23
     - Elemental Analysis.............................23
     - Enzyme Extraction..............................23

4. RESULTS...25
   - Morphology of the Complex Life Cycle...........25
     - Cocci..25
     - Matrix Development and Division Patterns.....26
     - Sarcinal Colonies..............................28
     - Colony Disaggregation..........................30

Morphology of the Limited Life Cycle...........58
  Methanosarcina mazei Strain S6...............58
  Resting Forms................................70
  Methanosarcina barkeri Strain 227 73
Disaggregation in Methanosarcina strain LYC................78
  Freeze-Fracture analysis.....................81
  Cytochemical Analysis of the Cell Surface....87
    Silver Stain...............................87
    Fluorescein-Labelled Lectins...............90
    Gold-Labelled Lectins......................93
    Enzyme Extraction..........................93
  Cytochemical Analysis of the Granules and Polyphosphate Bodies..........101
    Elemental Analysis.........................101
    Silver Stain...............................104
    Enzyme Extraction..........................104

4. DISCUSSION......................................110

LITERATURE CITED...................................136

BIOGRAPHICAL SKETCH................................147

Abstract of Dissertation Presented to the Graduate
School of the University of Florida in Partial
Fulfillment of the Requirements for the Degree of Doctor
of Philosophy

LIFE CYCLES IN THE METHANOGENIC ARCHAEBACTERIUM *METHANOSARCINA MAZEI*

by

RALPH WENDELL ROBINSON

May, 1985

Chairman: Henry C. Aldrich
Major Department: Microbiology and Cell Science

Methanosarcina mazei strains S6 and LYC along with *Methanosarcina barkeri* strain 227 were utilized to study the structure and differentiation of the aggregating methanogens. Cultures harvested under varying conditions are described at the ultrastructural level and qualitatively examined using cytochemical techniques. Cells are irregular and 1-2 μm in size. Cells of *Ms. mazei* strain S6 are enclosed by a protein layer 12 nm thick in contact with the plasma membrane. In sarcinal colonies, cells are held in close association by a fibrous matrix up to 60 nm thick.

Colony maturation was examined in *Ms. mazei* strain S6 over a period of one year. Changes occur in the shape and staining of individual cells. Also, various inclusion bodies were observed that either persist throughout colony maturation or are only found at certain growth stages. The inclusion bodies, cell surface, and matrix were analyzed with silver methenamine, fluorescein- and gold-labelled lectins, X-ray microanalysis, freeze-fracture, and various enzymatic treatments.

Based on electron microscopic examinations, two life cycles are described for *Methanosarcina*. A complex life cycle is described with two variations for *Ms. mazei* strains S6 and LYC. In addition, a limited cycle is described that contains the only morphotypes observed in *Ms. barkeri* strain 227. This limited cycle can also be observed in the two strains of *Ms. mazei* studied.

The complex life cycle of strain S6 begins with single cells that deposit matrix polysaccharide at the cell surface; this prevents complete daughter cell separation. These in turn divide forming sarcinae and, as more matrix material is deposited, become distorted into compact sarcinal colonies. The colonies dissociate by degradation of the matrix. When released cells of strain S6 are placed in fresh media, they can repeat the cycle.

Ms. barkeri is restricted to a limited cycle which also occurs in the *Ms. mazei* strains while the matrix remains intact. These colonies mature from 3-5 microns into larger masses (>3mm) that multiply by fragmentation. When *Ms. mazei* strain S6 remains in the limited cycle and does not disaggregate in stationary phase, several types of possible resting forms are found.

CHAPTER 1

INTRODUCTION

Methanogenic bacteria are strict anaerobes and generally obtain their energy from the oxidation of H_2 to CH_4 by the reduction of CO_2. A few genera can also utilize methanol, formate, methylamines, and acetate, forming methane as a reduced product (Mah *et al*. 1977, Mah and Smith, 1981). In general, methanogens can be isolated from environments that provide H_2 and CO_2 and exclude O_2. These include the rumen of cattle, the intestines of other animals and man, decaying tree trunks, stagnant water, ocean bottoms, thermal hot springs, and sewage treatment plants. Some sewage plants obtain much of their operating energy from collected methane.

The morphology of the methanogens is as diverse as their habitats. Cells are found as regular or irregular cocci, as rods, spirals, or as sarcinae in aggregates of large colony clusters. Such diversity in morphology contrasted with a relatively uniform and unique metabolic pathway led to the belief that methanogenesis is a very ancient process, pre-dating the morphological changes that occurred during evolution (Woese 1982).

Recently, an entire group of bacteria, including the methanogens, has been recognized as being phylogenetically separate from other prokaryotes (Balch 1982, Fox et al. 1980, Woese & Fox 1977). This group, called the archaebacteria, is believed to comprise a third kingdom, with the "eubacteria" (other prokaryotes) and the eukaryotes making up the other two kingdoms. Archaebacteria are not simply ancestors of the eubacteria but are a separate and independent group related to eukaryotes as much as they are to the eubacteria (Woese et al. 1982). Six characteristics shared by archaebacteria examined thus far are 1) the lack of peptidoglycan in the cell wall (Kandler & Koenig 1977, 1978, Kandler 1982, Koenig et al. 1982); 2) the presence of unusual ether-linked poly-isoprenoid glycerol lipids in the membrane instead of ester linked alkane lipids (Tornabene et al. 1978, Langworthy et al. 1982); 3) unique tRNAs and rRNAs (Woese 1982); 4) their existence in unusual, harsh environments (Woese 1977); 5) a eukaryotic-like DNA-dependent RNA polymerase structure (Stetter & Zillig, 1980); and 6) unique cofactors involved in metabolism (Cheeseman et al. 1972). The methanogenic bacteria were the first members recognized as being uniquely separate from other members of the Prokaryoteae and they still comprise the largest and most diverse group in the Archaebacteriaceae (Wolfe

1971, Fox et al. 1977, Mah et al. 1977, Zeikus 1977). Presently, other members of the archaebacteria include the aerobic extreme halophiles (e.g. Halobacterium), the thermoacidophiles (e.g. Sulfolobus and Thermoplasma), and the thermophilic acidophiles (e.g. Thermoproteus). Members of the group usually have a low percentage of rRNA homology with other bacteria and a high percentage of homology among themselves.

The sarcina-forming methanogens are currently placed in the genus Methanosarcina. They display a cellular arrangement that is unique, and several members exhibit complex life cyles which are rare among isolated archaebacteria. A life cycle has been partially described at the light microscope level for Ms. mazei where sedentary colonies break up into single cells which can grow into new colonies in fresh media (Mah, 1980). The ability of a colony-forming bacterium to dissociate into single cells in response to unfavorable environmental changes provides a unique means for dispersal. When cells regain a favorable habitat, they form colonies which attach via sedimentation and entanglement and are less likely to wash away. Indeed, colony-forming methanogens are major inhabitants of fixed bed reactors where the fluid components are periodically flushed from the system (Zinder and Mah 1979, Robinson et al. 1984).

This group is of prime importance in the final steps of biomass conversion to methane in mesophilic environments, with up to 70% of the methane formed derived from the acetate utilizing methanogens (Mah and Smith 1981). These two qualities, of displaying a complex life cycle and being of prime importance in bioconversion, warrant an in-depth examination of this group. This dissertation characterizes the structure and development of these aggregating methanogens at the ultrastructural level. The general objectives are 1) to describe the morphology using light and UV microscopy, scanning electron microscopy, and transmission electron microscopy; 2) to determine and describe the life cycles in *Methanosarcina mazei*; and 3) to obtain qualitative data on cellular composition using cytochemical techniques.

CHAPTER 2

LITERATURE REVIEW

Early Descriptions and Taxonomy

The genus Methanosarcina contains the most metabolically diverse methanogens isolated thus far. It was described in 1903 by Mazè (cited in Mazè 1915 and in Barker 1936) in mixed cultures as a "pseudo-sarcine" because of its ability to grow either as large sarcinal groups or as single cells. Soehngen (1906) later described a methanogenic sarcina that was more or less cubical and was not observed as single cells. Smit (1933) placed both of these bacteria into the genus Zymosarcina along with other anaerobic sarcinae, with the type species Z. methanica. In 1936 Kluyver and van Niel created two genera: Methanosarcina for the methane producing sarcina described by Soehngen with Ms. methanica as the type species, and the genus Methanococcus for the "pseudosarcina" described by Mazè with Mc. mazei as the type species (Barker 1936).

Since *Ms. methanica* and *Mc. mazei* had not been isolated or maintained in pure culture, they were omitted from the approved list of bacterial names (Ad hoc committee 1976). Balch *et al*. (1979) designated *Methanosarcina barkeri* and *Methanococcus vannielii* as neotypes. *Ms. barkeri* matches the descriptions of *Ms. methanica*, but *Mc. vannielii* is an irregular, highly motile, marine coccus that does not aggregate and has little resemblance to the early decriptions for *Mc. mazei* made by Mazè, Soehngen, or Barker (Jones *et al*., 1977). Then, in 1980, Mah reported the first successful isolation of a pure culture that exactly matched the "pseudosarcina" descriptions. Thus, the name *Methanococcus mazei* was temporarily revived. Recently though, there has been a re-evaluation of the taxonomic position of *Mc. mazei* and its relationship to other methanococci and methanosarcinae. Consequently, *Methanococcus mazei* has been moved into the genus *Methanosarcina* as *Ms. mazei*, with *Ms. barkeri* designated the type species (Mah & Kuhn 1984a and b).

Isolated Strains and Ultrastructure

Terminology. Since all methanogenic genera start with the letter "M," the abbreviations recommended by Daniels *et al*. (1984) will be used. These are as follows: *Mbr.*, *Methanobrevibacter*; *Mb.*, *Methanobacterium*; *Msp.*, *Methanospirillum*; *Mc.*, *Methanococcus*; and *Ms.*, *Methanosarcina*.

There is some confusion over the descriptive terms used for the various morphotypes of *Methanosarcina*, especially *Ms. mazei*. Mah (1980) designates types I, II, and III (Fig. 1). Zhilina (1976) had earlier designated different types I, II, and III (Fig. 2). To further complicate matters, Zhilina and Zavarzin (1979c) later described their type III as exhibiting a variety of morphotypes. Except when specifically describing others' work, this paper will use the 3 forms shown in figure 3 and refer to them as cocci, sarcinal colonies, or resting forms. These three morphotypes can be stable and long lasting in culture. The cocci correspond to type III described by Mah and by Zhilina. The sarcinal colony corresponds to type I descibed by Mah and type II described by Zhilina.

Mah's isolate of *Ms. mazei*, designated S6, has been described only at the light microscope level (Mah 1980). It exhibits three morphotypes at different growth stages (Fig. 1). When cultures are young, cells are found in small sarcinal aggregates (type I) that measure up to 20 μm in size and may form larger aggregations with each other. As the cultures mature and enter stationary phase, sarcinal aggregates go through a transitory stage

FIG. 1

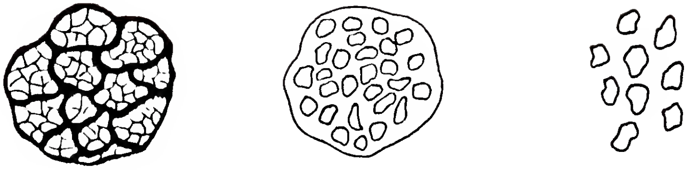

Type I Type II Type III

Mah, 1980

FIG. 2

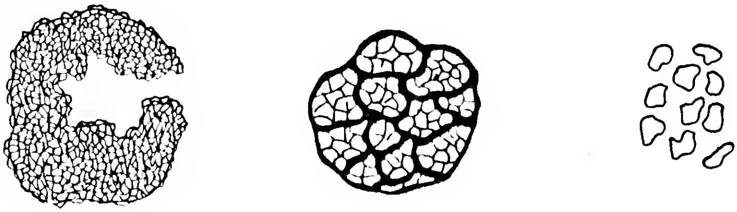

Type I Type II Type III

Zhilina, 1976

FIG. 3

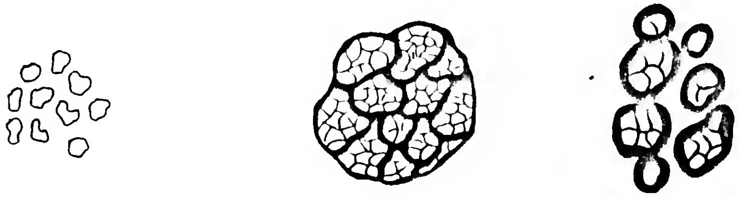

Cocci Sarcinal Colony Resting Forms

to form coccal cysts (type II). These are up to 100 µm in diameter and may form larger aggregates up to several millimeters in size. Mah reported that when the coccal cysts are physically disrupted, a cyst "wall" breaks, releasing individual cocci (type III) that are 1-3 µm in size. Each of these can grow into sarcinal forms when placed in fresh medium.

Several other strains of Ms. mazei have been reported: "MC_3" (Touzel and Albagnac 1983) exhibits a life cycle that is apparently identical to S6; "Juelich" (Scherer and Bochem 1983a) for which a life cycle is not described; and "LYC" (Liu et al. 1985). Strain LYC exhibits only two morphotypes with a unique mechanism of disaggregation. A sarcinal colony forms when the cells are grown at pH 6.0 but when the pH is raised to 7.0 the colony disaggregates into single cells. Apparently, an enzyme is activated that hydrolyzes the matrix holding the colony together. Unfortunately, the single cells cannot presently be induced to form aggregates so a complete life cycle cannot be delineated. Ms. mazei strains have not previously been described at the ultrastructural level.

The ultrastructure of Methanosarcina spp. from enrichment cultures were examined by Zhilina (1971, 1976), Zhilina and Zavarzin (1979a) and Bochem et al. (1982). Pure cultures of Methanosarcina spp. not designated Ms. mazei were examined by Zeikus and Bowen (1974), Zhilina and Zavarzin (1979b,c), Pangborn (In Mah 1981), Archer and King (1983, 1984), Scherer and Bochem (1983a,b), Ollivier et al. (1984), and Sowers et al. (1984a).

Zhilina (1971) first looked at sarcinal aggregates found in digester enrichments. They are composed of irregular cells measuring 1-3 µm with unequal division zones. Colonies are enclosed by a variably thick lamellar wall. Numerous gas vacuoles were described that are 70-80 nm wide and 200-400 nm long with a 2.5 nm membrane. Also present are electron dense granules measuring up to 100 nm and polyphosphate-like inclusion bodies of unreported size. Due to the ability to form gas vacuoles, Zhilina and Zavarzin (1979b) proposed a new species, Ms. vacuolata, but this epithet has not been officially recognized.

Zhilina (1976) also reported on three morphotypes of Methanosarcina in an enrichment culture (Fig. 2). Morphotype I corresponds to a large sarcinal aggregate that possesses a central cavity with a single pore. Morphotype II is a smaller aggregation of irregular cells tightly enclosed by matrix material. This type is a sarcinal colony and corresponds to Mah's type I (Fig. 1). Zhilina's type III is a single cell and corresponds to Mah's type III. Zhilina's morphotype III was later reported to occur as single cells, in groups forming loose aggregates, or in tightly packed cysts (Zhilina and Zavarzin, 1979c). However, these authors do not indicate any developmental changes that occur between the various forms. This biotype may be a strain of _Ms. mazei_ but this has not been confirmed.

Another isolate, designated _Methanosarcina_ strain MP, which may be a strain of _Ms. mazei_ was recently described by Ollivier _et al_. (1984). They describe sarcinal colonies that can break up into coccoid elements in old cultures. However, they only examined the ultrastructure of the sarcinal colonies.

Sowers _et al_. (1984a) recently reported on the isolation and ultrastructure of a third species of _Methanosarcina_, _Ms. acetivorans_, that grows in marine environments as irregular single cells that are motile. The cytoplasm contains electron dense granules and is enclosed by a plasma membrane and a closely associated protein layer. When cultures enter stationary phase the single cells begin to aggregate into loose associations that are eventually enclosed by a thin proteinacous cyst wall. A matrix is not present and when fresh medium is added the aggregates break up into single cells once again.

The electron dense granules and polyphosphate-like inclusion bodies have recently been the focus of several papers and presentations. Scherer and Bochem (1983 a and b) used X-ray microanalysis (see Moreton 1981) on ultrathin sections of 12 strains of Methanosarcina to determine the partial elemental composition. Polyphosphate-like globular inclusion bodies 150-250 nm in diameter contain Ca, P, and Fe. The electron dense granules have the same elemental composition but in lower amounts. Murray et al. (1984) examined crude cell extracts and reported that a carbohydrate is present when cells are grown under nitrogen limiting conditions and that the granules may be carbohydrate storage sites. However, there is little evidence presented and the granules have not been purified and analyzed.

CHAPTER 3

MATERIALS AND METHODS

Cultures and Growth Conditions

Methanosarcina mazei strains S6 and LYC and the type species Ms. barkeri strain 227 were examined. Colony development was examined only in Ms. mazei strain S6. Two different cultures of the same strain S6 were utilized. One exhibited a complex life cycle while the other grew only in sarcinal colonies in a limited cycle and is a variant of S6. The variant strain was obtained when cultures were repeatedly transferred in the laboratory. Ms. mazei strain S6 and Ms. barkeri were grown at pH 6.8 in B1 medium (Balch et al. 1979) modified according to Mah (1980) with H_2/CO_2, acetate, trimethylamine, or methanol used as energy sources. Ms. mazei strain LYC was grown at pH 6.0 in a medium described by Liu et al. (1985) with H_2/CO_2 or methanol used as energy sources.

Cultures were usually grown in serum tubes (Bellco) containing 9 ml of medium and sealed with butyl rubber stoppers. Inoculations consisted of 1 ml of a 10-14 day culture passed through the stoppers using 20 or 25 gauge needles. All cultures were incubated at 35° C without shaking.

Sarcina development from single cells and matrix deposition was examined in a series of tubes inoculated with cultures that had been filtered through a 3 μm filter to remove any remaining sarcinal forms. Tubes were incubated from 1-3 days, then prepared for transmission electron microscopy (TEM) using method 1 below.

Sarcinal colony maturation in the variant strain of S6 grown on acetate was monitored by inoculating a series of tubes through a 5 μm filter to select for the smallest sarcinal forms. No growth occurred when filters smaller than 5 μm were used (single cells are not released by this variant). Cells were collected at 5, 10, 12, 15, 21, 30, 90, 105, and 360 days and prepared for EM using method 1 below.

Colony disaggregation was monitored using strain S6 that spontaneously breaks apart into single cells. When a 200 ml culture grown in a 600 ml serum bottle showed the first signs of turbidity, the colonies were examined using light microscopy and the culture was prepared for EM using method 1 below.

Colony disaggregation in Ms. mazei strain LYC was monitored by growing the cultures at pH 6.0 for 5-7 days and then raising the pH to 7.0 by adding Na_2HCO_3 (10% in reduced medium). Cultures were collected at 0, 12, 24, 36, and 48 hrs and prepared for EM using method 1 below.

Light Microscopy

Two light microscopes were used to examine culture changes and to record micrographs. A Zeiss WL research microscope equipped with phase and Nomarski optics was used to make light micrographs on Kodak Plus-X 35 mm film. A Zeiss photostrobe was used when photographing single cells. Alternatively, a Nikon Labophot microscope equipped with UV epifluorescence was used for general culture monitoring and the recording of UV micrographs on Kodak Tri-X film.

Sample Preparation for Electron Microscopy

Method 1. For General Morphology

Samples were fixed in a modified (2.0% formaldehyde and 2.5% glutaraldehyde in 0.1M Na-cacodylate buffer) Karnovsky's fixative (Karnovsky 1965) for 30 min at pH 7.2 on ice. After washing in buffer for 1 hr, samples were fixed in 0.1M cacodylate buffered 1% OsO_4 at pH 7.2 for 1 hr on ice. Cells were washed once and then encapsulated in 1.5% agar (Difco). Samples were then dehydrated through a graded ethanol/acetone series, embedded through a resin/acetone series into 100% Spurr's resin (Spurr 1969), and polymerized in a 60° C oven for 24 hrs. Thin sections were cut on a LKB Ultrotome III ultramicrotome using a diamond knife and collected on copper grids. Sections were poststained with 1% uranyl acetate for 20 min followed by lead citrate (Reynolds 1963) for 5 min. Micrographs were taken on a Hitachi HU-11E or a JEOL JEM 100-CX transmission electron microscope operated at 75 and 60 KV respectively. For stereo micrographs, semi-thick sections (gold) were observed at a tilt angle of -5 and +5° using a goniometer stage (Rieder et al. 1985). The accelerating voltage was increased to 100 KV.

Method 2. For Gold Labelling and X-ray Microanalysis

Cells were fixed for 15 min in 2% formaldehyde and 0.2% glutaraldehyde in 0.1M cacodylate buffer at pH 7.2 on ice. After washing in buffer, cells were encapsulated in 1.5% agar then dehydrated in an ethanol series. Samples were further processed using one of two methods. In one, they were embedded through a series of ethanol/Lowicryl K4M plastic (Polaron Equipment Ltd.) to 100% plastic and polymerized by UV radiation overnight.

During this treatment, cells were kept on ice up to the 75% ethanol step and then placed at -40°C for subsequent steps until polymerization was complete. Alternatively, samples were placed directly in 100% LR White plastic (Polaron) from the 95% ethanol step and then, after 4 changes of plastic, were polymerized at 60°C overnight. Sections were cut and examined as in method 1 except they were collected on nickel grids and were not poststained.

Method 3. For Silver Staining and UV Fluorescence Analysis

This procedure was essentially the same as method 1 except samples were not exposed to osmium, and epon/araldite plastic (Mollenhauer 1964) was used for embedding. Sections were collected on nickel grids and were not poststained.

Method 4. For Scanning Electron Microscopy

Cells were harvested on a 0.2 µm syringe type filter and fixed with 2% glutaradehyde in 0.1M cacodylate buffer at pH 7.2 for 20 min. The cells were washed, treated with 1% buffered OsO_4 for 15 min, then washed again. The filter and cells were dehydrated in an ethanol series and dried by the critical point method using CO_2. The cells were then sputter coated with gold and viewed in a Hitachi S-450 scanning electron microscope.

Method 5. For Freeze-Fracture

Cells were collected on a 2.3 mm diameter 400 mesh gold grid, sandwiched between two 3 mm gold discs and immediately frozen in a propane jet freezing apparatus (Mueller *et al*. 1980). The frozen discs were stored in liquid nitrogen until being separated in a Balzers BA-360M freeze-fracture machine. The fracture faces were angle shadowed with platinum-carbon and replicated with carbon using electron guns. Replicas were cleaned in 50% aqueous chromic acid for 2 hrs, rinsed, then followed with sodium hypochlorite (50% household bleach) overnight before being collected on carbon and Formvar coated copper grids for viewing using TEM.

Method 6. For Negative Staining

Drops of cultures were placed on Formvar coated copper grids for 1-5 min depending on culture density. The medium was blotted away and the adsorbed cells stained with aqueous 2% phosphotungstic acid or aqueous 1% uranyl acetate for 5 min.

Changes in Cytoplasmic Fluorescence

Twelve-day old colonies of strain S6 grown on acetate and prepared for TEM using method 3 above were sectioned using a glass knife to obtain a single silver-gold thin section. This was poststained and observed using TEM. When an adequate thin section through a sarcinal colony was found, a 1 µm thick section was cut as the very next section. This was placed on a glass slide and observed with UV microscopy. A comparison was made between the morphology of cells observed in the thin section using TEM and the fluorescent properties of the same cells in thick section.

Cytochemical Analysis of the Cell Surface

All cytochemical analyses were performed on *Ms. mazei* strain S6. *Ms. mazei* strain LYC and *Ms. barkeri* were not examined.

Silver Stain

Sections prepared by method 3 were etched at room temperature by floating on 1% periodic acid from 1-15 min (Erlandsen _et_ _al_. 1979). After rinsing, the sections were stained for 30-45 min at 60°C with silver methenamine (de Martino and Zamboni 1967, modified by Picket-Heaps 1967). The grids were rinsed and then floated on Ektaflo fixer (Kodak, diluted 1:100) to remove non-specific silver deposits. Controls were run with sections receiving 1) no treatment; 2) periodic acid only; 3) silver methenamine only; and 4) periodic acid and silver stain only (no fixer).

Fluorescein-Labelled Lectins

Whole colonies of strain S6 grown on acetate were treated with 0.1M cacodylate buffered 1% OsO_4 at pH 7.2 for 1 min to quench autofluorescence and then rinsed with 0.1M PBS buffer at pH 7.2 supplemented with 0.1 mM $CaCl_2$, $MnCl_2$, and $MgCl_2$. The autofluorescence of single cells lasts only a few seconds, so for single cells this step was omitted. The samples were then treated for one hour with one of the following fluorescein-labelled lectins (Vector Labs, Burlingame CA): concanavalin A (Con A); wheat germ agglutinin (WGA); soybean agglutinin (SBA); _Dolichos_ _bifloris_ agglutinin (DBA); _Ulex_ _europaeus_ agglutinin (UEA-I); peanut agglutinin (PNA); or _Ricinus_ _communis_ agglutinin I (RCA_{120}). Controls were run with 0.1 M sugar (D-galactosamine, alpha-methylmannose, alpha-methyl-glucose, or L-fucose) present in the incubation mixture. Samples were washed in the supplemented buffer and fixed in buffered 3% glutaraldehyde for 20 min. After a final wash, samples were observed with UV microscopy.

Gold-Labelled Lectins

Colloidal gold approximately 15.0 nm in size was prepared by reducing chlorauric acid with sodium citrate according to the method of Frens (1973). A 4% gold chloride solution was prepared and 0.5 ml added to 200 ml of double distilled water. Four milliliters 1 of 1% sodium citrate was added and the solution was refluxed for 15 min After cooling to room temperature, the pH was adjusted to 7.0 with 0.1M K_2CO_3. The minimum amount of lectin required for stabilization of the gold was determined by the technique of Horisberger and Bauer (1976) as modified by Roth and Binder (1978). A 0.1 ml aliquot of serially diluted lectin was mixed with 0.5 ml of colloidal gold. After 15 min, 0.5 ml of 10% NaCl was added and flocculation due to insufficient stabilization of the gold was determined by a color change from pink to blue. A 20% excess of lectin needed for stabilization was added to 30 ml of colloidal gold. A 10% solution of PEG-20 was added for a final concentration of 0.5 mg/ml and the solution was centrifuged at 28,000 X g for 60 min. The clear supernatant containing any unbound lectin was discarded. The gold pellet was washed once by centrifugation in 20 mM $NaHPO_4$-KH_2PO_4 at pH 7.2 containing 0.5 mg/ml PEG-20 and 0.02% sodium azide and then resuspended in the same buffer to 1/10 the original volume.

Sections of strain S6 prepared using method 2 were floated for 20 min on drops of the lectin-stabilized gold which had been serially diluted with PBS. Sections were washed three times with PBS and then once with distilled water before viewing. Controls were run with sections receiving 1) colloidal gold only; and 2) D-galactosamine (0.1 M) in the reaction mixture.

Enzyme Extraction

Sarcinal colonies of strain S6 were exposed to 0.5% protease (type XIV, Sigma) in 0.1 M cacodylate buffer at pH 7.0 supplemented with 20% sucrose for 5, 10, and 30 minutes at 37°C. These were then fixed and embedded using method 1 above. Controls were run with colonies treated only with buffer. Alternatively, cultures containing single cells were fixed and embedded as in method 1 above except they were treated with 1.0% protease for 30 min after fixation. Also, thin sections of cells prepared according to methods 2 and 3 above were treated by protease digestion as described below.

Cytochemical Analysis of the Granules and Polyphosphate Bodies

Elemental Analysis

Thin sections of cells embedded by methods 2 or 3 were examined by energy- dispersive X-ray microanalysis (Kevex) in a JEOL JEM 100-CX TEM. Sections were held in a carbon specimen holder tilted 45-50°. The TEM mode was used at 60 KV and the condenser 1 spot size reduced to 2 or 3 to restrict the diameter of the area being counted.

Enzyme Extraction

Sections prepared by methods 2 or 3 using 12-day cells of strain S6 were collected on nickel grids and floated on 1% periodate for 15 min and washed. The sections were then exposed to one of the following solutions at 37° C: aqueous 0.5% protease at pH 7.0 (Anderson and Andre 1968); phosphate buffered 1% amylase at pH 7.0 for alpha amylase and at pH 5.8 for beta amylase activity (Palevitz and Newcomb 1970); phosphate buffered 0.5% pullulanase at pH 5.8 (Palevitz and

Newcomb 1970); bicarbonate buffered alkaline phosphatase (type 1-S, Sigma) at pH 10.4; or phosphate buffered 1% cellulase (type 2, Sigma) at pH 4.5. Sections were frequently monitored by TEM during treatment which lasted up to 24 hrs. Sections were also exposed to sequential treatments with pullulanase for 6 hrs followed by alpha and beta amylase each for 24 hrs. Controls were included with sections floated on their respective buffers. Positive controls of *Dictyostelium* myxamoebae were included to test for glycogen extraction by amylase. Embedded filter paper was included to test for cellulase extraction. Sections of *Sporosarcina ureae* which has a protein layer outside the gram-positive cell wall and protein layers on endospres were included to test for protease activity.

RESULTS

Morphology of the Complex Life Cycle

Cocci

When viewed with Nomarski optics, free cells of Ms. mazei strain S6 are approximately 1-2 μm in size (Fig. 4). The cytoplasm often contains 1 or 2 refractile granules up to 0.5 μm in size (not shown). Under UV microscopy, cells display moderate fluorescence which quenches within a few seconds. Scanning electron microscopy (SEM) shows cocci 1-2 μm in size and roughly spherical (Fig. 5). Negative staining (Fig. 6) reveals an uneven surface, and polyphosphate inclusion bodies can be seen which are up to 0.8 μm in size. Flagella or pili were not present.

Thin sections show irregular and regular cells up to 2.0 μm in size (Fig. 7 and 8) that differ in their degree of cytoplasmic staining. The nuclear region is not readily apparent. Electron dense granules are present in the cytoplasm that range from 40-100 nm in size. These are spheroid with very rough margins and

Figures 4-7. Single cells of *Methanosarcina mazei* strain S6.

Fig. 4. Cells viewed with Nomarski optics.

Fig. 5. Cells viewed with scanning electron microscopy (SEM).

Fig. 6. Transmission electron micrograph of negatively stained whole cells. One to two polyphosphate inclusion bodies can be seen in some cells.

Fig. 7. Thin section of cells showing a variety of shapes.

P= polyphosphate

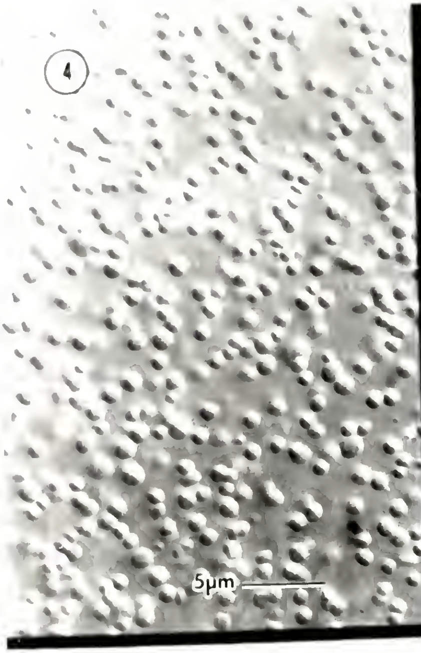
④
5μm

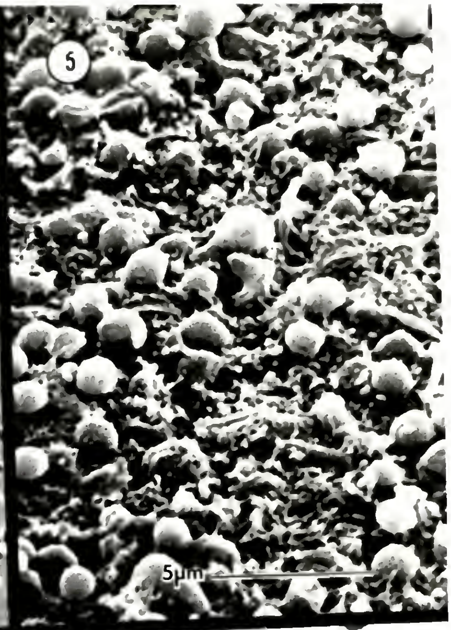
⑤
5μm

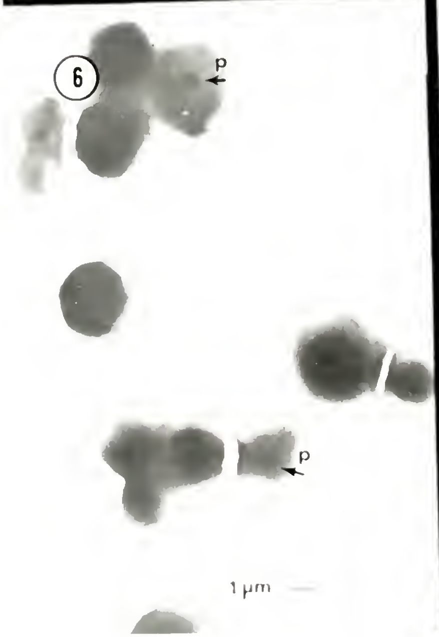
⑥
p
p
1 μm

⑦
1 μm

Figures 8-11. Transmission electron micrographs of single cells of Ms. mazei strain S6.

Fig. 8. Cells containing cytoplasmic granules and polyphposphate inclusion bodies.

Fig. 9. Smooth surface with protein layer in close contact with the plasma membrane (arrows). Material with a membranous appearance may be shedding from the cell surface (arrowheads).

Fig. 10. A cell that has lost most of the protein layer.

Fig. 11. Higher magnification of the cell in figure 10 shows the remaining protein layer as clumps on the cell surface.

g= granules

P= polyphosphate

L= protein layer

pm= plasma membrane

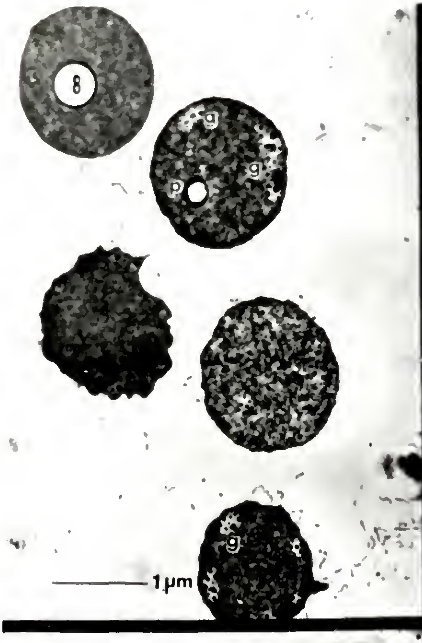
8
g
g
p
g
1 µm

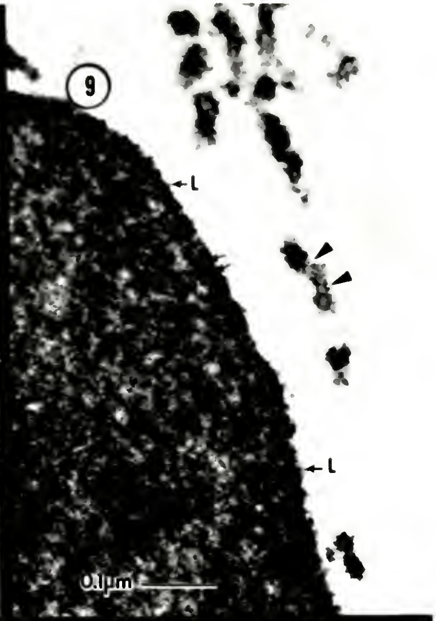
9
L
L
0.1µm

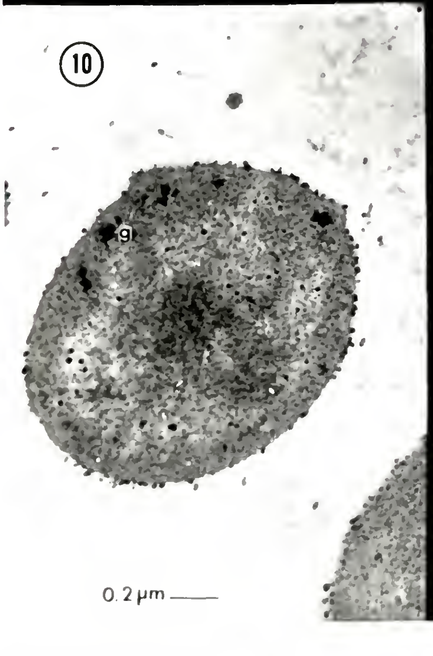
10
g
0.2 µm

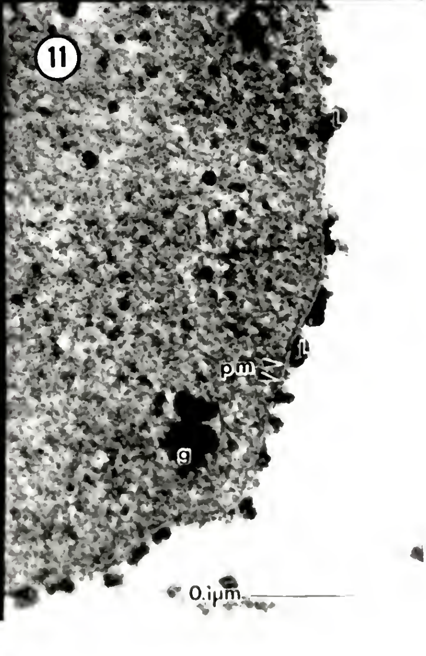
11
L
L
pm
g
0.1µm

are characteristically surrounded by an electron transparent halo. In single cells, the granules are not evenly distributed but tend to group into clusters at the periphery of the cytoplasm. Larger inclusion bodies similar to polyphosphate are common. The cytoplasm is bound by a unit membrane that is not very prominent and an additional closely associated protein (see below) layer 12 nm thick (Fig. 9). Frequently, material is observed that may have sloughed off the surface in strips. These sometimes have a membranous appearance (arrowheads Fig. 9). Occasionally cells are seen that have lost most of this layer (Figs. 10 and 11). The material on these cells is present as clumps approximately 14 nm in size just outside the plasma membrane.

Matrix Development and Division Patterns

A matrix material coats the outside of the cell surface and is probably responsible for cell-cell adhesion during colony formation. Matrix development begins as a fibrous layer close to the protein layer on the cell surface. During cell division and subsequent development into sarcinae, the matrix becomes thicker, denser, and more regular, somewhat resembling a gram-positive wall. As sarcinal colonies mature however, the matrix becomes very irregular as described below.

Figures 12-15. Various aspects of single cell division of *Ms. mazei* strain S6.

Fig. 12. Different stages of Cell division viewed under Nomarski optics.

Fig. 13. SEM of dividing cells.

Fig. 14. Thin section of a cell initiating septum formation.

Fig. 15. Thin section showing completed septum. Matrix material is incorporated in the septum.

M= matrix

g= granules

S= septum

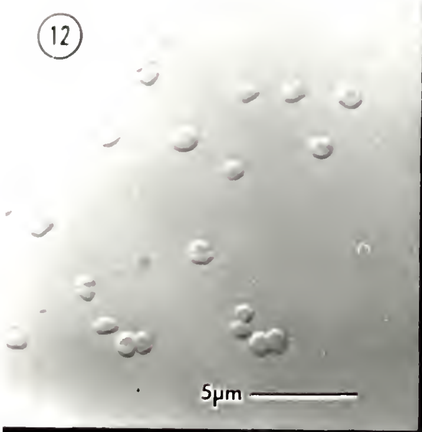
12
5μm

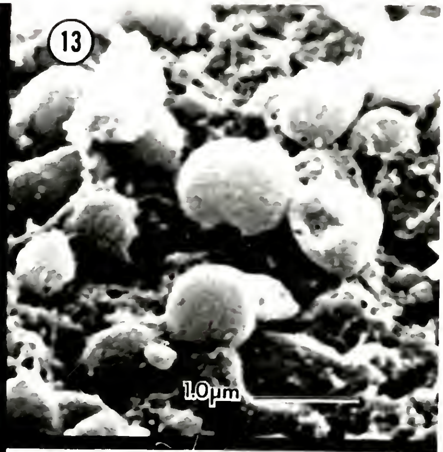
13
1.0μm

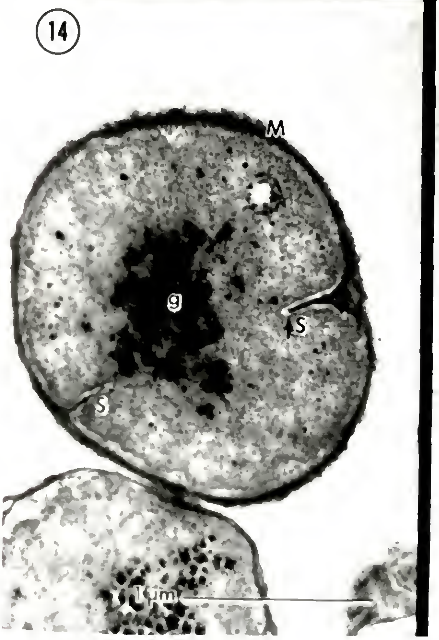
14
M
g
S
S
1μm

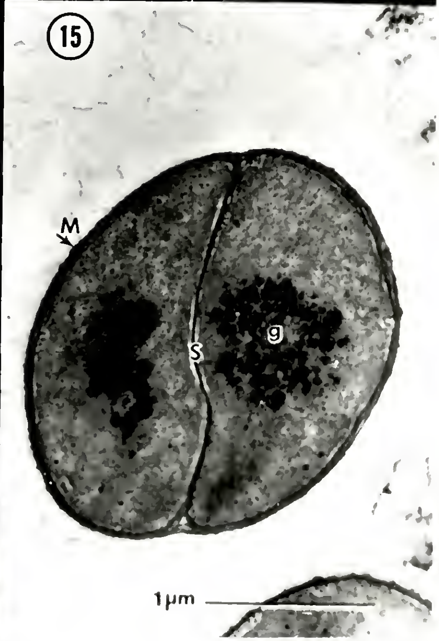
15
M
S
g
1μm

With Nomarski optics, cells in two-day cultures appear like diplococci in various stages of division (Fig. 12). The first division is by symmetrical binary fission with the two daughter cells remaining in contact. In SEM (Fig. 13), the dividing cells appear similar to those observed in light microscopy. Single cells initiate division with the plasma membrane, protein layer, and matrix invaginating as an annulus across the equator of the cell (Fig. 14). The matrix is 60 nm thick and has a fibrous structure.

After the septum has bisected the cell, the cross matrix thickens from the periphery inward (Fig. 15) until it is as thick as the outer matrix. The cells do not separate, presumably because of the tight association of the cross matrix. The second divisions that give rise to four daughter cells are initiated in the same plane with each other but perpendicular to the first cross septum (not shown). Sarcinae that develop from single cells have a regular shape when viewed with light microscopy and fluoresce brightly under UV microscopy (Fig. 16). In thin sections of three day cultures, the sarcinae show a fairly regular shape but the division septa are askew (Fig. 17). Unlike the first division where the completed septum is almost in the same plane, the second divisions are completed in an asymmetrical manner and two perpendicular septa are rarely seen.

Figures 16-19. Various aspects of Ms. mazei strain S6 sarcina structure.

Fig. 16. A sarcina-containing culture viewed under UV microscopy.

Fig. 17. Thin section of sarcina showing the involvement of the matrix in the cross septa.

Fig. 18. A culture of cells developing beyond the sarcina stage.

Fig. 19. Higher magnification of sarcina developing into colonies. The division planes are very irregular.

M= matrix

g= granules

s= septa

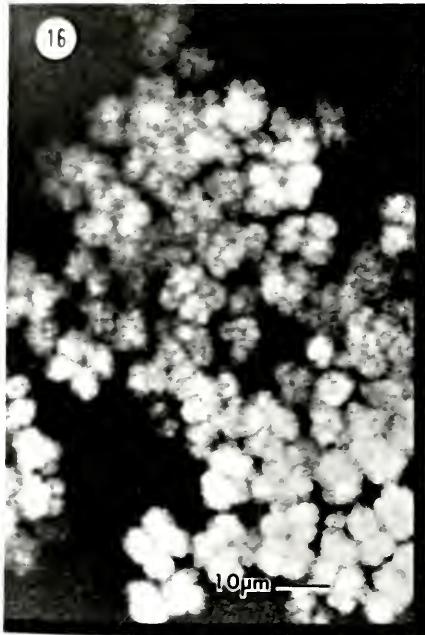
16
10µm

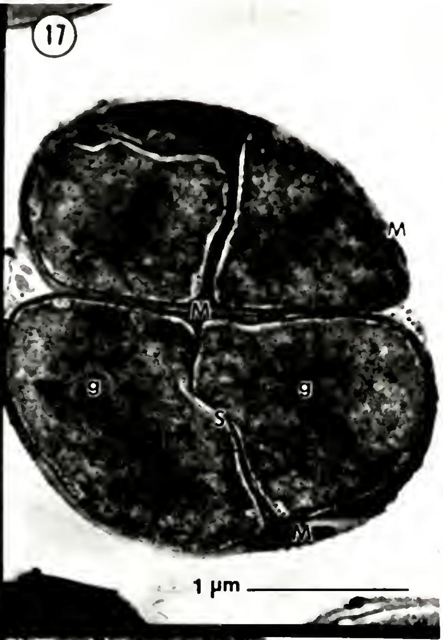
17
M
M
g
g
S
M
1 µm

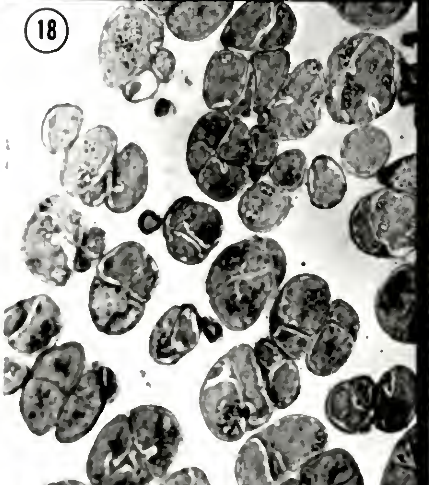
18
5µm

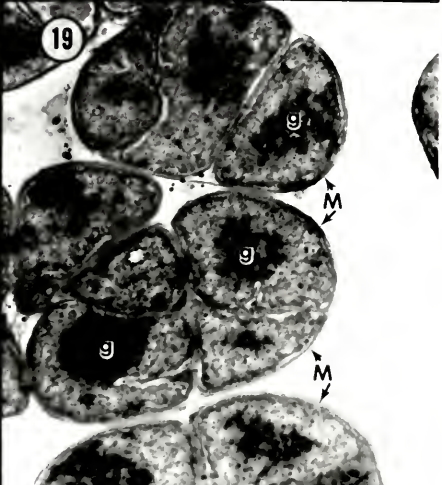
19
g
M
g
g
M
g
1 µm

Overall, the sarcinae are approximately 3.5 μm in size and the matrix is more condensed. Cytoplasmic granules are more numerous and tend to group towards the center of the cells. Further growth results in irregular masses at four days (Figs. 18 and 19). Each sarcina is derived from a single cell and is capable of eventually forming a large sarcinal colony. There is no evidence that sarcinae coalesce to form colonies. A large inoculum of single cells results in the growth of numerous small colonies while a small inoculum (i.e. a few cells) will give rise to just a few large colonies.

Sarcinal Colonies

Sarcinal colonies of strain S6 can reach up to 5 mm (Fig. 20). Light microscopy using Nomarski optics shows smaller colonies that are approximately 100 μm in size with an uneven surface (Fig. 21). Under phase and UV microscopy at lower magnifications, larger sarcinal colonies up to several hundred μm in size (Fig. 22) display a strong fluorescence which does not quench after several minutes (Fig. 23). The larger colonies are globular and are composed of smaller sized groupings which may fragment when disturbed (see limited cycle below).

SEM of broth cultures reveals a configuration somewhat like cauliflower (Fig. 24). Cells are either

Figures 20-23. Sarcinal colonies of Ms. mazei strain S6.

Fig. 20. Broth-grown culture poured into a staining dish. The colonies can reach up to 5 mm in size.

Fig. 21. Individual sarcinal colony viewed with Nomarski optics.

Fig. 22. Aggregates of colonies viewed with light microscopy.

Fig. 23. The same group of cells seen in figure 22 viewed with UV radiation. The cytoplasm fluoresces with a bright blue-green color.

20

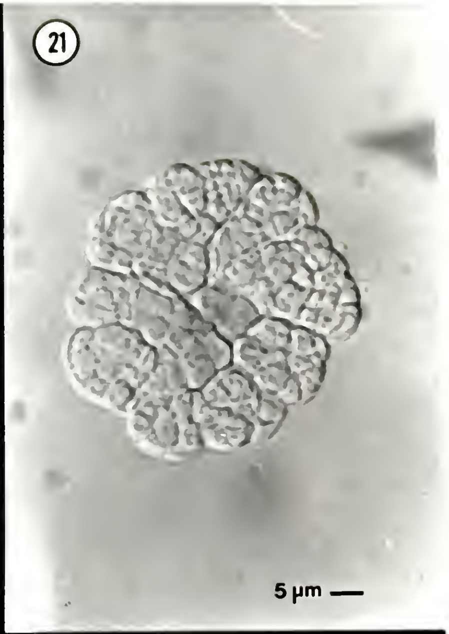
21
5 µm

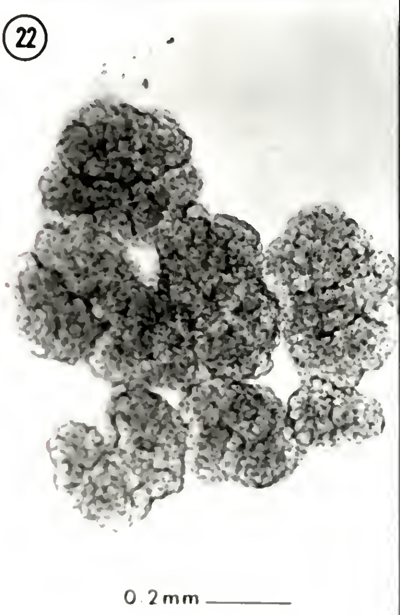
22
0.2mm

23
0.2mm

Figures 24 and 25. Scanning electron micrographs of sarcinal colonies of Ms. mazei strain S6.

Fig. 24. Large colony with an appearance somewhat like cauliflower.

Fig. 25. Enlargement of boxed area in figure 24 showing the close association of the cells covered with fibrous matrix material.

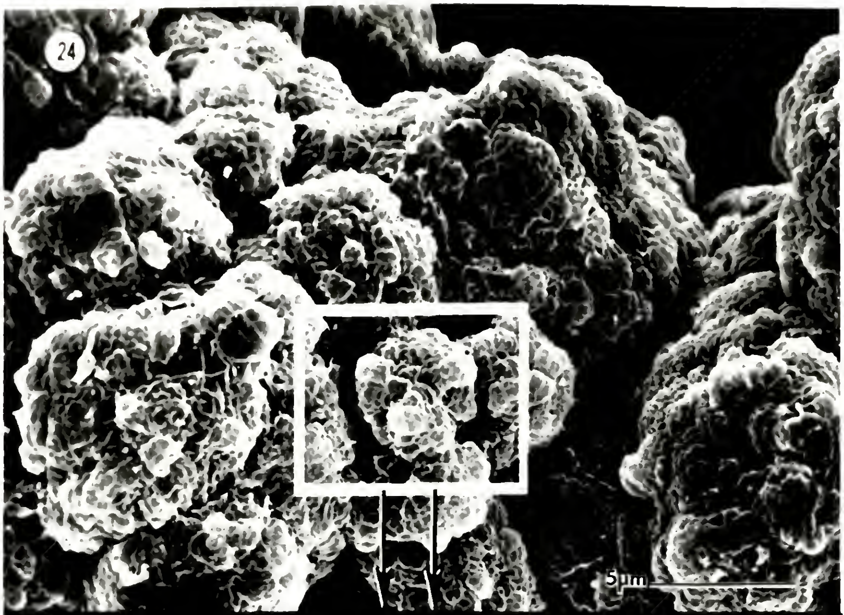
24
5µm

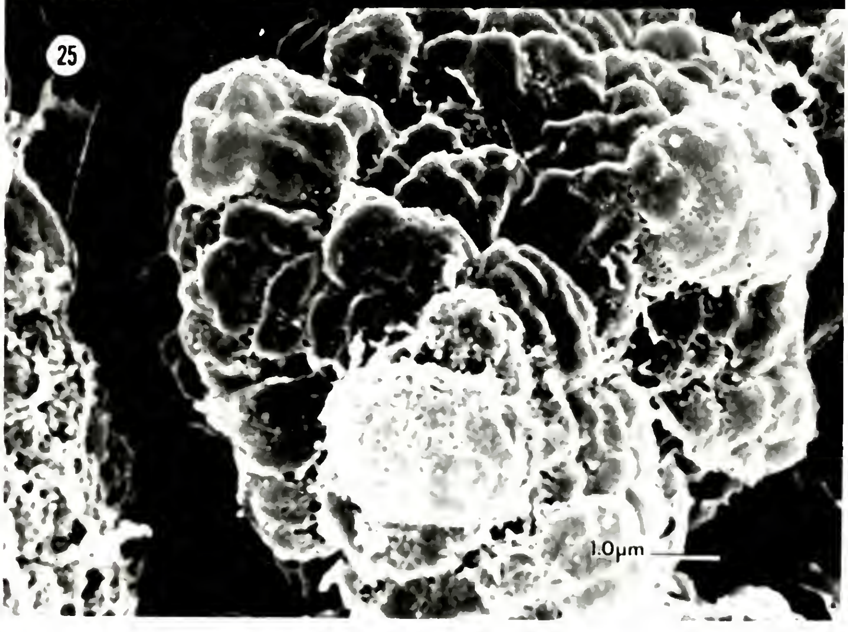
25
1.0µm

closely packed in the colony interior or are arranged in lobes at the surface. Individual cells can be seen at higher magnifications but these are difficult to discern due to the thick matrix material (Fig 25).

In thin sections, colonies are composed of a heterogeneously staining population of cells that are more irregular than the earlier sarcinal forms (Fig. 26). The matrix is approximately 40 nm thick and has a fibrous appearance. The granules are either dispersed throughout the cytoplasm or are concentrated at the cell center. The granules possibly come together and fuse to form the polyphosphate bodies since very compact groups of granules are sometimes observed which lack the characteristic electron transparent margins (Fig. 27). Clear areas are found where polyphoshate bodies have been removed during processing (Fig. 28). These are up to 0.8 μm in size and usually possess some residue around the margins. Occasionally, polyphosphate bodies are observed where some of the material is present in a loose reticular network (Fig. 29) or in bodies that are more condensed (Fig. 30).

A large number of curved tubules 14 nm thick that appear to contain membrane are trapped between the protein layer and the matrix (Figs. 27-37). These are sometimes in close association with the cell surface (arrows Figs. 31 and 32). When there is a high concentration of the tubules, they can intertwine with

Figures 26-30. Thin sections of sarcinal colonies of Ms. mazei strain S6. Numerous inclusion bodies are shown along with tubules associated with the cell surface.

Fig. 26. Low magnification showing the irregular arrangement of the cells. They contain numerous inclusion bodies and stain heterogeneously.

Fig. 27. Thin section showing the cytoplasmic granules that tend to group toward the center of the cells in thin sections and may fuse to form the polyphosphate bodies.

Fig. 28. Section through a polyphosphate body where most of the material has been removed during processing.

Fig. 29. A cell with two polyphosphate bodies that contain dark staining material in a characteristic reticular pattern.

Fig. 30. A polyphosphate body containing a dense arrangement of the dark staining material.

M= matrix

g= granules

P= polyphosphate

t= tubules

26

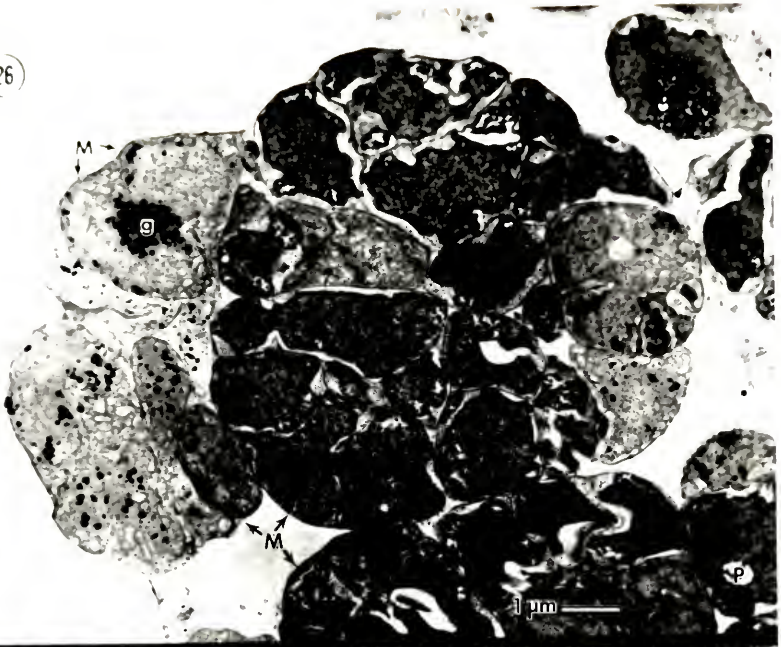

27

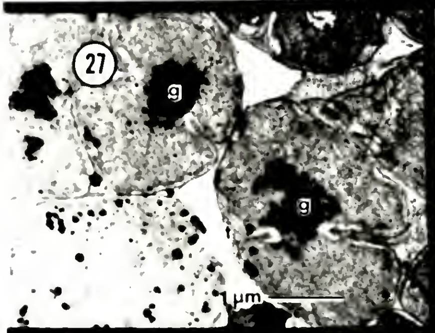

28

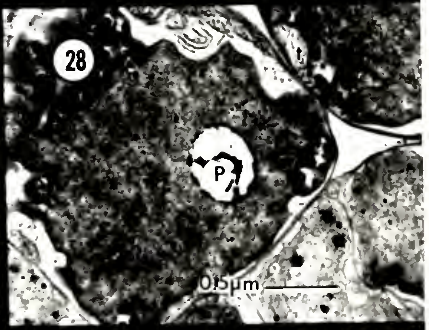

29

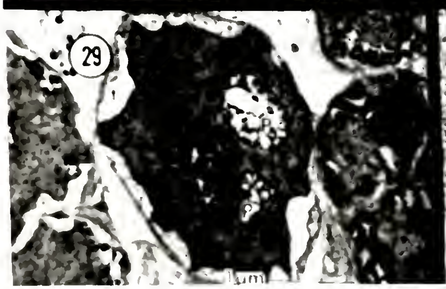

30

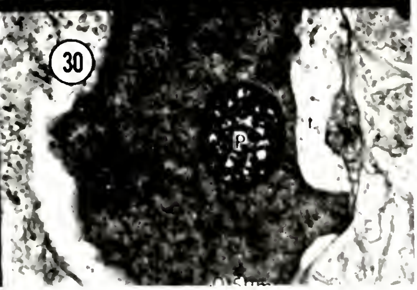

Figures 31-34. Thin sections of Ms. mazei strain S6 showing the cell surface and the close relationship of the tubules. Bar = 1 μm

Fig. 31. Micrograph of tubules found between two cells. The tubules are found in groups on the cell surface and appear to be attached in certain areas (arrows).

Fig. 32. Micrograph of the tubules and matrix. Frequently, the tubules are mixed with fibers of the matrix material. The tubules appear attached to the cell surface (arrows).

Figs. 33 and 34. Stereo pairs of micrographs that can be observed using a stereo viewer to obtain a three dimensional image. A tubular structure is clearly demonstrated.

M= matrix

g= granules

t= tubules

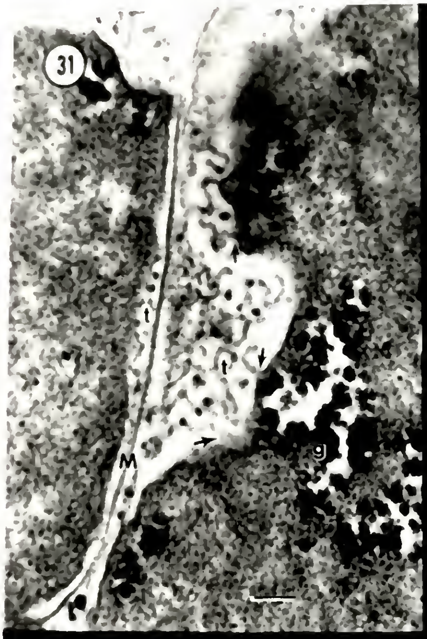
31

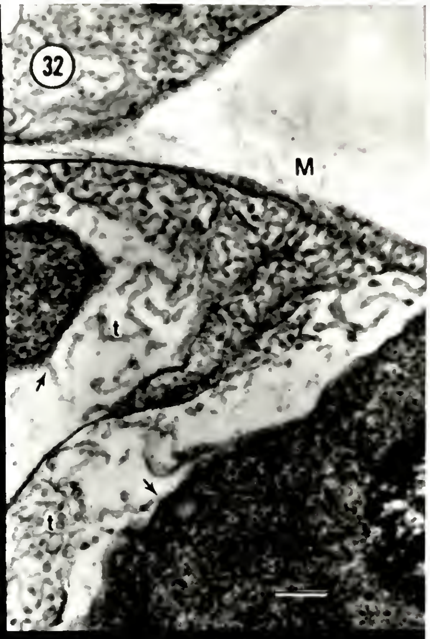
32

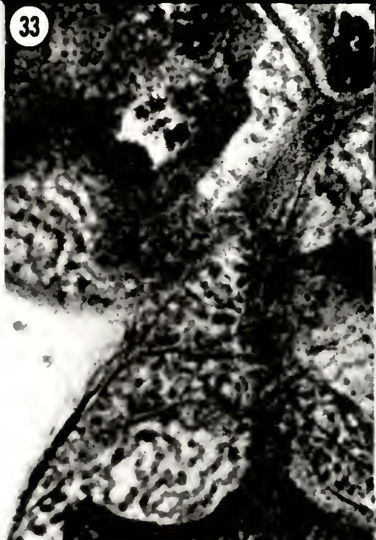
33

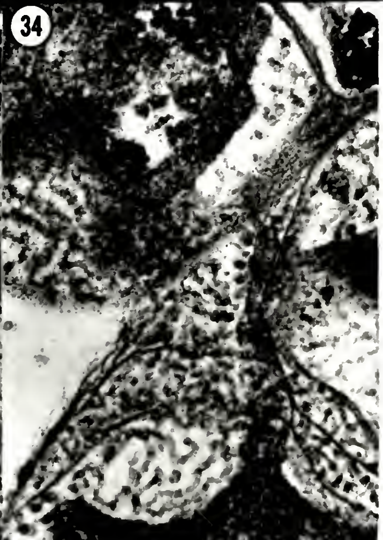
34

fibers of the matrix (Fig. 32). Stereo pairs of micrographs show the irregular arrangement and the mixing with fibers of the matrix (Figs. 33 and 34). In cross section (Fig. 35) they are circular and approximately 15 nm in diameter. They are usually distributed in clusters at areas on the cell surface; however, they can be found in grazing sections as threads stacked roughly parallel to each other and approximately 20 nm apart (Figs. 36 and 37).

After cells mature into sarcinal colonies during the complex life cycle, they possess most of the ultrastructural characteristics of colonies that are restricted to the limited cycle described below.

Colony Disaggregation

After an unspecified amount of time in stationary phase but usually not before two weeks, the colony matrix begins shedding from the cells. In dark field light microscopy at low magnification, single cells are seen shedding from sarcinal colonies (Fig. 38). Under phase contrast at higher magnifications, numerous cocci are present with sarcinal colonies (Fig. 39). It is common to find intermediate forms where both sarcinae and cocci are present. Under UV microscopy (Fig. 40), the colonies appear as coccal colonies held together by what remains of the matrix. These coccal colonies

Figures 35-37. Thin section micrographs of Ms. mazei strain S6 showing tubules associated with the cell surface.

Fig. 35. High magnification micrograph of a group of tubules cut in cross section showing a hollow tubule structure.

Fig. 36. A cell showing four groups of tubules at the cell surface. The one at the upper right is cut in a grazing section of the surface.

Fig. 37. High magnification of the grazing section of the cell surface seen in figure 36. The tubules are in a parallel arrangement.

M= matrix

T= tubules

35

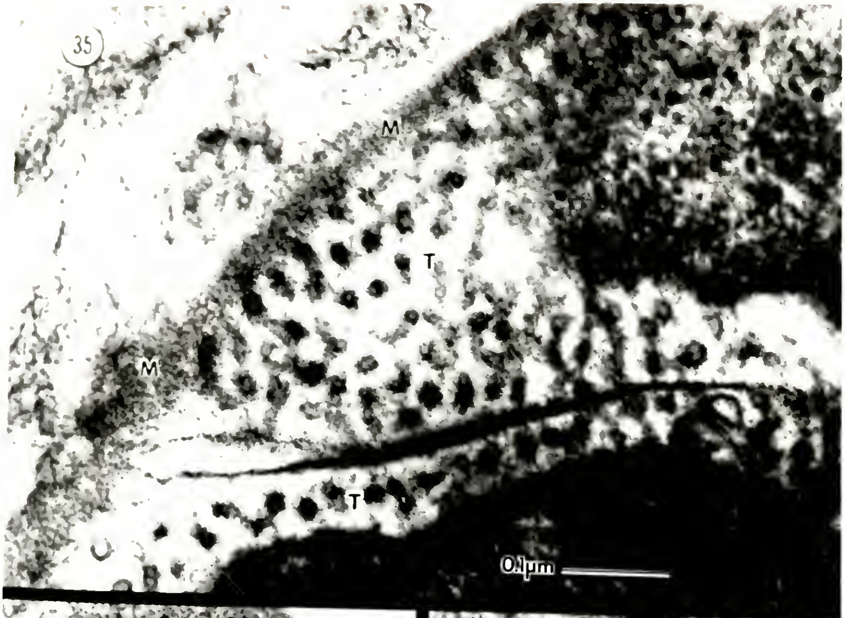

36

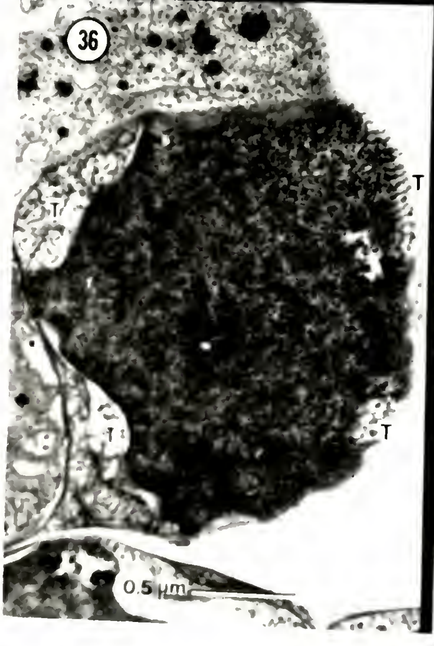

37

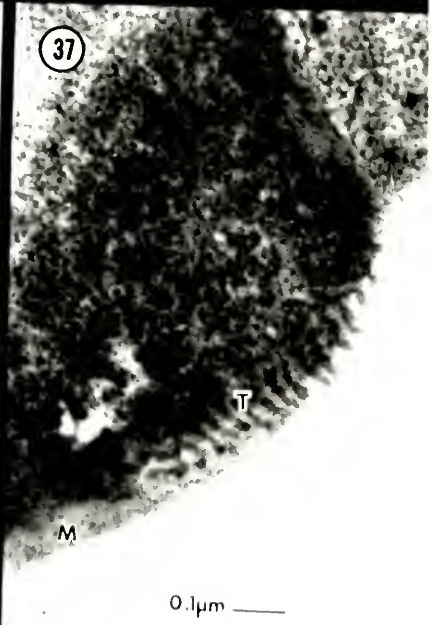

Figures 38-40. Microscopic examination of gross colony morphology of *Ms. mazei* strain S6 during disaggregation.

Fig. 38. Dark field light micrograph of two disaggregating colonies releasing single cells.

Fig. 39. Disaggregating culture observed with phase contrast microscopy shows intact colonies together with free single cells.

Fig. 40. Disaggregating colonies observed with UV microscopy. Single cells that fluoresce brightly are held together by the remaining matrix material.

38

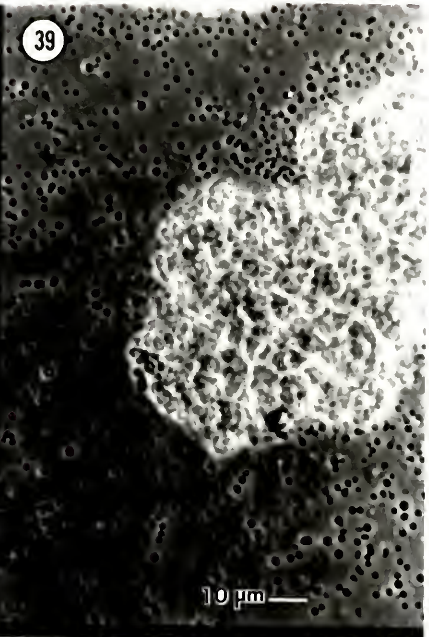
39

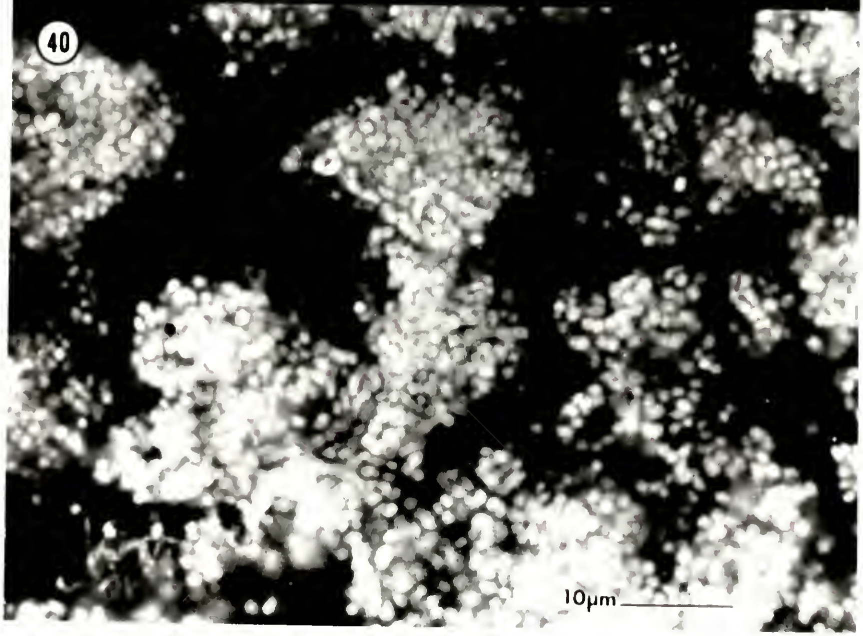
40

usually break up spontanously or can persist until physically disrupted.

In SEM, cells in a cluster of colonies are not arranged in a tight fashion (Fig. 41) and less matrix material is present between cells. Individual cells are easily observed at high magnifications (Fig. 42) and measure 1.3 to 2.2 µm. Lobes and crevices are not as apparent as in whole colonies (compare with Figs. 24 and 25).

When observed in thin sections, the matrix has a loose fibrous nature when the colony degrades into a coccal colony (Fig. 43). The fibrous matrix has a laminated appearance at higher magnifications and involves uncompleted division septa (Fig. 44). The membrane tubules between the matrix and the protein layer are scattered throughout this region. The matrix layers may number 20-30 per cell and shed or peel from the surface (Fig. 45). At very high magnifications of a cell nearly devoid of matrix, fibers 4-8 nm thick are shedding from the surface (Fig. 46). Colony disaggregation is usually completed 48 hrs after initiation. However, coccal colonies are sometimes not completely degraded, with the cells held together by the remaining fragments of matrix (Figs. 47 and 48). Slight physical pressure can break these colonies apart. Single cells within these colonies still possess a remnant of the matrix (Fig. 49). This layer is dense, Figures 41 and 42. Scanning electron micrographs of disaggregating colonies of Ms. mazei strain S6.

Fig. 41. A disaggregating colony with little matrix material holding the cells together.

Fig. 42. Higher magnification of colony with sarcinae on the surface.

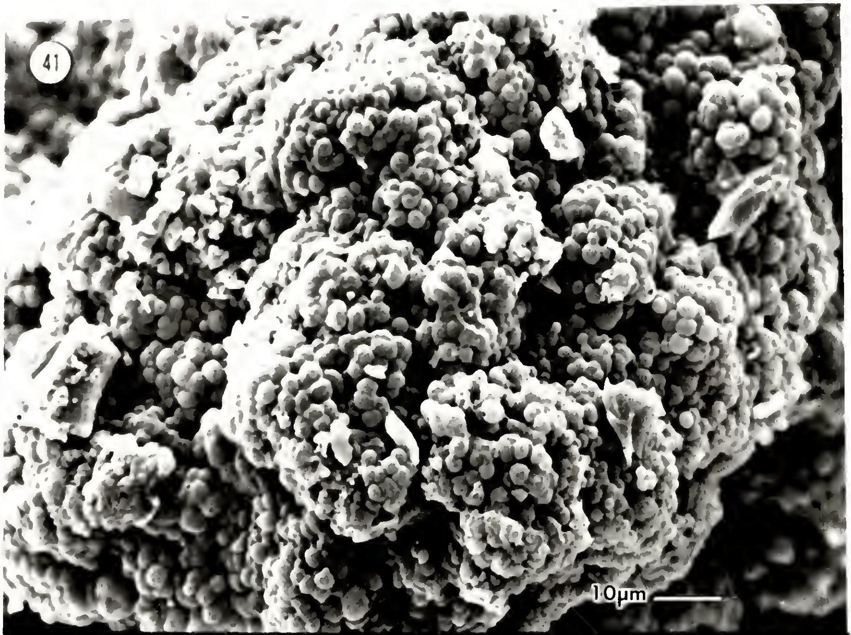
41
10µm

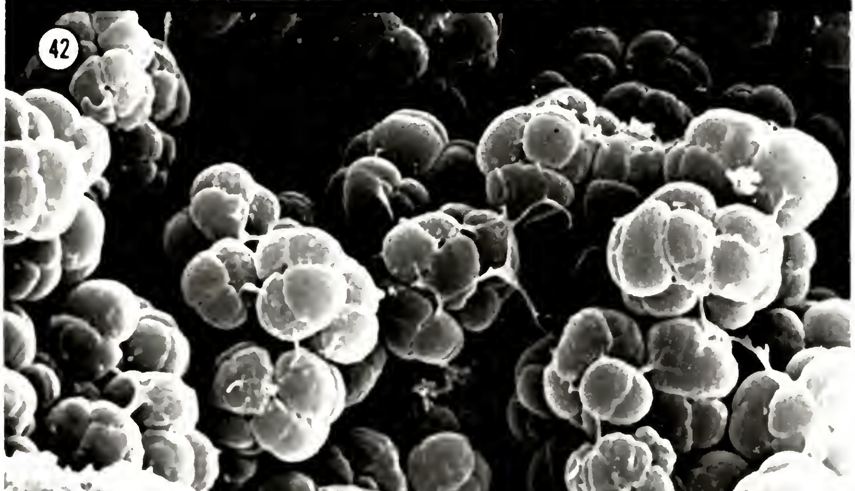
42
1.0 µm

Figures 43-46. Thin sections of Ms. mazei strain S6 showing the matrix material during colony disaggregation.

Fig. 43. Disaggregating colony held together by a loose fibrous matrix.

Fig. 44. Individual cell arrested during division. The matrix in the septum has the same fibrous appearance as the matrix on the cell surface.

Fig. 45. Micrograph showing the matrix peeling or shedding from the cell surface in layers.

Fig. 46. High magnification of the matrix on a cell that has almost lost all of the matrix. The matrix material is present as thin fibers and tubules are still associated with the cell surface.

M= matrix

g= granules

pm= plasma membrane

t= tubules

S= septum

43

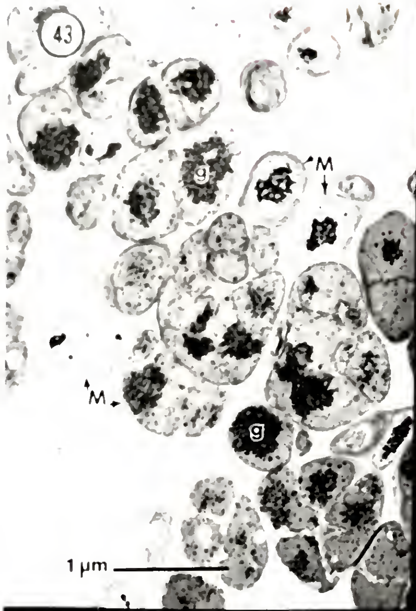

44

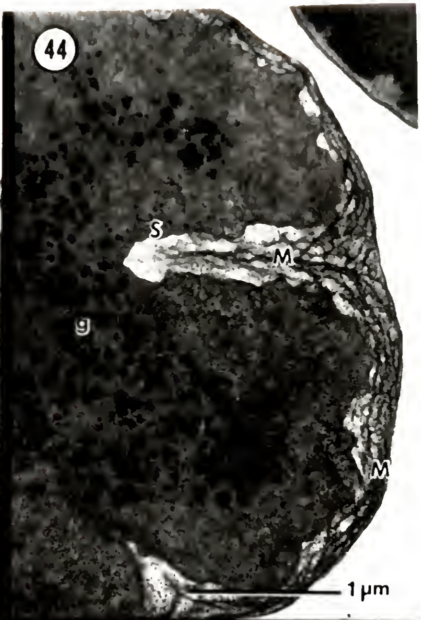

45

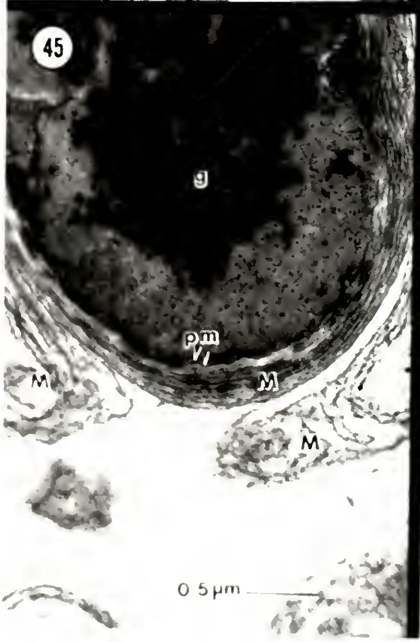

46

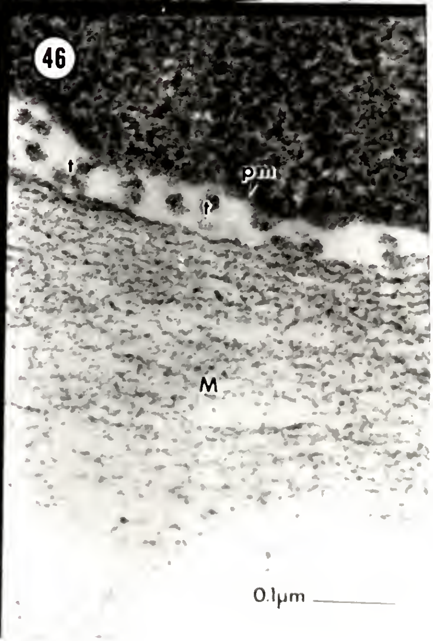

Figures 47-49. Thin sections of Ms. mazei colonies in the later stages of colony disaggregation.

Fig. 47. Low magnification of a loose colony held together by remnants of the matrix.

Fig. 48. Higher magnification of a partially disaggregated colony. A thin layer of matrix material remains around each cell in the colony while the associated free cells lack this material.

Fig. 49. A single cell that is surrounded by remaining matrix. Tubules are present between the matrix and the cell surface.

M= matrix

L= protein layer

g= granules

pm= plasma membrane

t= tubules

㊼

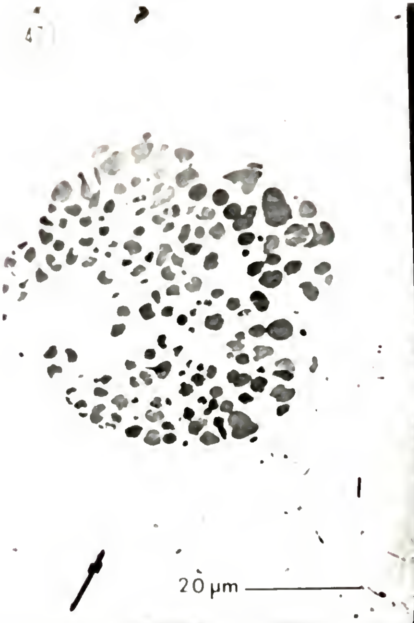

㊽

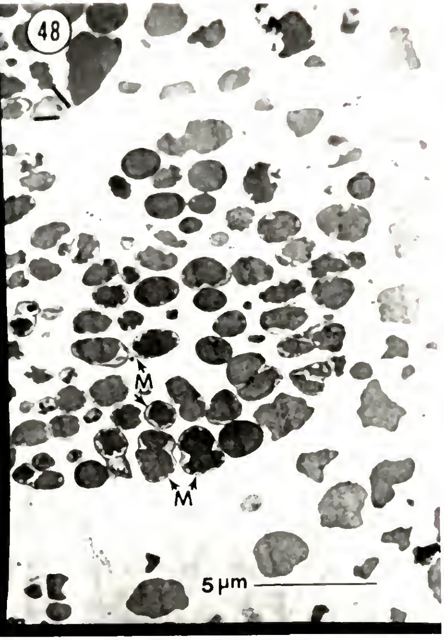

㊾

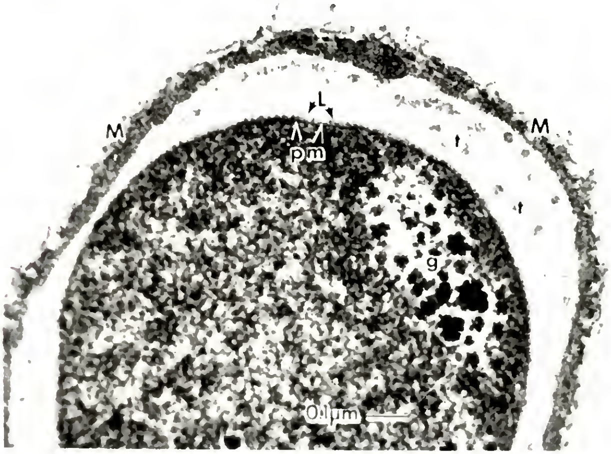

uneven, approximately 50 nm thick, and is not laminated. The layer is located several hundred nanometers from the cell surface. Such cells are less frequent as the cultures age.

Morphology of the Limited Life Cycle

Methanosarcina mazei Strain S6

A limited cycle occurs in the wild type *Ms. mazei* when the colonies are still actively growing before matrix degradation and colony dissagregation begins. When the wild type *Ms. mazei* was repeatedly transferred in the laboratory, it gradually lost the ability to undergo the complex life cycle. It failed to disaggregate into single cells and the matrix remained intact. This variant strain can only disperse by fragmentation of the sarcinal colony. *Ms. barkeri* and the variant of *M. mazei* strain S6 are limited to this cycle and do not break up into individual cells. When these cultures are passed through 5 µm filters into fresh media, colonies have the same general morphology as mature colonies found in the complex life cycle. If these colonies are disturbed sufficiently by methane gas evolution or by shaking, they will fragment into smaller masses. The size depends on the severity of the shaking, and if very hard (vortexing for 1 min), then individual units approximately 3.0 µm in size are released (see boxed area in Fig. 24). These will again grow into larger masses when placed in fresh media. The developmental changes of maturing sarcinal colonies of Ms. mazei S6 were examined in the variant strain over a period of 360 days. Cultures of Ms. barkeri were examined after 14 and 90 days of growth.

In thin sections, the cytoplasm of the cells of 5-day colonies grown on acetate stains rather evenly (Fig. 50). At this stage the colonies are found singly in the culture medium and are uniform with a diameter of 3-5 µm. The individual cells themselves are 0.6-1.0 µm in diameter and are surrounded by a 30-60 nm matrix. The electron dense granules are scattered throughout the cytoplasm and polyphosphate bodies are rarely seen. Membrane tubules between the protein layer and the matrix are not commonly observed in cultures restricted to the limited cycle.

Within 10 days, the colonies enlarge to 8-10 µm and the cells to 1.5 µm (Fig. 51). Cells of this age show a variability of cytoplasmic staining correlated with three morphological types. These cell types are arbitrarily defined and intermediate forms can be found. The first type (A) has a dense rather dark staining cytoplasm, while that of the second type (B) appears less dense and stains lightly. The third cell type (C) appears highly degenerated and is usually found near the

Figures 50 and 51. Young colonies of the variant strain of Ms. mazei strain S6 growing in the limited cycle.

Fig. 50. Five-day old colony with fairly uniform staining cells.

Fig. 51. Ten-day old colony showing a variability in the cytoplasmic staining of cells. Cell type "A" stains rather dark while cell type "B" stains lighter. Cell type "C" is highly degenerated with numerous inclusion vescicles. A granule-containing membrane bound core is present (arrowheads).

M= matrix

g= granules

50

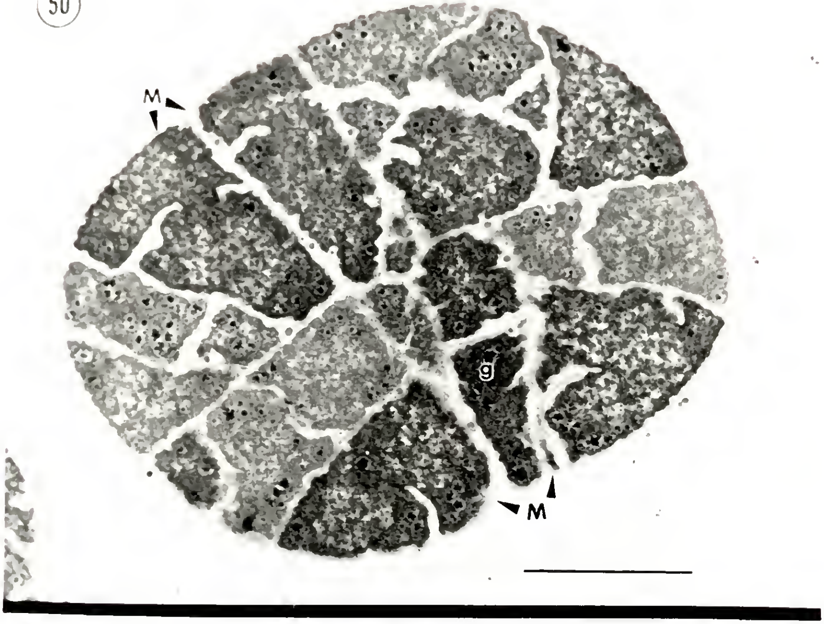

51

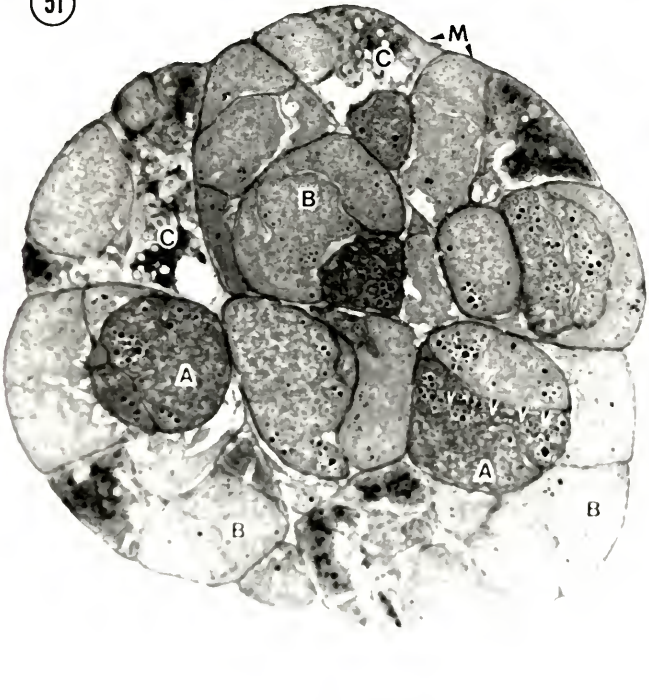

periphery of the colony. This type has numerous inclusions and membranous structures and does not show the cytoplasmic staining homogeneity seen in younger-looking cells.

Two kinds of membrane cores are found in the cytoplasm of cells restricted to the limited cycle. One kind is found in cell types A and B (Figs. 52-55 and arrowheads Fig. 51). They are 90 nm in diameter and appear to have a double membrane surface 25 nm thick. The membranes are straight and have a rigid appearance. A trilamellar unit structure is only rarely demonstrated (Fig. 54). There can be up to three cores of this kind per cell and when more than one is present they are arranged parallel to each other (Fig. 53). Inside the cylindrical cores are electron dense granules arranged in single file. These granules are of the same appearance as those found in the cytoplasm but are much more uniform in size at 40 nm. These cores are observed in less than 1% of the cells in thin sections but almost traverse the cytoplasm and are closely associated with the plasma membrane. A connection with the plasma membrane has not been observed and the ends appear to open into the cytoplasm (Fig. 55).

The second kind of core is associated with the plasma membrane in cell type C (Figs. 56 and 57). These are 100 nm in diameter and are shorter than the cores seen in younger cells (above). They are more numerous

Figures 52-57. Thin sections of membrane cores found in Ms. mazei strain S6. Figs. 52-55 are of the granule-containing cores found in cell types "A" and "B". Figs. 56 and 57 are of plasma membrane-associated cores found in cell type "C".

Fig 52. A high magnification of the core present in figure 51 (arrowheads). The core nearly bisects the cell and contains a single file of cytoplasmic granules.

Fig. 53. A cell with two of the granule-containing cores arranged parallel to each other (arrowheads).

Fig. 54. A granule-containing core at high magnification showing the double membrane structure.

Fig. 55. A granule-containing core with one end opening into the cytoplasm.

Fig. 56. A grazing section of a plasma membrane-associated core. A regular pattern is observed in the core surface.

Fig. 57. A cell containing several randomly arranged cores, one of which shows a connection with the plasma membrane (arrows).

M= matrix

g= granules

im= inner core membrane

om= outer core membrane

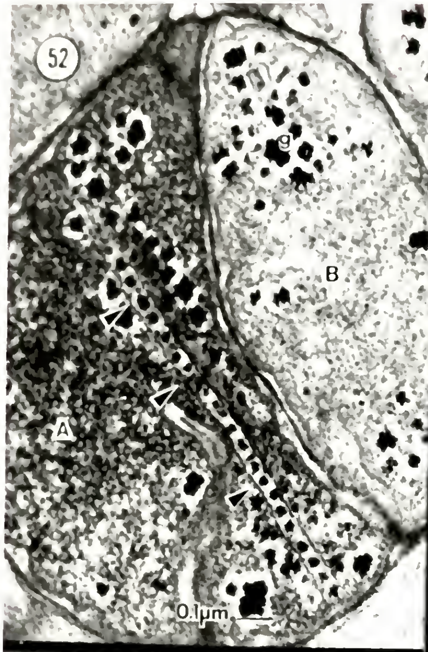
52
g
B
A
0.1µm

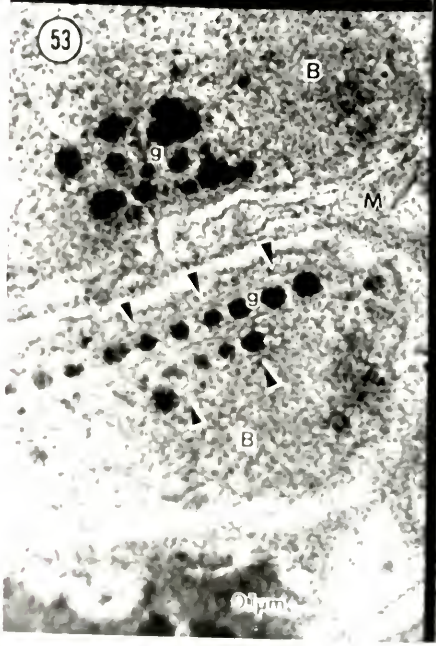
53
B
g
M
g
B
0.1µm

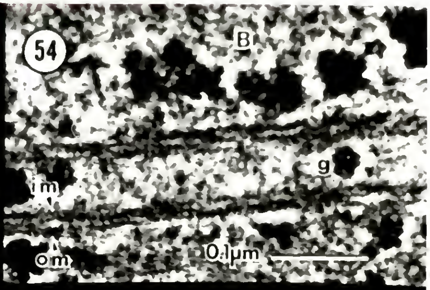
54
B
g
im
om
0.1µm

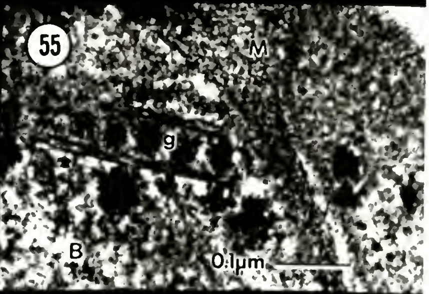
55
M
g
B
0.1µm

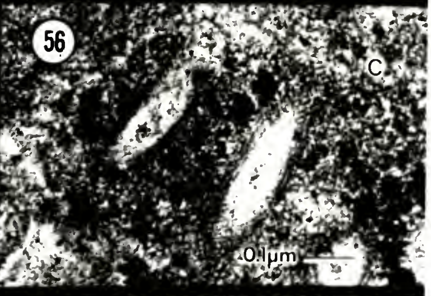
56
C
0.1µm

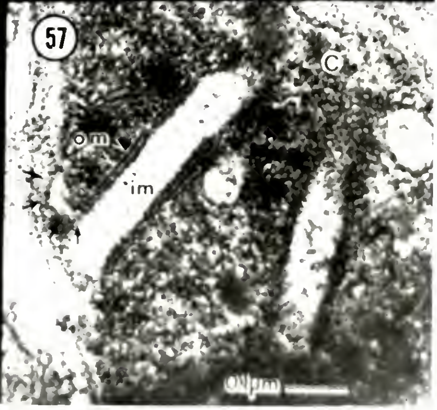
57
C
om
im
0.1µm

however, and are not in an ordered arrangement. These cores do not possess electron dense granules and appear empty. The inner membrane is continuous with the plasma membrane (arrows Fig. 57) and in grazing sections, a regular helical pattern is observed (Figs. 56 and 57). This regular pattern is probably due to the protein layer in close contact with the inner membrane. The ends of the outer membrane have not been resolved.

Twelve-day sarcinal colonies of strain S6 fixed only with glutaraldehyde and embedded in epon/araldite still fluoresce when viewed under UV irradiation. A comparison of cells observed in TEM (Fig. 58) and the same cells under UV epifluorescence (Fig. 59) reveals a correlation between the intensity of fluorescence and the type of cell observed within the colonies (see above). The dark staining type A cells observed in thin sections fluoresce brightly while the lighter staining type B cells and degenerated type C cells fluoresce very weakly or not at all.

At 12 days the three cell types within a colony are present in approximately equal numbers but by day 15 the second lighter staining cell type predominates (Fig. 60) and in cultures older than 21 days the degenerative cell type is most common (Fig. 61). By 90 days only a few of the younger cell types can be found (Fig. 62), and at 105 and 360 days (Fig. 63), which appear the same, only a few single cells look viable. The matrix

Figures 58 and 59. Sections showing the correlation between cell type and autofluorescence.

Fig. 58. Thin section of colonies showing the various cell types.

Fig. 59. Thick section of the same cells in figure 58 but viewed with fluorescence microscopy. The dark staining cells in thin sections (type "A") are the same cells that fluoresce brightly in thick sections.

58

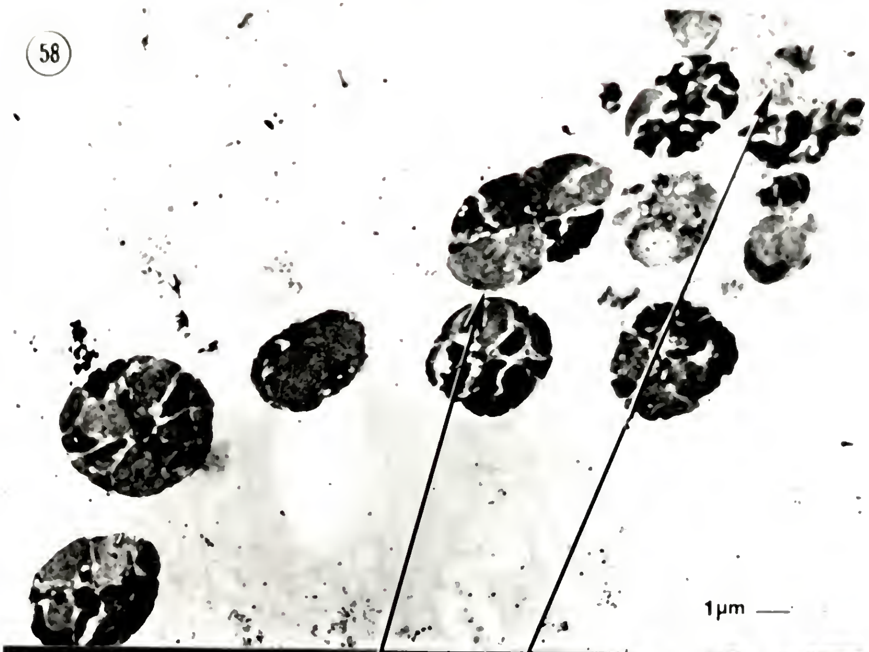

59

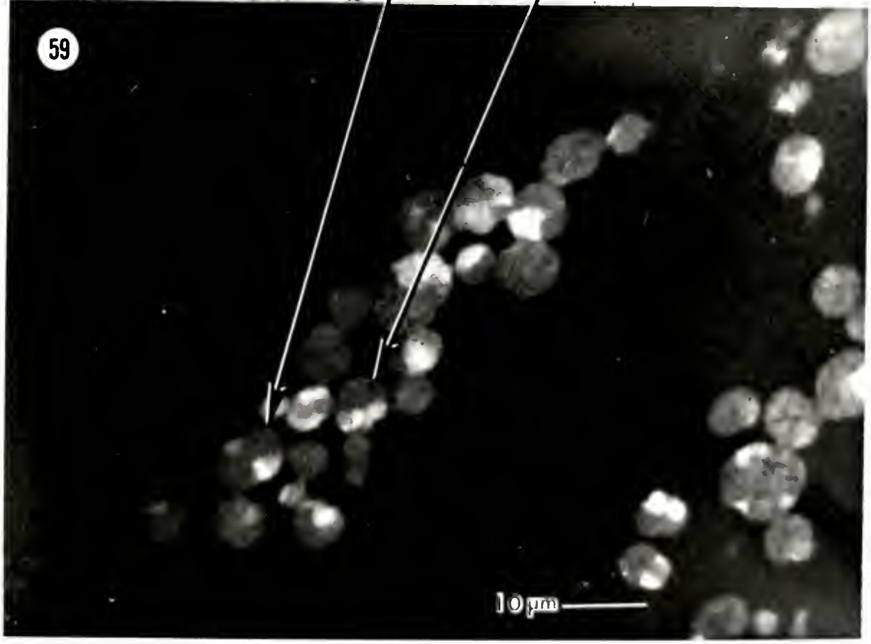

Figures 60-63. Thin sections of older cultures of the variant strain of *Ms. mazei* S6 grown in the limited cycle.

Fig. 60. Fifteen-day old colony showing the three cell types (see text).

Fig. 61. Twenty-one-day colony with cell type "C" predominating.

Fig. 62. Ninety-day colony where most of the cells are dead.

Fig. 63. One-hunded-twenty-day colony that appears the same as one-year-old colonies (not shown). Only a few viable looking cells are present.

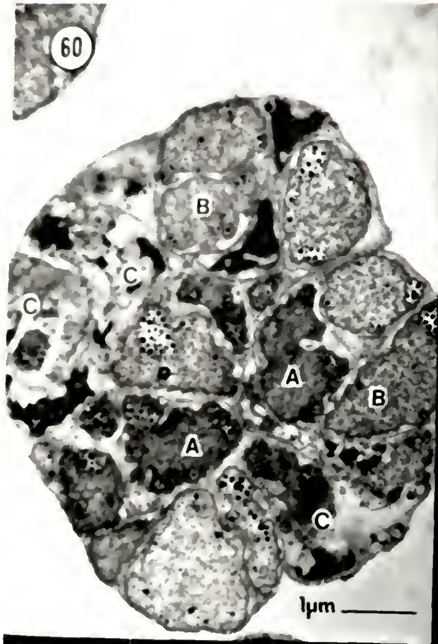
60
B
C
C
A
B
A
C
1µm

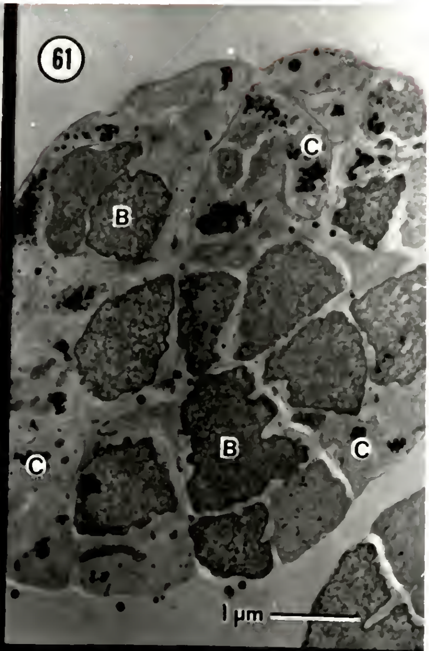
61
C
B
B
C
C
1 µm

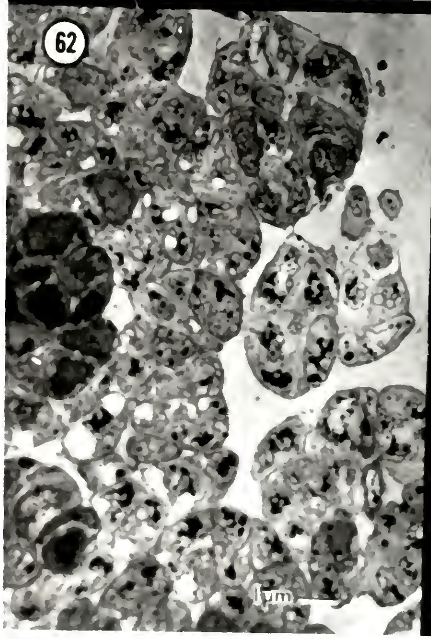
62
1µm

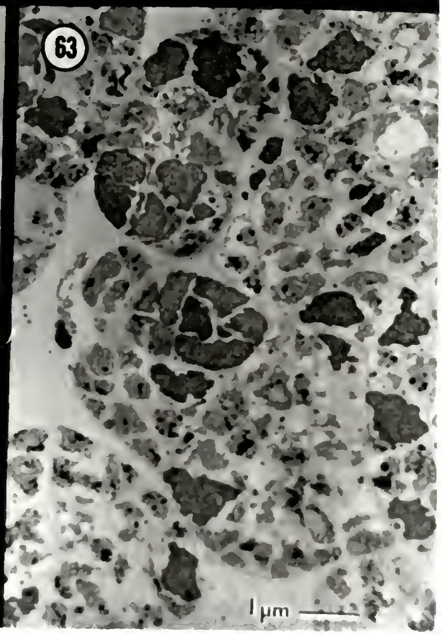
63
1 µm

between degenerated cells is poorly defined and the granules and polyphophate bodies persist. Possible resting forms (see below) can be found in these older cultures that have thick specialized walls.

Possible Resting Forms

Cultures of the variant Ms. mazei strain S6 older than three months are largely composed of dead cells. However, several types of structures which may be resting forms are found (Figs. 64-66). Islands of viable looking cells can be found toward the center of the colonies (Fig. 64). In thin sections these are usually composed of 10-15 cells each surrounded by a dense layer of matrix material 100-200 nm thick. Frequently, individual cells can be found with a specialized uniform layer 40 nm thick that is apparently derived from the matrix but appears more dense (Fig. 65). Numerous membrane tubules may be found outside the protein layer and division septa were never observed in these cells. The single-cell forms are usually spherical but they are sometimes rod shaped. They may or may not contain cytoplasmic granules or polyphosphate bodies. A specialized layer sometimes develope around cells in younger cultures when the other cells still look viable (Fig. 66).

Figures 64-66. Thin sections of resting forms found in old colonies of the variant strain of _Ms. mazei_ growing in the limited cycle.

Fig. 64. One type of resting form is composed of many cells enclosed by a thick specialized matrix.

Fig. 65. Single-cell resting forms surrounded by a thick specialized layer.

Fig. 66. A group of viable looking cells with a specialized layer (arrowheads) around one of them.

R= resting forms

t= tubules

64

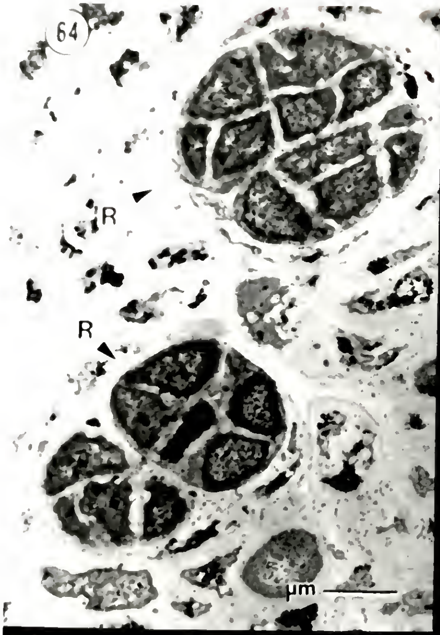

66

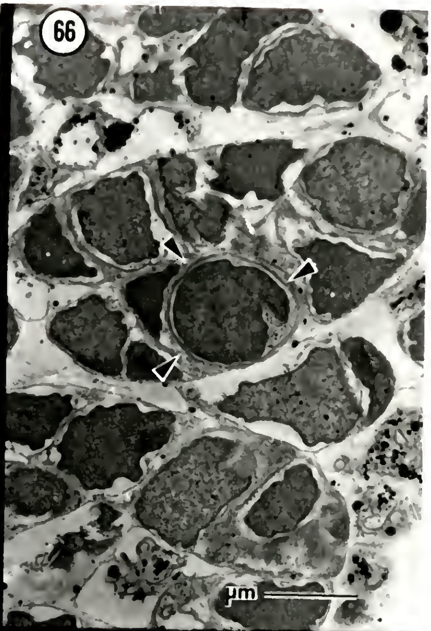

65

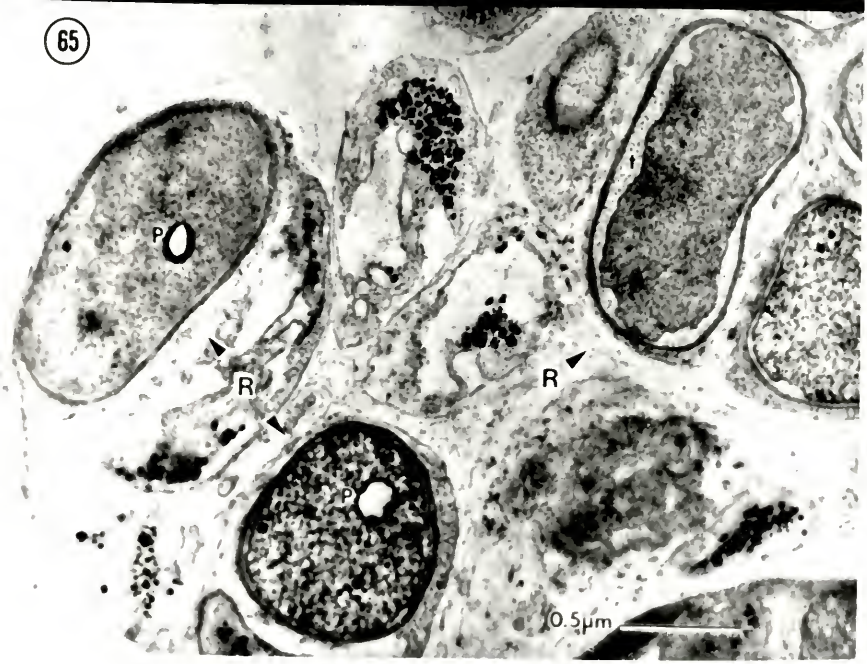

Methanosarcina barkeri Strain 227

Young colonies of *Ms. barkeri* strain 227 (Fig. 67) appear similar to the 5-day cultures of *Ms. mazei* (compare with Fig. 50) and exhibit morphotypes similar to those in the limited cycle. The nuclear regions are prominent and granules are present in the cytoplasm. The matrix is up to 150 nm thick, approximately twice the thickness of the matrix in *Ms. mazei*, and is closely packed between the cells. An additional layer approximately 10 nm thick could be observed between the plasma membrane and the matrix but this is usually difficult to discern due to the close association of the matrix (Fig. 68). Colonies at 90 days (Fig. 69) are highly degenerated, much more so than older cultures of *Ms. mazei* (compare with Figs. 62 and 63). A few viable looking cells are present but these do not have specialized layers and do not appear to be resting forms. The degenerated cells contain laminated or concentric stacks of membranes that form a variety of structures (Fig. 70). The rest of the cytoplasm is filled with membrane particles and electron dense granules (Fig. 70). Occasionally, membrane bound areas are found with dark staining spherical bodies (Fig. 71). These are up to 80 nm in diameter and are made of

Figures 67 and 68. Thin sections of 14-day colonies of *Methanosarcina barkeri* strain 227.

Fig. 67. Cells within a colony are enclosed by a closely associated matrix. The cells stain rather homogenously.

Fig. 68. High magnification of the cell surface showing a layer in contact with the plasma membrane.

M= matrix

g= granule

pm= plasma membrane

Nu= nuclear region

L= probable protein layer

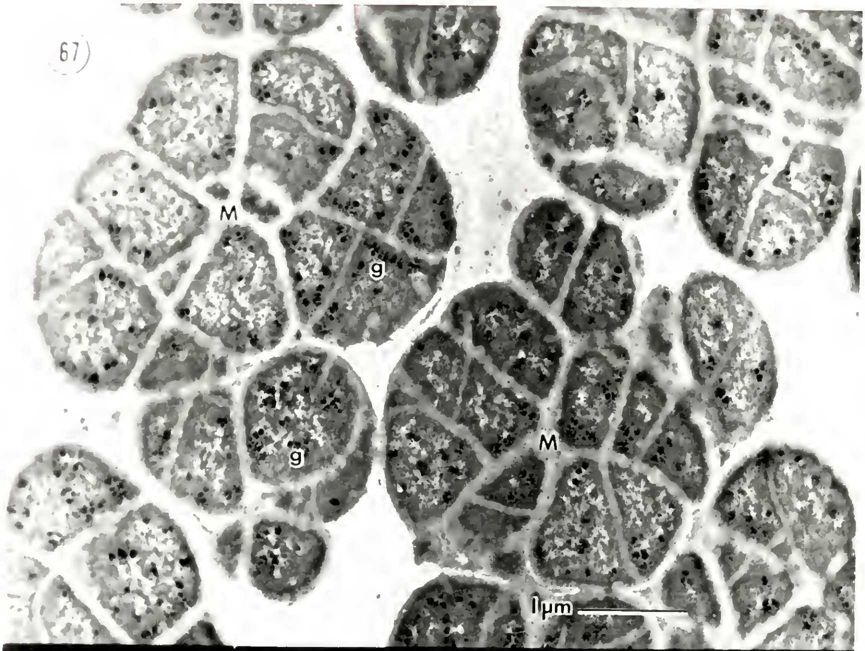
67

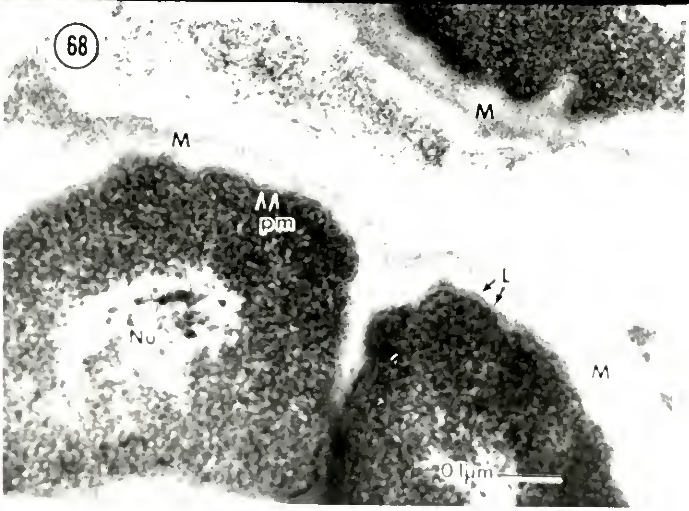
68

Figures 69-71. Thin sections of 90-day colonies of Ms. barkeri strain 227.

Fig. 69. Degenerative cells in these old cultures do not show any regular structure. Membrane vescicles are present along with the electron dense granules.

Fig. 70. A higher magnification showing the vescicles (arrowheads) and granules.

Fig. 71. A membrane bound vescicle containing several very dark staining structures. These are apparently made of coils of membrane (inset).

M= matrix

g= granules

pm= plasma membrane

m= vescicle membrane

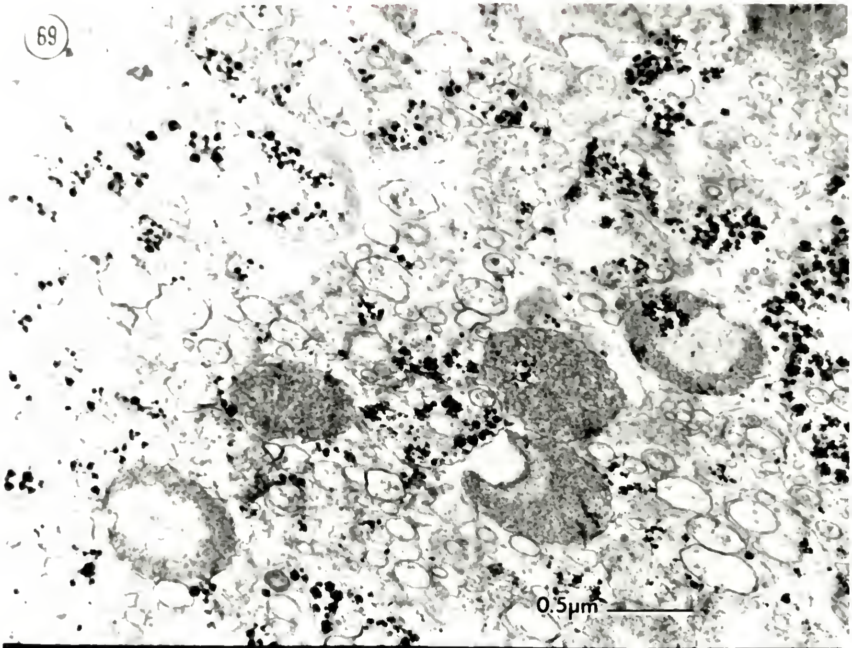
69
0.5μm

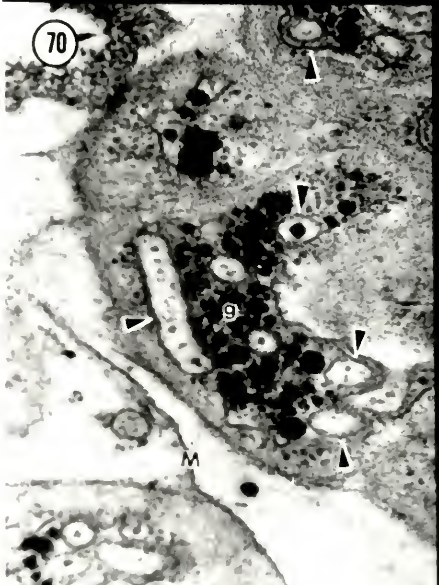
70
g
M
0 5μm

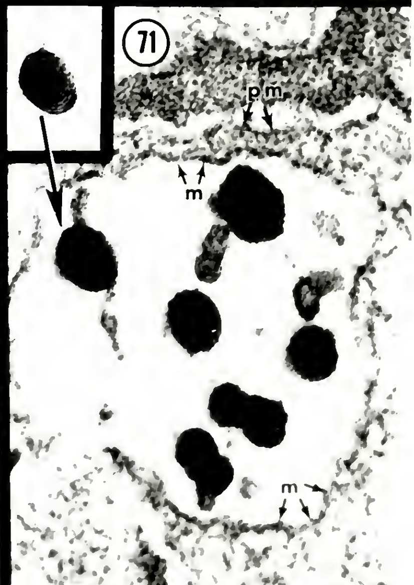
71
pm
m
m
0.1μm

closely packed concentric rings 5.0 nm thick (insert). The nature of these structures is unknown.

Disaggregation in Methanosarcina Strain LYC

Ms. mazei strain LYC when grown at pH 6.0, has a morphology and life cycle similar to Ms. barkeri. When colonies are viewed in SEM, cells are 1.0-2.5 μm in size and are held in lobes that make up the sarcinal colony (Fig. 72). The matrix is not as thick on the surface as in strain S6 and individual cells can easily be seen. If cultures are maintained at pH 6, the larger colonies will fragment into smaller colonies when agitated. When the pH of a culture is changed to 7.0 however, single cells begin shedding from the colonies.

When the disaggregating colonies are observed in SEM, cells on the colony surface are not tightly associated (Fig. 73). These are similar to cells in disaggregating colonies of strain S6 (compare with Figs. 41 and 42). Thin sections, however, show that cells are being released from the matrix at the colony surface and only the outermost cell layers are affected (Fig. 74). The cells in the colony interior have a homogeneous staining cytoplasm which contains only a few electron dense granules and polyphosphate-like bodies. The matrix is dark staining and is approximately 50 nm

Figures 72-75. Disaggregation in *Methanosarcina mazei* strain LYC.

Fig. 72. SEM of a sarcinal colony growing at pH 6.0.

Fig. 73. SEM of a colony after changing the pH of the medium to 7.0. Free single cells are apparent on the colony surface.

Fig. 74. Thin section of disaggregating colony. The matrix is only being degraded at the colony surface.

Fig. 75. High magnification of the colony surface showing a single cell breaking through the remaining matrix. The single cells are osmotically sensitive and the cell surface is not well preserved. However, dark areas are present (arrowheads) that may correspond to a protein layer.

M= matrix

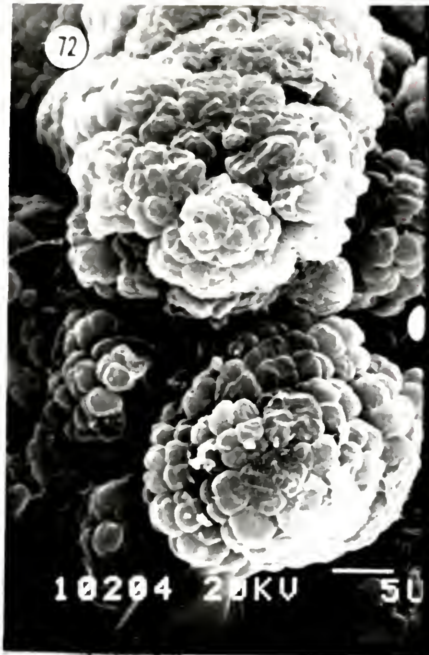
72
10204 20KV
5U

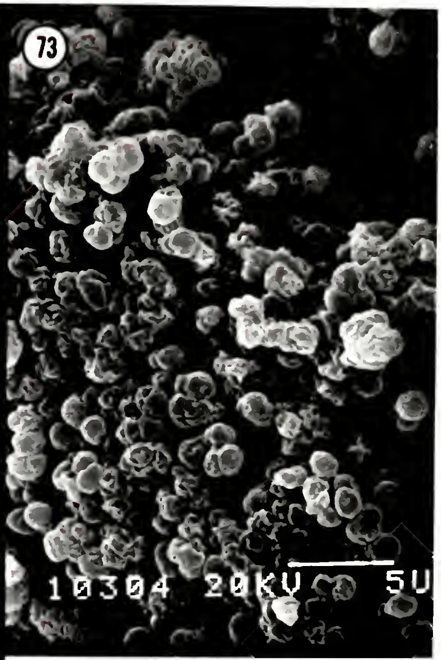
73
10304 20KV
5U

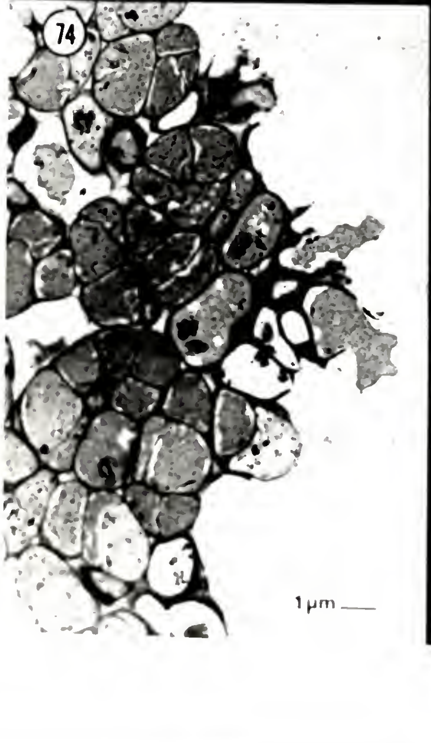
74
1 μm

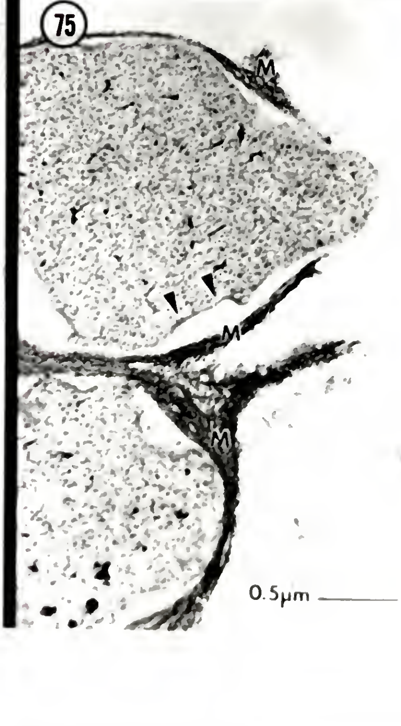
75
M
M
M
0.5μm

thick. It is fibrous and generally not in close association with the plasma membrane. The matrix has a loose appearance in the colony periphery and is approximately 150 nm thick. At the very outer edge, the matrix thins (Fig. 150) until the underlying cell breaks through and migrates away from the colony. The cells become contorted in this process and retain an irregular appearance. A protein layer was not observed outside the plasma membrane, which is poorly preserved. The cytoplasm stains lighter than that of cells within the colony and there are regions along the cell surface that stain darker than the cytoplasm but lighter than the matrix (arrows Fig. 75). It is possible that the cells are osmotically sensitive and a layer, if present, was damaged during processing.

The sarcinal colonies of strain LYC will sometimes completely dissociate over a period of 48 hours. Usually though, degradation stops before the entire colony is broken up and colonies, although reduced in size, are still seen at the bottom of culture tubes.

Freeze-Fracture Analysis

Unfixed, propane jet frozen, sarcinal colonies of Ms. mazei strain S6 and Ms. barkeri strain 227 show a tendency to fracture through the cytoplasm rather than the plasma membrane and membrane faces are only rarely

Figures 76-81. Freeze-fracture analysis of the variant strain of Ms. mazei strain S6 and of Ms. barkeri strain 227.

Figs. 76 and 77. Cytoplasmic fractures through Ms. mazei grown in the limited cycle showing two types of particles.

Fig. 76. A high magnification of the smaller class of cytoplasmic particles.

Fig. 77. Low magnification with larger particles (arrows) wich probably correspond to the polyphosphate bodies.

Figs. 78 and 79. Plasma membrane fractures through Ms. mazei growing in the limited cycle revealing a high number of intramembrane particles.

Fig. 78. High magnification of intracytoplasmic particles.

Fig. 79. Low magnification of plasma membrane fractures of several cells.

Fig. 80. Cytoplasmic fracture through Ms. barkeri showing irregular particles and a smooth fracture surface through the matrix.

Fig. 81. Plasma membrane fracture through Ms. barkeri showing a high number of membrane particles arranged in regular patterns.

M= matrix

Cy= cytoplasm

pf= protoplasmic fracture

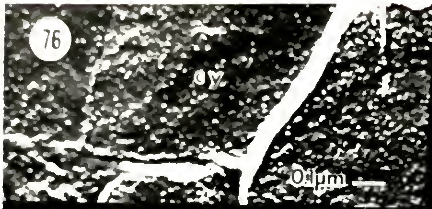
76
cy
0.1µm

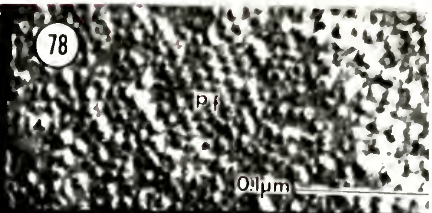
78
pf
0.1µm

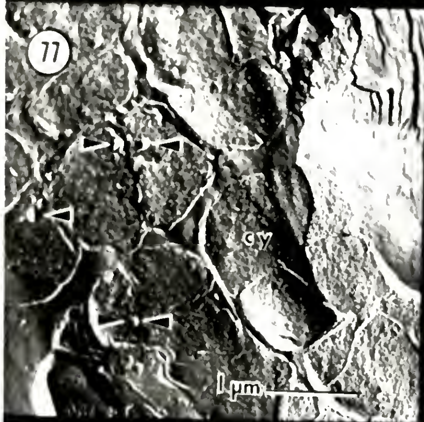
77
cy
1 µm

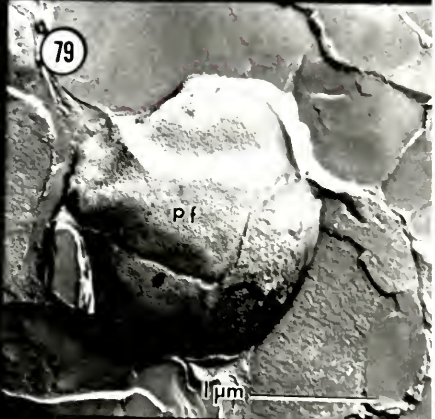
79
pf
1µm

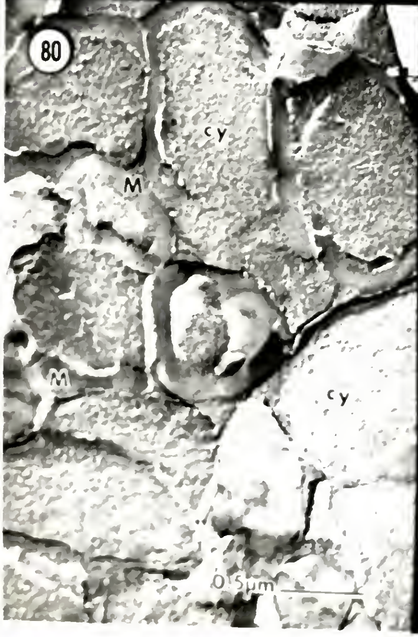
80
cy
M
M
cy
0.5µm

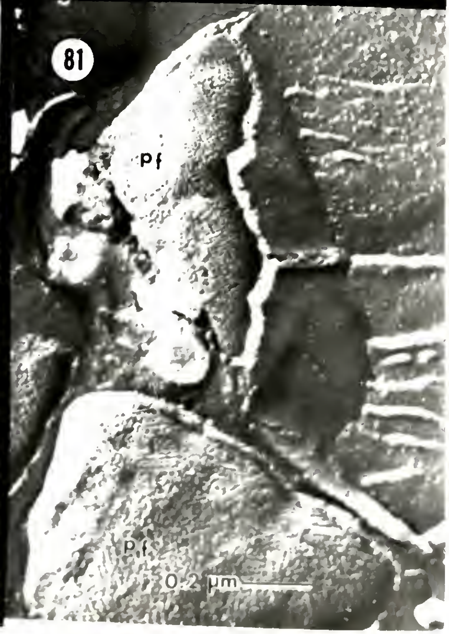
81
pf
pf
0.2 µm

observed. Replicas of the variant strain S6 growing in the limited cycle show two classes of intracellular particles (Figs. 76 and 77). One ranges in size from 10 to 20 nm and the other measures from 80 to 200 nm. The latter number 1-2 per cell and are probably the polyphosphate bodies. A dense arrangement of protein particles 9.0 nm in size was found in the plasma membrane (Figs. 78 and 79). Cultures of S6 examined at 5, 10, 14, and 21 days showed no difference in the particle distribution in the fracture planes. Free single cells of strain S6 were not observed to fracture through the plasma membrane.

Ms. barkeri strain 227 possessed a heterogeneous population of cytoplasmic particles ranging from 10 to 30 nm. with approximately the same distribution as observed in Ms. mazei. The larger class of particles corresponding to the polyphosphate bodies was not observed (Fig. 80). The matrix is approximately 120 nm thick and fractures with a smooth surface. The plasma membrane contains a large number of particles 9.0 nm in size that are commonly arranged in regular arrays in many areas (Fig. 81).

Colonies of strain S6 growing in the complex life cycle showed a similar tendency to fracture through the cytoplasm rather than the plasma membrane. However these showed a more complex structure than those of colonies growing in the limited cycle. Fracture planes

Figures 82-85. Freeze-fracture analysis of Ms. mazei strain S6 grown in the complex life cycle.
Figures 83-85. Specialized areas found associated with the plasma membrane.

Fig. 82. Fracture through the cytoplasm and a large polyphosphate body.

Fig. 83. A fracture through a stack of laminated material.

Fig. 84. A fracture through several laminated areas that curve around and back on the stack.

Fig. 85. A fracture through a lamminated region where individual layers can be clearly observed. The layer folds back on itself and may be one continuous layer.

P= polyphosphate

cy= cytoplasmic fracture

82

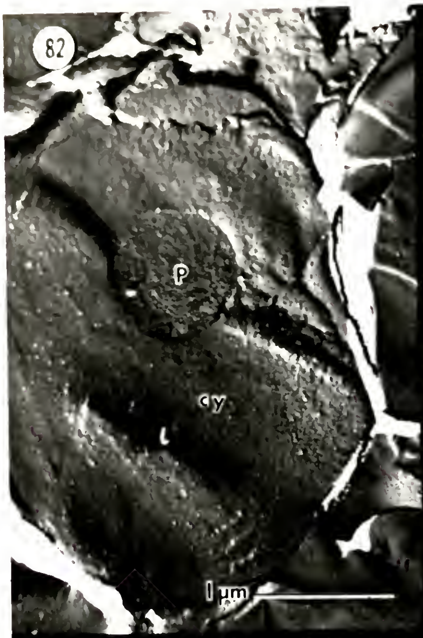

83

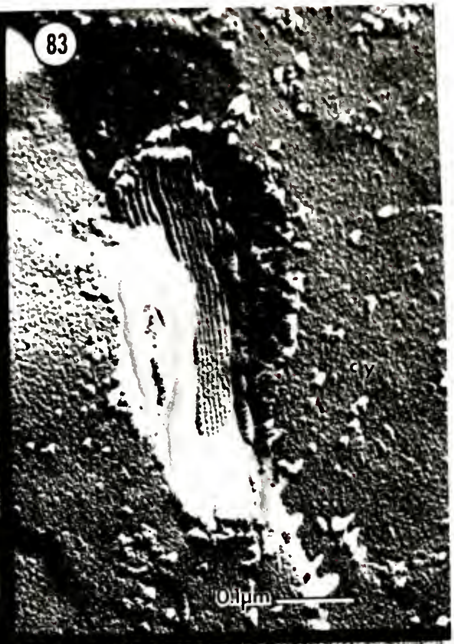

84

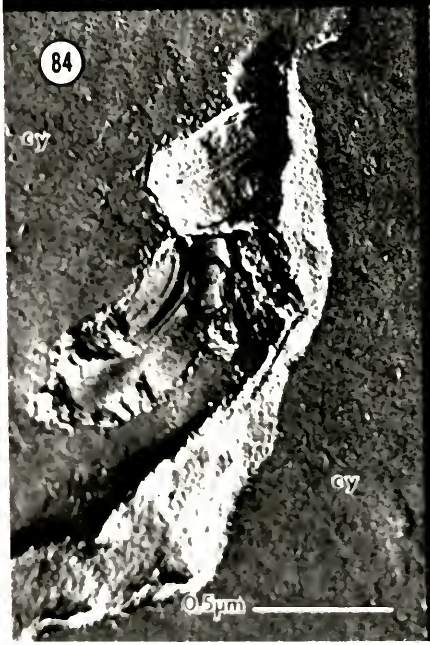

85

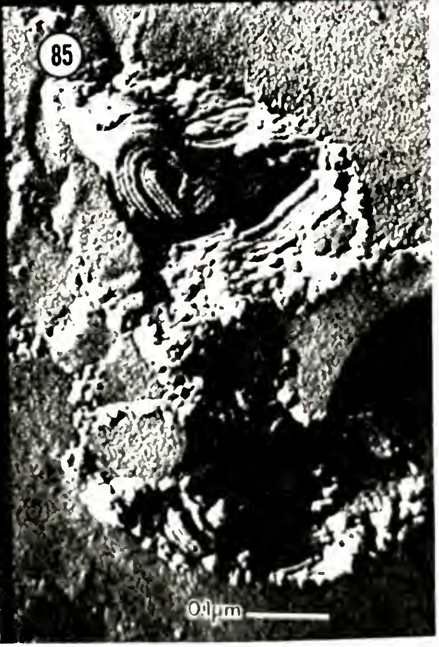

would frequently pass through polyphosphate bodies (Fig. 82). These are very large up to 0.8 μm in size with a rough even fracture surface. Specialized laminated structures are associated with the plasma membrane (Figs. 83-85). These usually consist of stacks of material in curved or convoluted forms with individual layers approximately 12 nm thick. Sometimes the structures appeared as tightly packaged folded layers 11.4 nm thick arranged in parallel coils (Fig. 85). These areas may correlate to groups of tubules observed at the cell surface in thin sections.

Cytochemical Analysis of the Cell Surface

Silver Stain

When thin sections of 12-day sarcinal colonies of strain S6 are etched with 1% periodic acid for one min and then stained with silver, the colonies show moderate labelling of the matrix material (Fig. 86) indicating a general polysaccharide composition. The layer just outside the plasma membrane does not label. When sections of disaggregating colonies were etched for 15 min before staining, the matrix shows a much higher level of staining (Figs. 87 and 88). The matrix material is evident and fibers throughout the extracellular space are prominent. Again, the layer

Figures 86-88. Siver methenamine staining of Ms. mazei strain S6.

Fig. 86. Sections of cells etched for 1 min show a light labelling of the matrix (arrowheads). The cell surface has a dark appearance due to the etching but does not label with silver (arrows). The cytoplasmic granules show heavy labelling.

Fig. 87. Thin section showing an intact colony, disaggregating colony, and free cells. The sections were etched for 15 min and the staining is much heavier than in figure 86. Only the matrix material stains. The free cells do not stain.

Fig. 88. Higher magnification of a cell with some remaining matrix material. The cell surface and associated tubules do not stain while the matrix stains heavily (arrowheads).

g= granules

t= tubules

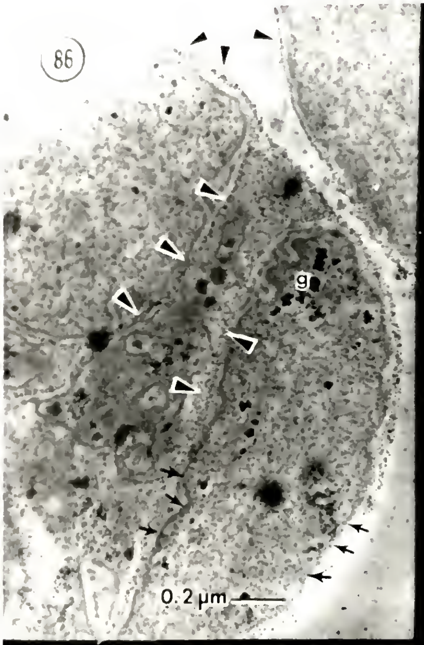

86

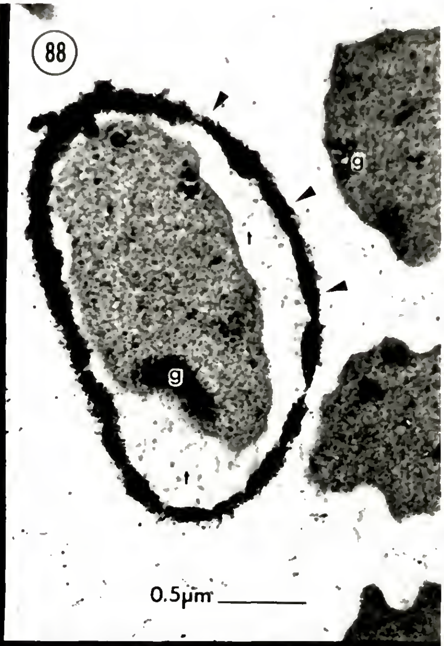

88

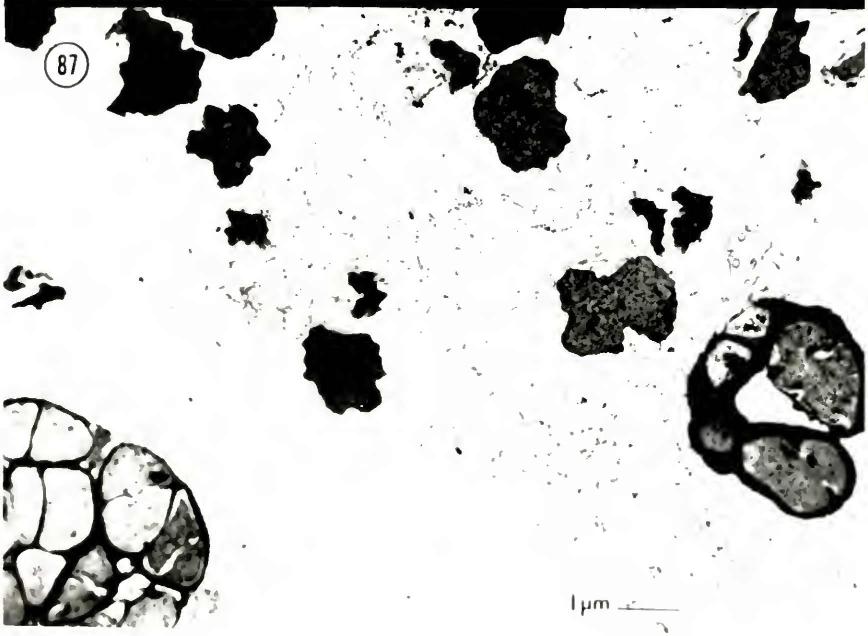

87

close to the plasma membrane and the associated membrane tubules do not stain. Free cells do not show any specific labelling of the cell surface, indicating a lack of matrix material. Controls not treated with fixer after silver staining had the same level of non-specific backround labelling and this step was subsequently eliminated. The other controls did not label.

Fluorescein-Labelled Lectins

A strong fluorescence was observed at the colony surface when strain S6 was treated with fluorescein-labelled PNA, SBA, DBA, or RCA_{120} lectins (Fig. 89). These lectins are specific for galactosyl groups. Fluorescence was not observed when galactosamine was present in the reaction mixture. Free cells generally did not label with only an occasional cell showing fluorescence (not shown). This is expected due to the lack of matrix material. No fluorescence was observed in samples treated with ConA, UEA I, or WGA lectins. These are specific for mannosyl and glucosyl, fucosyl, and glucosaminyl groups respectively.

Figures 89-91. Lectin labelling of the matrix of intact colonies of *Ms. mazei* strain S6.

Fig. 89. UV micrograph of fluorescein-labelled soybean lectin binding to whole cells. Peanut, *Dolichos*, and *Ricinus* lectins showed a similar fluorescence (not shown).

Fig. 90. Unstained thin section treated with colloidal gold-soybean lectin. The labelling is heaviest over the matrix material (arrowheads).

Fig. 91. Control section with the blocking hapten sugar galactosamine added to the reaction mixture. The labeling is non-specific.

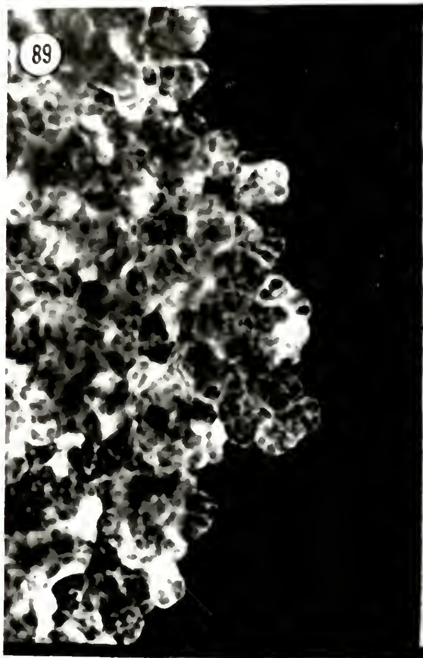
89

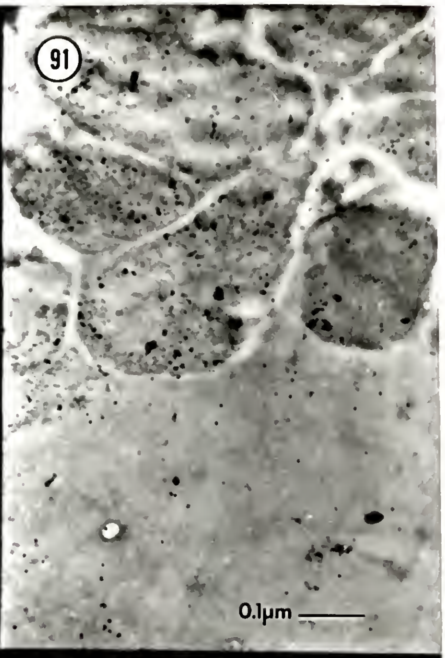
91
0.1µm

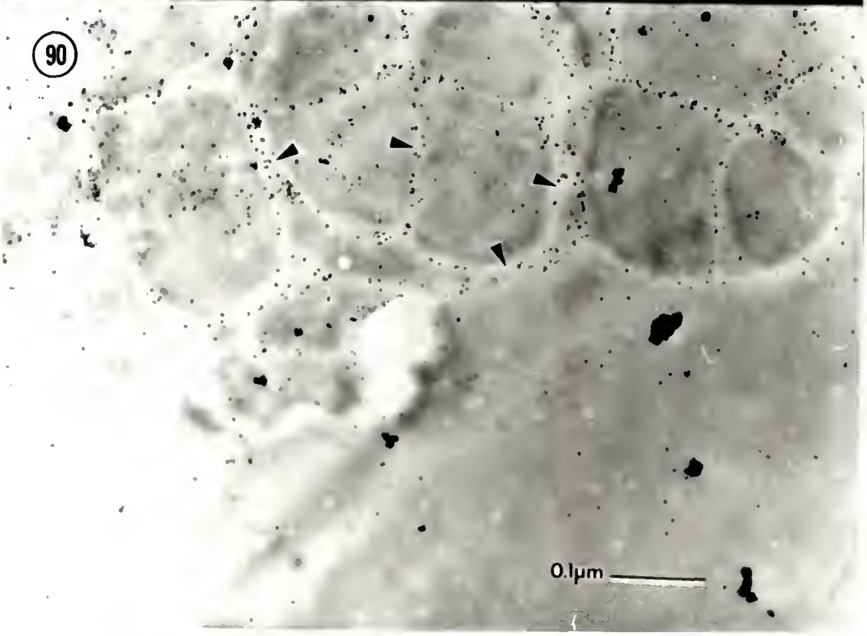
90
0.1µm

Gold-Labelled Lectins

Based on the results obtained using fluorescein-labelled lectins, an attempt was made to stabilize colloidal gold with PNA, SBA, and RCA. PNA and SBA stabilizations were successful but RCA-gold would flocculate during centrifugation and could not be used. PNA and SBA-gold treated cells are labelled lightly over the entire matrix (Fig. 90). These lectins are specific for N-acetyl galactosamine. Only non-specific labelling was observed on thin sections of single cells. The controls that included galactosamine in the labelling mixture (Fig. 91) show only non-specific labelling. Sections receiving colloidal gold only did not label (not shown).

Enzyme Extraction

The layer just outside the plasma membrane can be removed when colonies are treated with protease before fixation. Colonies treated for 5 or 10 min show protoplasts enclosed by the intact matrix which is 20-70 nm thick (Fig. 92). At higher magnifications (Fig. 93), the cytoplasm is bound solely by the plasma membrane, and the region between the cell surface and the matrix is free of particulate matter. Extensive cell damage

Figures 92-96. Whole colonies of Ms. mazei strain S6 treated with protease before fixation.

Fig. 92. Colonies treated with protease for 10 min lack the tubules associated with the cell surface.

Fig. 93. A high magnification of the cell surface of protease treated colonies shows the cytoplasm bound only by the plasma membrane. The protein layer is digested away.

Fig. 94. Cells treated with protease for 30 min show considerable cytoplasmic extraction with only the matrix remaining.

Fig. 95. Control culture treated with buffer for 30 min prior to fixation exhibits poor preservation but still contains the tubules.

Fig. 96. Control culture at high magnification shows the tubules and an intact protein layer.

M= matrix

L= layer

pm= plasma membrane

t= tubules

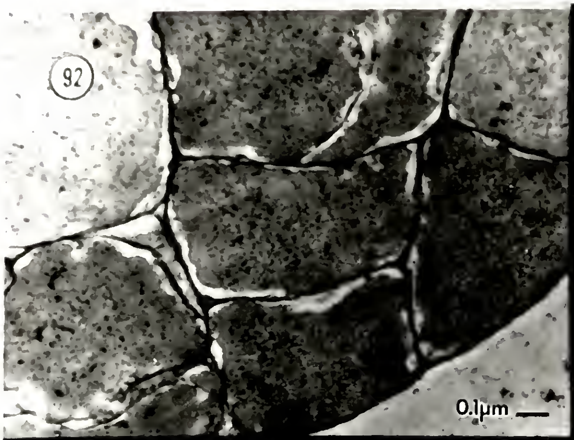
92
0.1µm

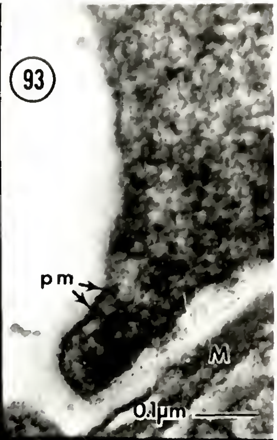
93
pm
M
0.1µm

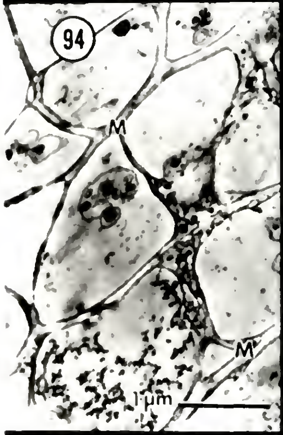
94
M
M
1 µm

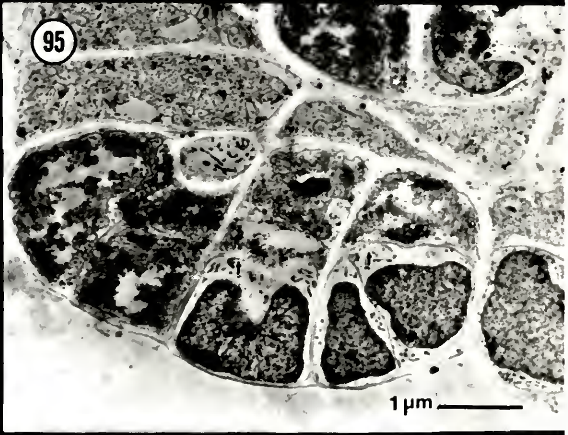
95
1 µm

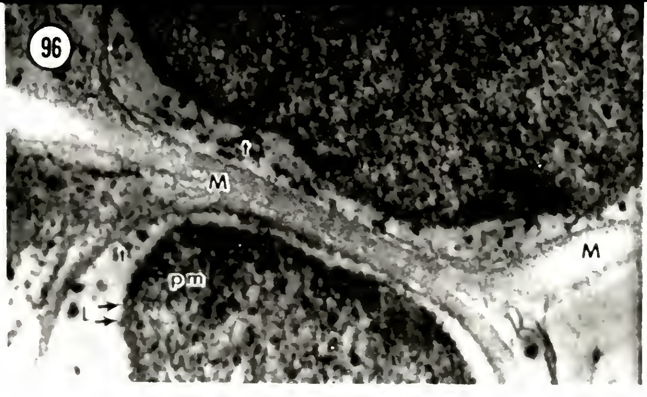
96
M
M
pm
L

occurs when colonies are treated for 30 min (Fig. 94). The controls treated with buffer for 30 min show an intact layer just outside the plasma membrane (Figs. 95 and 96). The preservation is poor due to air exposure before fixation.

When a culture of sarcinal colonies and single cells was fixed and subsequently treated with protease for 30 min, the layer just outside the plasma membrane is removed from single cells but not from intact colonies (Figs. 97-99). Single cells are enclosed only by the plasma membrane and strands of material are not associated with the cell surface (compare with figs. 7-9). The layer is not removed from cells in sarcinal colonies probably because the enzyme cannot penetrate the matrix after it is fixed.

Treatment of thin sections of Ms. mazei strain S6 with protease for four hours causes extensive extraction of the cytoplasm, but the granules and the polyphosphate bodies remain intact (Fig. 100). The layer in contact with the plasma membrane is removed (Fig. 102). The associated tubules are also removed indicating that protein from the surface layer may be associated with the tubules (Fig. 102). Controls treated with buffer retain this layer and the tubules (Fig. 103). Sporosarcina ureae has a protein layer just outside of the vegetative cell wall and also has protein coats in mature endospores (Fig. 104). These layers are removed

Figures 97-99. Free cells and colonies of _Ms. mazei_ strain S6 treated with protease after fixation.

Fig. 97. Single cells remain intact after fixation but protease digests away the protein layer.

Fig. 98. Higher magnification of the cell in figure 97 showing the cytoplasm bound only by the plasma membrane.

Fig. 99. Intact colonies still possess the protein layer and the tubules associated with the cell surface.

M= matrix

pm= plasma membrane

L= protein layer

g= granules

T= tubules

97

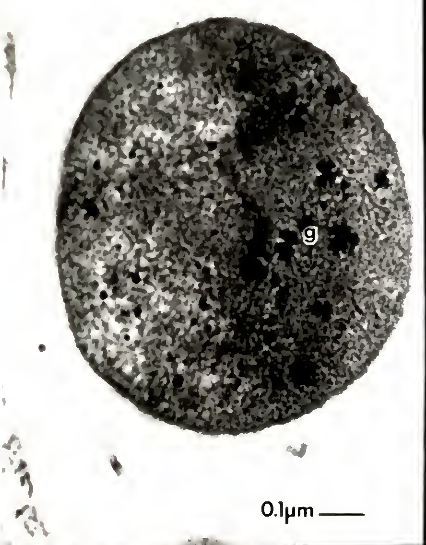

98

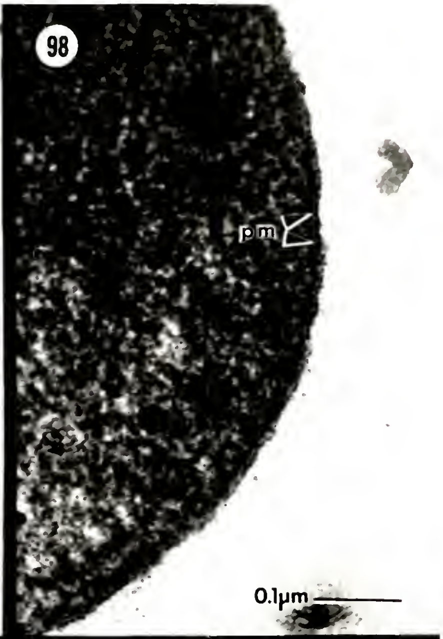

99

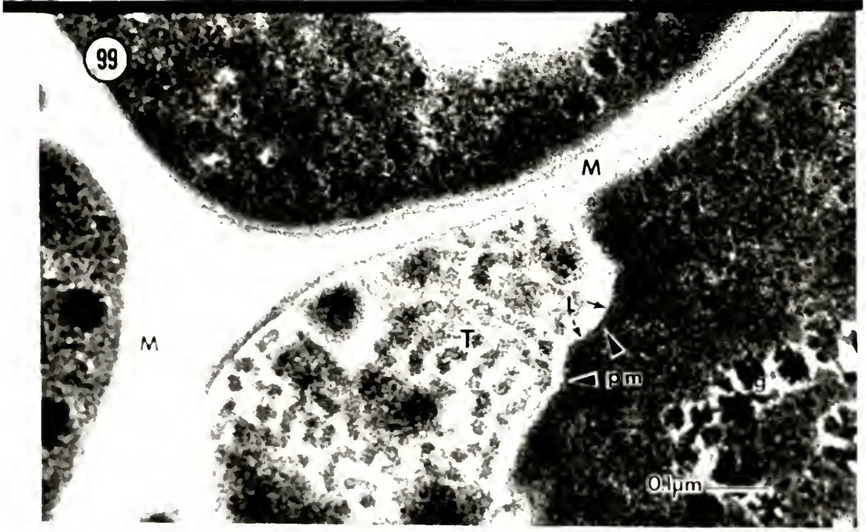

Figures 100-105. Protease treatment of thin sections of Ms. mazei strain S6.

Fig. 100. Low magnification of an unstained section treated with protease. There is considerable cytoplasmic extraction but polyphosphate bodies and cytoplasmic granules persist.

Fig. 101. High magnification of an unstained, protease-treated sections lack the tubules associated with the cell surface.

Fig. 102. Very high magnification of the cell surface treated with protease. The protein layer and the associated tubules have been digested away. Section poststained.

Fig. 103. Control section that was only etched shows less cytoplasmic extraction and retained the protein layer and associated tubules. Section poststained

Fig. 104. Control section of Sporosarcina ureae showing intact spore coats and outer protein layer after etching.

Fig. 105. Section of S. ureae after protease treatment. The endospore and the cell walls are completely removed (*).

M= matrix

L= protein layer

pm= plasma membrane

g= granules

Sp= spore

Sc= spore coats

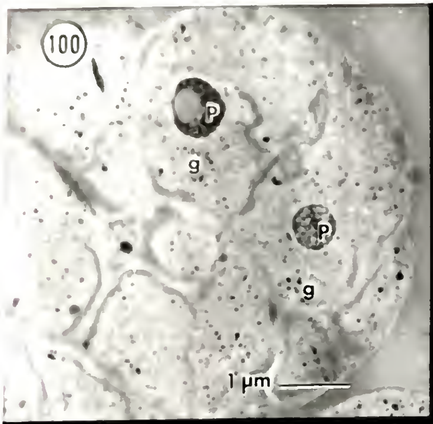
(100)

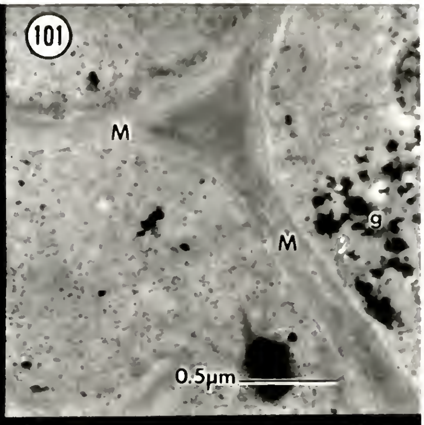
(101)

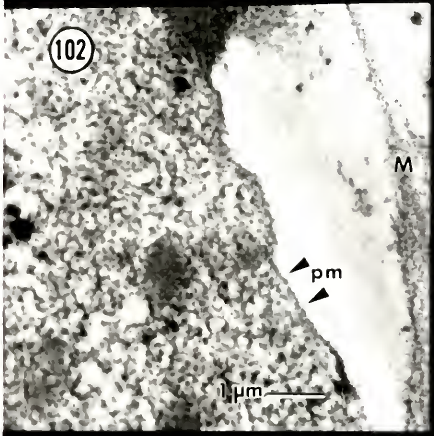
(102)

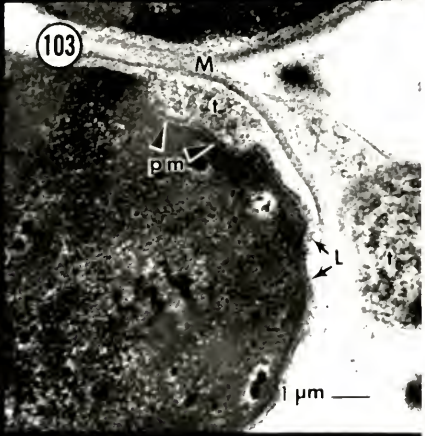
(103)

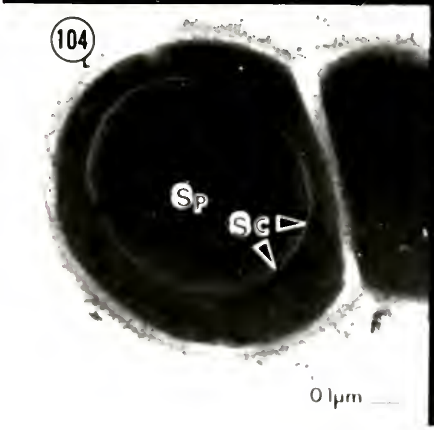
(104)

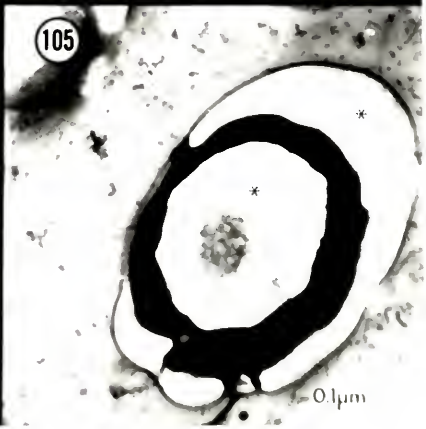
(105)

along with most of the gram-positive wall when treated with protease (Fig. 105). It is not known why the gram-positive wall is removed but it might contain a high amount of outer layer protein associated with it.

Cytochemical Analysis of the Granules and Polyphosphate Bodies

Elemental Analysis.

In cells fixed only with glutaraldehyde and formaldehyde (no osmium), the polyphosphate bodies are electron dense and can readily be identified in unstained sections (Fig. 106). The cytoplasmic granules are also electron dense but are difficult to observe unless they are in groups. Intact polyphosphate bodies give an energy spectrum that shows peaks corresponding to phosphorus and calcium (Fig. 107). The cytoplasm gives a spectrum with much smaller peaks for phosphorus and calcium (Fig. 108) and these elements are not detected in the embedding resin (Fig. 109). Cytoplasmic areas where the granules are prominant give an energy spectrum that is identical with the cytoplasm. This may indicate a difference in elemental concentration that is too low to detect, or that the calcium and phosphorus present in the spectrum of the cytoplasm is due to granular material that is difficult to see in unstained sections.

Figures 106-109. X-ray analysis of thin sections of Ms. mazei strain S-6 not treated with heavy metals. Sections were collected on nickel grids and not etched or poststained.

Fig. 106. Thin section used to represent areas tested.

Fig. 107. Energy spectrum obtained when the polyphosphate body is analyzed.

Fig. 108. Energy spectrum obtained from cytoplasm.

Fig. 109. Energy spectrum obtained from the plastic embedding medium.

M= matrix

P=polyphosphate

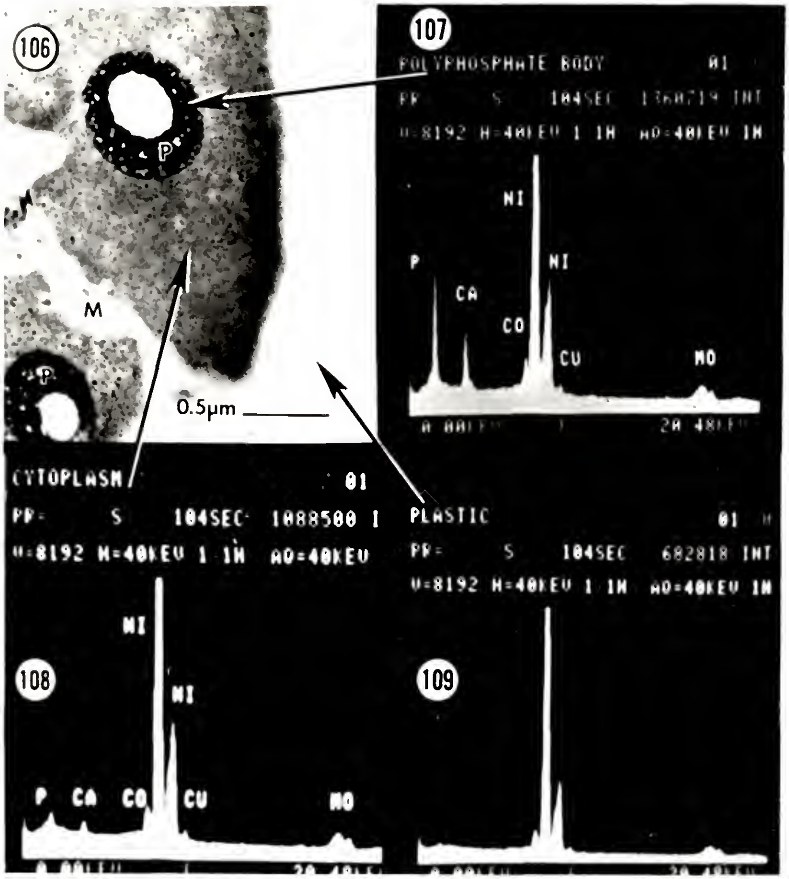
106
P
M
P
0.5μm
107
POLYPHOSPHATE BODY 01
PR= S 104SEC 1360719 INT
V=8192 H=40KEV 1 1N AQ=40KEV 1N
P
CA
CO
NI
NI
CU
MO
0.00KEV
20.48KEV
CYTOPLASM 01
PR= S 104SEC 1088500 I
V=8192 H=40KEV 1 1N AQ=40KEV
108
P
CA
CO
NI
NI
CU
MO
0.00KEV
20.48KEV
PLASTIC 01
PR= S 104SEC 682818 INT
V=8192 H=40KEV 1 1N AQ=40KEV 1N
109
0.00KEV
20.48KEV

Silver Stain

Granules and the polyphosphate bodies stain heavily with silver methenamine which may indicate the presence of reducing sugars and/or disulfide bonds (see Figs. 86-88).

Enzyme Extraction

When unetched thin sections are treated with phosphatase for 6 hrs the polyphosphate bodies are partially removed and the electron density is diminished (Fig. 112). The reticular nature is maintained, and when this material is examined using X-ray analysis, no peaks for phophorus or calcium are obtained (Fig. 113, compare with Fig. 105). The electron dense granules are not extracted after 24 hours (Fig. 110). Controls treated with buffer for 24 hrs retains the dark staining polyphosphate bodies (Fig. 111).

Treatment of etched thin sections for up to 24 hours with cellulase, amylase, or pullulanase, alone, or sequentially with pullulanase followed by alpha and beta amylase does not extract the electron dense granules or the polyphosphate bodies (Fig. 114). The amylase control does extract glycogen from thin sections of *Dictyostelium* myxamoebae within 30 minutes (Fig. 115).

Cellulase extracts cellulose from embedded filter paper (Figs. 116 and 117).

Figures 110-113. Thin section analysis of Ms. mazei strain S6 treated with phosphatase.

Fig. 110.	Section treated with phosphatase shows a cell with a partially extracted polyphosphate body. The cytoplasmic granules remain intact. Section poststained.
Fig. 111.	Etched, buffer-treated control shows intact electron dense granules and polyphosphate bodies.
Fig. 112.	Partialy extracted polyphosphate body examined by X-ray analysis in figure 113.
Fig. 113.	X-ray specrum of the partially extracted polyphosphate body in figure 112. The phosphorous and calcium peaks are missing (compare with Fig. 107)

M= matrix

g= granules

P= polyphosphate

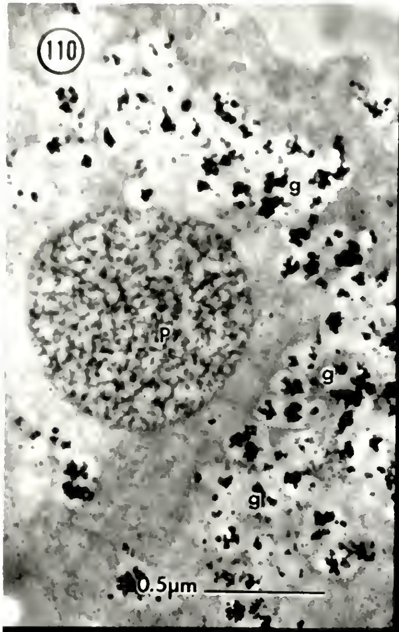
(110)

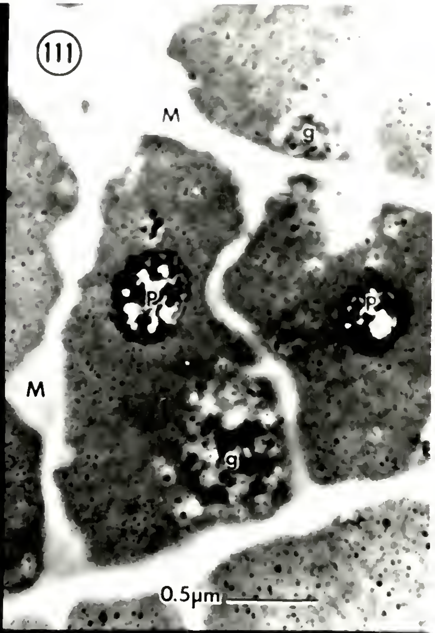
(111)

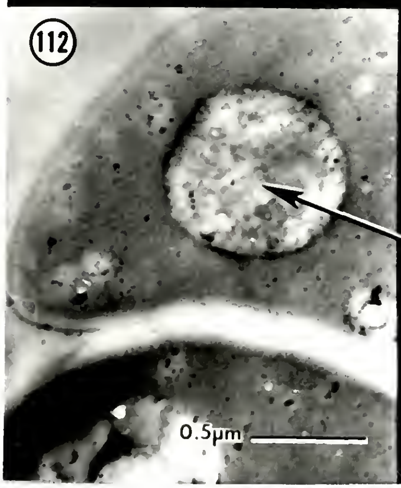
(112)

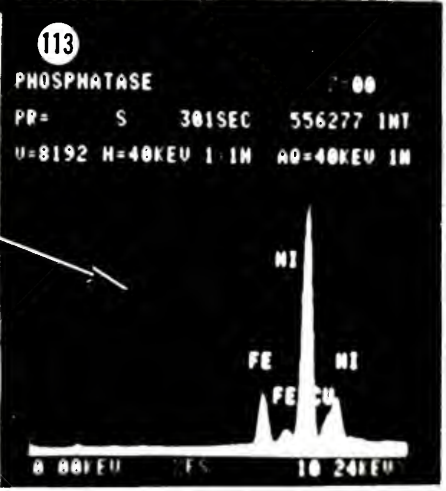
(113)

Figures 114-117. Enzymatic treatments of thin sections.

Fig. 114. Section of Ms. mazei strain S6 treated with pullulanase followed with alpha and beta amylase contain intact granules. Sections treated with cullulase were similar.

Fig. 115. Control section of Dictyostelium treated with amylase lacks the glycogen storage granules (*).

Fig. 116. Control section of embedded filter paper to test for cellulase activity after etching.

Fig. 117. Control section for cellulase activity after cellulase treatment. The filter paper is removed from the section (*).

g= granules

r= resin

(114)

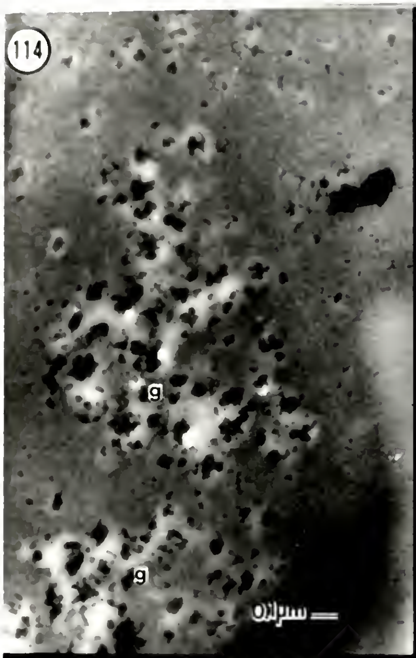

(115)

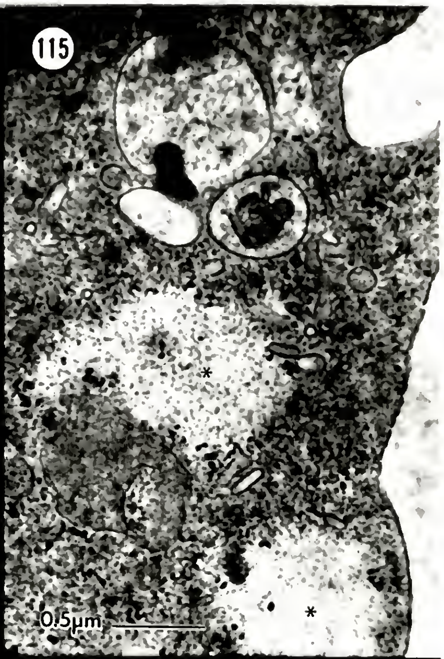

(116)

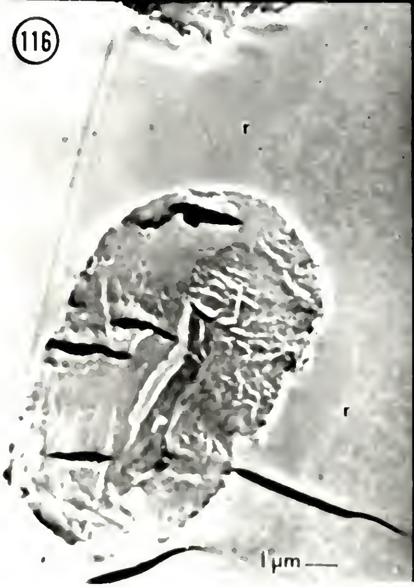

(117)

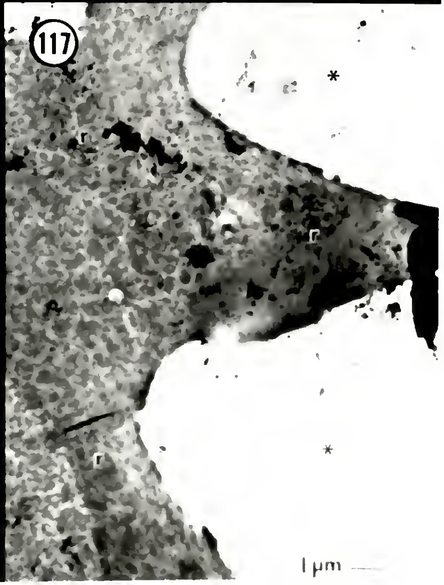

CHAPTER 5

DISCUSSION

This is the first report on the ultrastructure of the developmental cycle of Ms. mazei. Described developmental cycles or "life cycles" in archaebacteria are rare and generally limited to the genus Methanosarcina. The complex life cycle involving the release of single cells may provide a mechanism for cell dispersal during unfavorable growth conditions while the limited cycle would facilitate colony division during growth in favorable conditions.

Results of this study show that single cells of Ms. mazei can be released via two different mechanisms (Fig. 118). When strain S6 is in stationary phase, the matrix material begins to degrade causing the colony to disaggregate into single cells. Alternatively, strain LYC grown at pH 6.0 presumably produces an enzyme that is inactive until the pH is raised to 7.0, then the matrix material at the periphery of the colony begins to degrade. This results in a slow sequential release of single cells. Introduction of the supernatant from strain LYC will also disrupt colonies of strain S6 in a similar fashion (Liu et al. 1985).

Fig. 118 LIFE CYCLE FOR METHANOSARCINA MAZEI

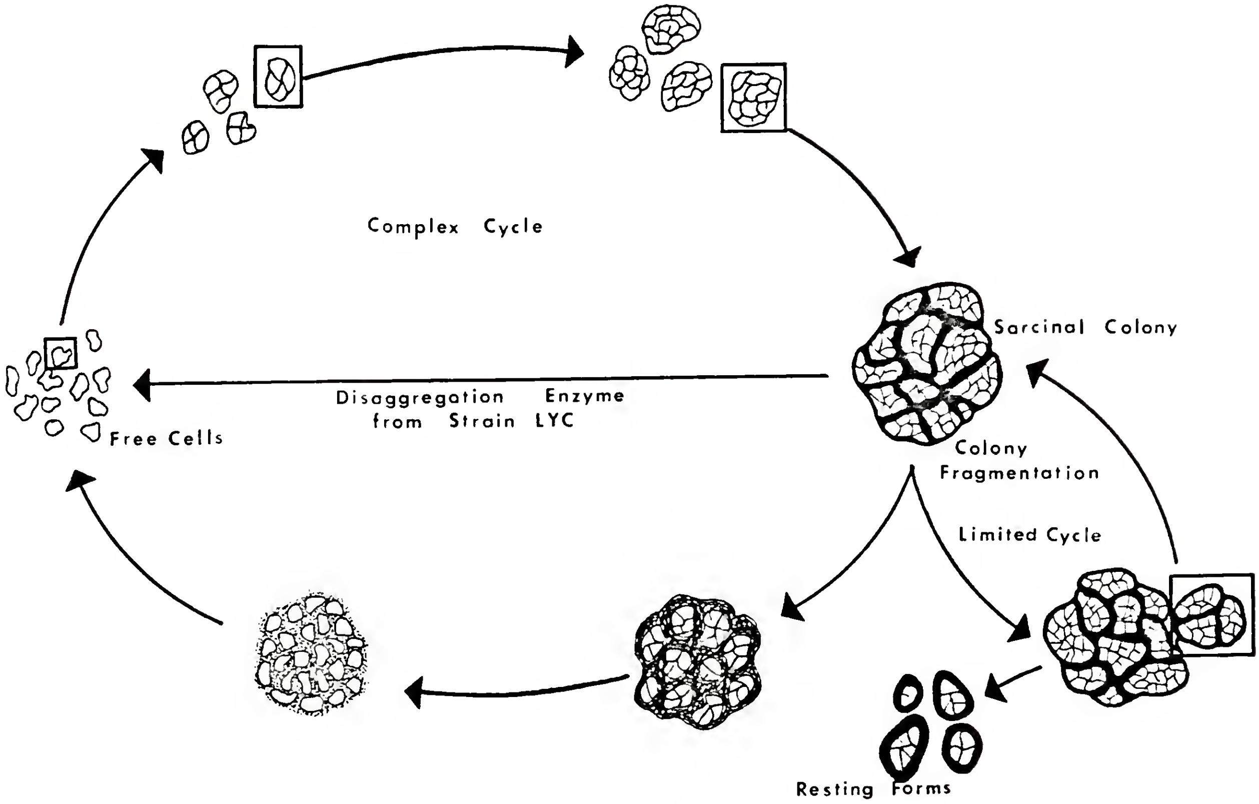

The colony disaggregation reported by Mah (1980) using light microscopy is explained mechanistically at the ultrastructural level through changes in the matrix enclosing the cells. As the matrix degrades into a loose fibrillar network, the cells become less tightly associated within the colony. A layered arrangement of the matrix is apparent as it sheds from the cells. When colonies reach a critical point during disaggregation, slight pressure from a cover slip as reported by Mah (1980) will dislodge individual components. If colonies are left undisturbed, the matrix may degrade sufficiently to release single cells. Although Mah reported that a "cyst wall" ruptures when single cells of _Ms. mazei_ strain S6 are released, no structure was observed at the ultrastructural level enclosing the colonies. Since he had observed a "cyst wall" in cultures grown on agar, cells grown on agar were examined thin sections (data not shown). Again, a structure was not apparent surrounding the colonies. It is possible that the "cyst wall" may be a layer of waste material that accumulates when cells are grown on agar and this is normally washed away in broth grown cultures. However, in examining thin sections of digester samples, groups of cells which are similar to _Ms. mazei_ have been observed with a definite enclosing layer (personal observations). Thus, the presence of a cyst wall may depend on environmental conditions.

When viewed with UV and light microscopy (Fig. 4), single cells of Methanosarcina mazei strain S6 resembled those described by others for Ms. mazei (Mah 1980, Touzel and albanac 1983), Methanosarcina TM-1 (Zinder and Mah 1979), Ms. acetivorans (Sowers et al. 1984a), and the single cells reported by Zhilina and Zavarzin (1976) for biotype 3. They are similar except for motility to the methanogenic marine cocci studied thus far (Ferguson and Mah 1983, Huber et al. 1982, Jones et al. 1983, Konig and Stetter 1982, Rivard et al. 1983, Rivard and Smith 1982, Romesser et al. 1979, Sowers and Ferry 1983). They are irregular, non-motile, gram-negative, and display a blue-green fluorescence that quenches within a few seconds.

The ultrastructure of the single cells of Ms. mazei has not been reported with the possible exception of Methanosarcina biotype 3 described by Zhilina and Zavarzin (1979c). They describe single cells approximately 1.0 µm in diameter enclosed by a "microcapsule" of varying thickness which probably corresponds to remaining matrix material. A cell wall near the protoplasm is described but is difficult to discern. This may be identical to the protein layer observed in strain S6 that is just outside the plasma membrane (Figs. 9-11). The existance of a protein layer in the Methanosarcineae was first proposed by Sowers et al. (1984) based on the antigenic cross reactivity observed with several marine methanogens that possess a protein wall, and the matrix-containing Methanosarcinae.

The layer in Ms. mazei strain S6 is demonstrated here to be composed of protein by protease digestion in whole colonies (before fixation, Figs. 92-96), single cells (after fixation, Figs. 97-99), and embedded colonies in thin sections (Figs. 100-105). Also, this layer does not stain with silver methenamine (Figs .86 and 87) indicating the absence of reducing sugars that are present in the matrix. For Ms. mazei strain S6, single cells are irregular and possess a cell surface that is very similar to the methanogenic marine cocci that have a protein layer of regular size in close association with the plasma membrane and lack a heteropolysaccharide wall (see references above). The thickness of the protein layer varies slightly between 10-15 nm for most species. In thin sections of Ms. mazei strain S6, the protein layer appears to shed from the surface as strands (Figs. 8-11) and a few cells are nearly devoid of this layer. A membranous appearance is observed in some of the material shedding from the surface (Fig. 8). This implies that the tubules are shedding along with the protein layer. In micrographs of Ms. acetivorans, material also appears to be shedding from the protein layer (Sowers and Ferry 1984a). This shedding is not evident in the reports of other marine methanogens (see references above) and may be restricted among the archaebacteria to cells of the Methanosarcineae. Protein shedding is common from eubacterial gram-positive bacteria that possess protein layers outside the peptidoglycan layer. (Thornley 1975, Sleytr 1978).

This is the first report on events that occur during division of a methanogenic coccus (Figs. 12-19). In the light microscope and scanning electron microscope, the first division gives rise to two equal daughter cells. In thin sections, the second division is also somewhat symmetrical giving rise to tetrads. These have a spherical surface due to the packing of matrix material. Zhilina and Zavarzin (1979) describe a similar cellular arrangement for their biotype 3 that they called "pseudococci" because it appeared to be one large cell in the light microscope. With Ms. mazei strain S6 the first two division planes have a symmetry similar to the divisions observed in the eubacterial sarcinae (Holt & Canale-Parola 1967, Sleytr 1978, Thornley _et_ _al_. 1965). However, the similarity is superficial since the matrix has a much more fibrous nature than a gram-positive wall, and a protein layer separates the matrix from the plasma membrane. The subsequent divisions are asymmetrical, thus preventing the formation of regular packages of cells as seen in the eubacterial sarcinae. Also, the cells do not separate until the colony is larger (Figs. 20-25).

The ultrastructure of sarcinal colonies has been reported using SEM for agar grown strains of _Ms. barkeri_ (Mah _et_ _al_. 1978, Mah 1981) and _Ms. mazei_ (Mah 1981). They are similar to the SEM micrographs presented here (Figs. 24 and 25) except that the matrix is thinner on the colony surface because the cells were grown on agar and individual cells are easier to discern.

The general ultrastructure of intact sarcinal colonies of _Ms. mazei_ strain S6 growing in the limited cycle did not differ significantly from other reports on the freshwater Methanosarcineae. Colonies display a pseudoparenchymal morphology with random division planes (Fig. 26). Previous reports differ in morphological details such as matrix thickness, and the presence or absence of various inclusion bodies. These include the electron dense granules, polyphosphate-like bodies, vacuoles, protein arrays, and the cylindrical core-like structures (see below). Overall, these differences may be related more to different growth conditions rather than to genetic differences between isolates.

The morphology of sarcinal colonies in thin sections of M. mazei strain S6 differed depending on which cycle the cultures were undergoing when harvested. Sarcinal colonies that developed from single cells during the complex cycle had a large number of tubules in localized areas between the cell surface and the matrix (Figs. 26-37). Similar specialized membranous structures associated with the plasma membrane have been called plasmalemmasomes in the fungi (Kahn 1976, Marchant and Moore 1973) and mesosomes in bacteria (Burdett and Rogers 1972, van Iterson 1984). Both of these structures are believed to have specialized functions and may be involved with membrane storage. However, these structures are found in the cytoplasm under the inner surface of the plasma membrane while the structures described here are on the cell surface.

In freeze-fracture replicas, specialized structures closely associated with the plasma membrane sometimes contain neatly packaged material in strands approximately the same thickness as the tubules (Figs. 83-85). The structures with the coiled thread-like appearance (Fig. 85) may be a close packing of the tubules. This may represent the "natural state" since the freeze-fractured cells are quick frozen and do not show the artifactural damage that may be induced during preparation for thin sectioning. The specialized structures appear similar to fractures of plasmalemmasomes observed in the fungi by Marchant and Moore (1973). Freeze-fracture analysis did not reveal the cell surface or the membrane tubules, however, it is common for fracture planes to miss protein layers (Sleytr and Robards 1983).

The number of tubules increased as the colonies aged indicating that synthesis continues throughout the life cycle. Sarcinal colonies that developed from the variant strain S6 that only exhibited the limited life cycle showed small amounts of this material which remained at a relatively low level during colony growth (Figs. 50-63). Since single cells are not released by these colonies, any benefits that these tubules have for the cell may be diminished by the persistence of the matrix and the cells may be synthesizing less of this material. Indeed, all of the freshwater Methanosarcina strains reported in the literature, except for biotype 3 (Zhilina and Zavarzin 1979c) which may be a strain of Ms. mazei, resemble the sarcinal colonies of this variant of strain S6 rather than colonies which can undergo the complex life cycle. Since other investigators did not include an ultrastructural investigation of colony development or high magnifications of the cell surface, it is difficult to observe subtle differences in the cell surfaces of these strains. However, the gross morphology of the colonies does not differ very much in these reports and it can be assumed that the cell surface is not as dynamic as observed in the complex life cycle of strain S6.

The cell surface does have a profound effect during the life cycle of the single marine *Methanosarcina* studied (Sowers *et* *al*. 1984). Single cells of *Ms. acetivorans* which are similar to *Ms. mazei* strain S6 have a protein wall 10 nm thick. Cultures of *Ms. acetivorans* divide and grow as single cells in log phase growth but aggregate in stationary phase to form communal cysts. These are enclosed by a cyst wall 6 nm thick that appears similar to the protein wall surrounding individual cells. The communal cysts differ from sarcinal colonies because they lack a matrix and develop from the aggregation of cells rather than from the multiplication of a common mother cell.

Cytochemical analysis of the matrix reveals a general polysaccharide nature by staining with silver methenamine (Figs 86-87). Further analyses using fluorescein and gold-labelled lectins demonstrate the location of N-acetylgalactosamine in the matrix (Figs. 89 and 90). Indeed, subsequent chemical analyses of the isolated matrix performed by Bleiweis and Hurst (in Robinson _et al_. 1985) reveal the major polymer to consist of equimolar amounts of N-acetylgalactosamine and galacturonic acid. They did not detect polymers containing glucuronic acid, although preliminary analyses showed the presence of this acid in the matrix. Destruction of this moiety during acid hydrolysis or exclusion of glucuronic acid-containing polymers during preparative procedures is possible.

_Ms_. _mazei_, therefore, does not possess a eubacterial cell wall containing murein or a typical methanogenic wall containing pseudomurein (Kandler & Koenig 1978, and Koenig and Kandler 1979a), and extensive peptide cross linkages were not found in the matrix. Instead, it consists of polyuronides. These are viscous, negatively charged polymers that promote adherence between adjacent cells and would explain the extensive colonization shown above.

Freeze-fracture replicas of _Ms. mazei_ S6 and _Ms. barkeri_ 227 reveal fracture planes that preferentially pass through the cytoplasm rather than the hydrophobic region of the plasma membrane (Figs 76-86). This has also been reported by Doddema et al. (1979) when they tried to fracture Mb. thermoautotrophicum, and by Sprott et al. (1984) working with Mb. bryantii. Neither of these groups obtained fracture planes through the plasma membrane. Only Jones et al. (1977) managed to get cleavage planes through the plasma membrane of Mc. vannielii. It has been suggested that the ratio of C_{40} to C_{20} diether lipids may influence the ability of the frozen membranes to fracture (Langworthy et al. 1982, Sprott et al. 1984). C_{40} lipids which have only been found in the arechaebacteria, cross the entire membrane and would presumably provide more structural rigidity (Langworthy et al. 1982). Fifty-five percent of Mb. thermoautotrophicum membranes are of the C_{40} type while Mc. vannielii contains only the C_{20} type lipids (Langworthy 1982). The plasma membrane of Ms. barkeri also contains only C_{20} lipids. No data are available of Ms. mazei lipid composition but there does seem to be a correlation between membrane lipid composition and the ability for the membrane to fracture. Also, when these membranes do fracture there may be more damage during the fracturing process. As the resistance to the fracture plane increases due to transmembrane covalent bonds (protein and lipid) there is a greater amount of localized heat generated. This may affect the final conformation of the membrane particles (Sleytr & Robards 1982). Covalent bonds may also be introduced if the cells are fixed with glutaraldehyde before freezing. The fact that these cells were quick frozen with a propane jet without fixation may have increased the number of membrane cleavages obtained.

Plasma membrane particle density for Ms. mazei and Ms. barkeri are approximately the same and are similar to the particles found in the plasma membrane of Mc. vannielii (Jones et al. 1977 , Figs. 78-81). The particle size is approximately the same at 9-14 nm for all three and specialized areas where the particles are arranged in regular arrays are similar. The protein arrays are presumed to reflect functional differentiation sites (Jones et al. 1977).

The granule containing cores observed in young sarcinal colonies (Figs 52-55) do not resemble any of the common bacterial inclusions described thus far (see reviews by Shively 1974 and van Iterson 1984). Initially, the possibility that they were pairs of collapsed gas vacuoles was investigated. Gas vacuoles have been described for several isolates of Methanosarcina (Archer & King 1983 & 1984, Zhilina 1979b). These do easily collapse and appear in thin section as pairs of closely opposed membranes (Walsby 1972).

However, the cores are much larger and are shown to be cylindical in cross and serial sections (D. Williams, personal communication). The exact nature of the cores is unclear. They appear to consist of two membranes with a trilamellar unit structure. The cores nearly bisect the cytoplasm and are in close association with the plasma membrane. The ends are not clearly resolved but they apparently are not attached to the plasma membrane (Fig. 57). The second type of core structure does not contain granules and is continuous with the plasma membrane and protein layer. Grazing sections indicate a regular helical arrangement around the core.

Cores have been described in Streptococcus by Coleman and Bleiweis (1975). They are common depending on the growth conditions of the cells. However, these are up to three times the diameter and have a thicker surface than the cores described here. They do not contain granules and are disrupted when the pH is higher than 6.5. The cores contain mostly protein and their function is unknown.

The function of the granule-containing cores is also unknown but since the granules are smaller and more uniform in size than the cytoplasmic granules, they may be involved in the sequestering of storage material during granule formation. Although they were observed in pure cultures of *Ms. mazei* strain S6 in less than 1% of the cells in thin section, they are much more prevalent in mixed cultures. Thin sections of digester samples have been observed where nearly 75% of the methanosarcinal cells possess one or more of the granule-containing cores (personal observation).

An attractive function for the cores would be for localized sites of methane production. Extensive internal membrane systems not associated with division such as mesosomes, are restricted to the photosynthetic (Holt & Marr 1966), nitrifying (Murray & Watson 1965), and the methane-oxidizing bacteria (Smith & Ribbons 1970a and b). Less complex internal membranes are more common in many bacteria and were first described in the methanogens by Landenberg *et al*. (1968). These were suggested to play a role in methane production by Zeikus and Wolfe (1973) who examined the fine structure of *Methanobacterium thermoautotrophicum* and found internal membrane structures typically consisting of three layers of closely packed concentric rings. This idea was expanded by Dodemma *et al*. (1979) using tetrazolium dyes on *Mb. thermoautotrophicum* to act as hydrogen acceptors for hydrogenase. The reaction products were shown in thin sections to be localized on internal membranes. However, these membranes have not been isolated and the specificity of the staining techniques is uncertain (Sprott et al. 1984). Similar internal membranes were later observed by other investigators in Mb. thermoautotrophicum (Sauer et al. 1980, Sprott et al. 1984), Methanospirillum hungatei (Zeikus & Bowen 1975), Methanogenium marisnigri (Romesser et al. 1979), and Methanothermus fervidus (Stetter et al. 1981).

Recently, the term "methanomitochondrion" was used to describe internal membranes which might be sites for methane production (Kell et al. 1981). Biochemical studies on cell extracts indicate that methane synthesis from CO_2 occurs in the particulate fraction (Sauer et al. 1977, 1980, 1981, Spencer et al. 1980). However, it is difficult to differentiate plasma membrane from internal membranes in these preparations. There is considerable debate over the existence of this "organelle" due to inconsistencies in observing internal membranes (Sprott et al. 1984). They are lacking in many recently described genera (Huber et al. 1982, Konig & Stetter 1982, Jones et al. 1983, Sowers & Ferry 1983) and they have been shown to increase or decrease in number depending on growth conditions and the culture strain used (Sprott et al. 1984). Thus, the presence of specialized internal membranes (or "methanomitochondrion") for methane production is in doubt.

Ultrastructurally, there is no evidence that the cores are sites for methane production. In exponential growth phase cultures, they ussually possess the electron dense granules which are probably storage products (see below) that may not be involved with methane production. Also, although the ends of the granule-containing cores have not been clearly demonstrated, they may open out to the cytoplasm and not form a closed vescicle which would be required for organelle function (Spencer *et al*. 1980). The granule-containing cores in *Ms. mazei* grown on acetate are observed in less than 1% of the cells in thin sections and are rarely observed in cells grown on methanol or trimethylamines. It is more likely they are involved in granule synthesis since the enclosed granules are smaller than the free cytoplasmic granules. Also, in this respect they would not be required at all times during the life cycle.

The electron dense granules described here for *Ms. mazei* and *Ms. barkeri* strain 227 are characteristic for the Methanosarcinaceae. The rough margins with an electron transparent halo distinguish them from other types of inclusions seen in the archaebacteria. They are usually found in groups, and in cells where they are numerous, the groups become compact. Granules approximately 50 nm in size are described for *Ms. hungatei* (Zeikus & Bowen 1975) but these are of low electron density and appear globular. Similar sized granules described as "glycogen-like" were also found in *Mc. vannielii* (Jones *et al*. 1977). These have electron transparent margins which are smoother than those described here. Also, the granules in *Mc. vanneilii* were only found in agar grown cells.

It is doubtful that the granules described here for *Ms. mazei* are glycogen, or possess a high concentration of other carbohydrates with cross linkages that would be susceptible to alpha and beta amylase, pullulanase or cellulase since they are not extracted from thin sections by these enzymes. Although they stain with silver methenamine, it should be noted that silver staining is indicative for reducing sugars but is not specific and will stain sulfhydryl groups (Swift 1973) and possibly other reducing sites present in the tissues (Lewis and Knight 1977). Scherer and Bochem (1979a) analyzed the granules in *Ms. barkeri* and found phosphorus, calcium, and iron. X-ray analysis of the granules in *Ms. mazei* shows the same composition as the cytoplasm, but this may be due to a concentration of granular material too low to be detected with the procedure used here.

Polyphosphate bodies are common in the eubacteria, fungi, and algae (see reviews by Harold 1966 and by Shively 1979). Polyphosphate-like bodies are found in the archaebacteria in the genera *Methanolobus*, and *Methanoplanus* (Koenig & Stetter 1982, Wildgruber *et al.* 1982), and in *Methanosarcina*. The electron dense nature, smooth surface, and lack of enclosing membranes are characteristics of polyphosphate bodies (Shively 1974). Another electron dense smooth storage body found in *Beggiatoa* can be distinguished from polyphosphate because it is membrane bound and contains mostly sulfur (Strohl *et al.* 1981). Webster *et al.* (1984) used X-ray microanalysis to determine the partial elemental composition of eubacterial inclusions including polyphosphate (volutin or metachromatic granules) and poly-beta-hydroxy-butyrate. They found poly-beta-hydroxybutyrate to be electron transparent and give a low energy spectrum. When they analysed the electron dense polyphosphate they found phosphorus, potassium, and calcium. The elemental composition of polyphosphate bodies in algae and fungi also includes phosphorus, potassium, calcium, along with smaller amounts of magnesium, and sulfur (Doonan *et al.* 1979).

Scherer and Bochem (1983a) analyzed twelve strains of *Methanosarcina* at the ultrastructural level and found polyphosphate-like bodies to be common. Using X-ray microanalysis they demonstrated that the granules and polyphosphate-like bodies have the same elemental composition, with energy peaks corresponding to phosphorus, calcium, and iron, with phosphorus predominating. The findings here with X-ray analysis of the polyphosphate-like bodies from Ms. mazei only show energy peaks corresponding to phosphorus and calcium (Figs 110-113). Iron was not detected. In another study, Scherer and Bochem (1983b) determined that heavy metals (Cd, Pb, & Cu) added to the growth medium are sequestered in the granules and polyphosphate-like bodies. Thus, differences in elemental composition may reflect differences in the growth medium or culture age. Enzyme treatments of thin sections indicate that the phosphorus is present as phosphate by the partial removal of the polyphosphate-like bodies (Figs. 106-109). X-ray analysis of the phosphatase treated cells shows that all of the detectable phosphorus has been removed.

Due to the results obtained here showing extraction of the inclusions using phosphatase and the elemental studies here and by Scherer and Bochem (1983a), the term "polyphosphate" probably is correct when describing the larger electron dense inclusions. Other inclusion bodies that are commonly called polyphosphate have been shown to also contain calcium, potassium, and magnesium (Shively 1979). These other elements should probably not be considered significant when referring to the inclusions as polyphosphate.

The mechanism of polyphosphate formation is unknown but there are several theories. Jensen (1969) suggests a cytoplasmic clearing is followed by deposition of electron dense material. Voelz *et al*. (1966) propose that long polymers precipitate onto cytoplasmic components which contract into granules. The reticular pattern of the polyphosphate bodies in strain S6 that remains after phosphatase digestion may be the cytoplasmic components proposed by Voelz. However, the polyphosphate bodies described here for *Ms. mazei* may not form from the precipitation of long polyphosphate polymers. They probably form by the pooling of cytoplasmic granules (Figs. 27-30). When only a few granules are present they tend to be scattered throughout the cytoplasm of cells in sarcinal colonies or along the periphery in free single cells. When they increase in number, they pool together in tight associations. These could coalesce to form the smooth round inclusions. Also, elemental analysis by Scherer and Bochem (above) shows the same elemental composition for the granules and polyphosphate bodies.

Sarcinal colonies of Ms. mazei strain S6 that remain in stationary phase for longer than three months contain several morphotypes of viable looking cells that appear to be resting forms (Figs. 64-66). These are surrounded by matrix material that is thicker than that observed in younger cultures. While investigating cell death in Methanosarcina exposed to air, Zhilina (1972) found specialized cyst-like forms under light microscopy. These were larger than vegetative cells and appeared more dense. Zhilina and Zavarzin (1979c) later described a "microcyst" at the ultrastructural level that is a single cell surrounded by a thick specialized wall. They do not speculate that this may be the same structure observed earlier in the light microscope. Here the term "resting form" is used based on six observations 1) they do not resemble "endospores" described for Methanobacterium strain M.o.H (Steyn et al. 1980) or typical eubacterial spores; 2) cultures remain viable for over six months; 3) these viable looking cells are present in thin sections of year-old cultures; 4) they have a thicker cell covering than vegetative cells (probably Zhilina's "microcyst"); 5) they occur as several different morphotypes; and 6) The cultures are more tolerant to oxygen exposure than other methanogens. This last observation was the focus of a study by Kiener and Leisinger (1983) who examined the oxygen sensitivity of several methanogens. *Ms. barkeri* was found to withstand up to 30 hrs exposure to air. They believed this was due to the large sarcinal arrangements of cells that would slow oxygen diffusion to the center of the colony. Also, they noted that several methanogenic cofactors are very oxygen sensitive and that oxygen exposure may be more bacteriostatic than bacteriocidal for these cells. Three of the methanogenic species they found to be the most aerotolerant were *Ms. barkeri*, *Mb. arboriphilus*, and *Mb. thermoautotrophicum*. All three were originally isolated from digester environments where they would periodically be exposed to oxygen stress during digester charging or draining. The large sarcinal colonies probably do provide some protection from oxygen diffusion but the existence of resting forms could also provide for long term survival during oxygen exposure or nutrient depletion. Parkin *et al*. (1983) found that if digesters poisoned by toxic heavy metals were left undisturbed they would regenerate after a lag period of up to six months. This may be due to the persistence of resting forms in the digesters and the ability of *Methanosarcina* to sequester heavy metals rom the environment. In a fixed bed digester where there are no 5, 10, or 90-day cultures; colonies are immobilized in a biofilm and regions are found, usually at the colony periphery, where cells appear similar to 5-day pure cultures. Also, there are areas, usually toward the colony center, where cells appear similar to older cells observed in pure culture (Bochem _et_ _al_. 1982, Robinson _et_ _al_. 1984, personal observations). Thus, with colonies simultaneously exhibiting various stages of development, resting forms may be present in digesters in low numbers all the time.

There is a difference of morphology between the sarcinal colonies in pure culture and the colonies found in digester samples or mixed enrichment samples. Colonies embedded in digester biofilms (Robinson _et_ _al_. 1984) and enrichments (Bochem _et_ _al_. 1982) simultaniously exhibit the characteristics of young and old colonies examined in pure cultures. The colonies in mixed cultures are very large and possess a central cavity. This form corresponds to Zhilina's Type I (Fig. 2) that has a central pore for gas evolution. This morphotype was not observed in this study and has not been described for pure cultures of _Methanosarcina_. While this morphotype is rare or non-existant in pure cultures, it may be the predominating cellular arrangement in the environment.

So far, the complex life cycle has only been described (or implied by the presence of single cells) for *Ms. mazei* which presently includes strains S6 (Mah 1980), MC6 (Touzel & Albanac 1983), and LYC (Mah 1985). The undesignated *Methanosarcina* strains MB (Ollivier *et al*. 1984) and biotype 3 (Zhilina & Zavarzin 1979c) should also be included in this list. *Ms. acetivorans* undergoes a reverse life cycle described above. *Ms. barkeri* is apparently restricted to the limited cycle which can also be observed in *Ms. mazei*.

The transition in *Ms. mazei* strain S6 from colonial forms to single cells is triggered by unkown factors. If the inducing conditions are found (carbon/nitrogen ratio, pH, etc.), then large numbers of single cells could be harvested for fractionation. The exact composition of the inclusions and the amino acid content of the protein layer could then be determined. Alternatively, the disaggregation enzyme produced by *Ms. mazei* strain LYC (Liu *et al*. 1985) holds promise by allowing one to directly manipulate the life cycles of several strains of *Methanosarcina*.

Future work with *Ms. mazei* should examine the effects of different growth media on the cellular ultrastructure. Specifically, the presence and concentration of the cytoplasmic granules and polyphosphate inclusions may be related to the concentration of phosphorus or nitrogen available at different stages of the life cycle. If the granules are carbohydrate storage sites, as suggested by Murray *et al*. (1984), then they should increase in number under nitrogen limiting conditions. If, however, they are precursors to the polyphosphate bodies as implied here, then their number should change depending on the phosphorus concentration. Ultimately, the granules and polyphosphate bodies should be isolated so their chemical structure can be directly determined.

REFERENCES

Ad Hoc Committee of the Judicial Commission of the International Committee on Systematic Bacteriology. 1976. First draft. Approved lists of bacterial names. Internat. J. System. Bacteriol. 26:563-599.

Anderson W. A., and J. Andre. 1968. The extraction of some cell components with Pronase and pepsin from thin sections of tissue embedded in an epon-araldite mixture. J. Microscopie 7:343-354.

Archer, D. B., and N. R. King. 1983. A novel ultrastructural feature of gas vacuolated Methanosarcina. FEMS Microbiol. Lett. 16:217-223.

Archer, D. B., and N. R. King. 1984. Isolation of gas vesicles from Methanosarcina barkeri. J. Gen. Microbiol. 130:167-172.

Balch, W. E. 1982. Methanogens: their impact on our concept of prokaryote diversity. Zentralb. Bakteriol. Parasitenkd. Infektionskr. Hyg., I. Abt. Orig. Reihe C, 3:295-303.

Balch, W. E., G. E. Fox, L. J. Magrum, C. R. Woese, and R. S. Wolfe. 1979. Methanogens: reevaluation of a unique group of bacteria. Microbiol. Rev. 43:260-296.

Barker, A. 1936. Studies upon the methane producing bacteria. Arch. Microbiol. 7:420-438.

Bochem, H. P., S. M. Schoberth, B. Sprey, and P. Wengler. 1982. Thermophilic biomethanation of acetic acid: morphology and ultrastructure of a granular consortium. Can. J. Microbiol. 28:500-510.

Burdett, I. D. J., and H. J. Rogers. 1972. The structure and development of mesosomes studied in Bacillus licheniformis. J. Ultrastruct. Res. 38:113-133.

Cheeseman, P., A. Toms-Wood, and R. S. Wolfe. 1972. Isolation and properties of a fluorescent compound, factor 420, from Methanobacterium strain M.o.H. J. Bacteriol. 112:527-531.

Coleman, S. E., and A. S. Bleiweis. 1975. Ultrastructural, physiological, and cytochemical characterization of cores in group D Streptococci. J. Bacteriol. 129:445-456.

Daniels, L., R. Sparling, and G. D. Sprott. 1984. Bioenergetics of methanogenesis. Biochim. Biophys. Acta. 768:113-163.

de Martino, C., and L. Zamboni. 1967. Silver methenamine stain for electron microscopy. J. Ultrastuct. Res. 19:273-282.

Doddema, H. J., C. van der Drift, G. D. Vogels, and M. Veenuis. 1979. Chemiosmotic coupling in Methanobacterium thermoautotrophicum: hydrogen-dependent adenosine 5'-tripphosphate synthesis by subcellular particles. J. Bacteriol. 140:1081-1089.

Doonan B. B., R. E. Crang, T. E. Jensen, and M. Baxter. 1979. In situ X-ray energy dispersive microanalysis of polyphosphate bodies in Aureobasidium pullulans. J. Ultrastr. Res. 69:232-238.

Erlandsen, S. L., J. A. Parsons, and C. B. Rodning. 1979. Technical parameters of immunostaining of osmicated tissue in epoxy sections. J. Histochem. Cytochem. 27:1286-1289.

Ferguson T. J., and R. A. Mah. 1983. Isolation and characterization on an H_2-oxidizing thermophilic methanogen. Appl. Environ. Microbiol. 45:265-274.

Fox, G. E., L. J. Magrum, W. E. Balch, R. S. Wolfe, and C. R. Woese. 1977. Classification of methanogenic bacteria by 16S ribosomal RNA characterization. Proc. Nat. Acad. Sci. U.S.A. 74:4537-4541.

Fox, G. E, E. Stackebrandt, R. B. Hespell, J. Gibson, J. Maniloff, T. A. Dyer, R. S. Wolfe, W. E. Balch, R. S. Tanner, L. J. Magrum, L. B. Zablen, R. Blakemore, R. Gupta, L. Bonen, B. J. Lewis, D. A. Stahl, K. R. Luehrsen, K. N. Chen, and C. R. Woese. 1980. The phylogeny of prokaryotes. Science 209:457-463.

Frens, G. 1973. Controlled nucleation for the regulation of the particle size in monodisperse gold suspensions. Nature Phys. Sci. 241:20-22.

Harold, F. M. 1966. Inorganic polyphosphates in biology: structure, metabolism, and function. Bacteriol Rev. 30:772-794.

Holt, C. S., and E. Canole-Parola. 1967. Fine structure of Sarcina maxima and Sarcina ventriculi. J. Bacteriol. 93:399-410.

Horisberger, M., J. Rosset, and H. Bauer. 1975. Colloidal gold granules as markers for cell surface receptors in the scaning electron microscope. Experientia 31:1147.

Horisberger, M., and J. Rosset. 1977. Colloidal gold, a usefull marker for transmission and scanning electron microscopy. J. Histochem. Cytochem. 25:295-305.

Huber, H., M. Tomm, H. Koenig, G. Thies, and K. O. Stetter. 1982. Methanococcus thermolithotrophicus, a novel thermophilic lithotrophic methanogen. Arch. Microbiol. 132:47-50.

Jensen, T. E. 1969. Fine structure of developing polyphosphate bodies in a blue-green alga, Plectonema boryanum. Arch. Mikrobiol. 67:328-338.

Jones, J. B., B. Bowers, and T. C. Stadtman. 1977, Methanococcus vannielii: Ultrastructure and sensitivity to detergents and antibiotics. J. Bacteriol. 130:1357-1363.

Jones, J. B., J. A. Leigh, F. Mayer, C. R. Woese, and R. S. Wolfe. 1983. Methanococcus jannaschii sp nov., an extremely thermophilic methanogen from a submarine hydrothermal vent. Arch. Microbiol. 136:254-261.

Jones, W. J., M. J. B. Paynter, and R. Gupta. 1983. Characterization of Methanococcus maripuludis sp nov., a new methanogen isolated from salt marsh sediment. Arch. Microbiol. 135:91-97.

Kandler, O. 1982. Cell wall structure and their phylogenetic implications. Zentralb. Bakteriol. Parasitenkd. Infektionskr. Hyg., I. Abt. Orig. Reinhe C, 3:149-160.

Kandler, O., and H. Hippe. 1977. Lack of peptidoglycan in the cell walls of Methanosarcina barkeri. Arch. Microbiol. 113:57-60.

Kandler, O., and H. Koenig. 1978. Chemical composition of the peptidoglycan-free cell walls of methanogenic bacteria. Archiv. for Microbiol. 118:141-152.

Karnovsky, M. J. 1965. A formaldehyde-glutaraldehyde fixative of high osmolarity for use in electron microscopy. J. Cell Biol. 27:137A.

Kell, D. B., H. J. Doddema, J. G. Morris, and G. D. Vogels. 1981. Energy coupling in methanogens. Microb. Growth C-1 Compd. Proceed. Int. Symp. 1981. Edited by H. Dalton. Heyden & Sons, Ltd. London. pp 159-170.

Khan, S. 1976. Paramural bodies of Albugo candida. Archiv. Microbiol. 109:271-275.

Kiener, A., and T. Leisinger. 1983. Oxygen sensitivity of methanogenic bacteria. System. Appl. Microbiol. 4:305-312.

Kluyver, A. J., and C. B. van Niel. 1936. Prospects for a natural system of classification of bacteria. Zentralbl. Bakteriol. Parasitenkd. Infektionskr. Hyg. Abt. Orig. Reihe C, II. 94:396.

Koenig, H., and O. Kandler. 1979. N-acetyltalosaminuronic acid a constituent of the pseudomurein of the genus Methanobacterium. Arch. Microbiol. 123:295-299.

Konig, H., R. Kralik, and O. Kandler. 1982. Structure and modifications of the pseudomurein in Methanobacteriales. Zentalb. Bakteriol. Parasitenkd. Infektionskr. Hyg., I. Abt. Orig. Reihe C, 3:179-191.

Koenig, H., and K. O. Stetter. 1982. Isolation and characterization of Methanolobus tindarius, sp. nov., a coccoid methanogen growing only on methanol and methylamines. Zentralb. Bakteriol. Parasitenkd. Infektionskr. Hyg., I. Abt. Orig. Reihe C, 3:478-490.

Landenberg K. F., M. P. Bryant, and R. S. Wolfe. 1968. Hydrogen-oxidizing methane bacteria. II. Electron microscopy. J. Bacteriol. 95:1124-1129.

Langworthy, T. A., T. G. Tornabene, and G. Holzer. 1982. Lipids of the archaebacteria. Zentralb. Bakteriol. Parasitenkd. Infektionskr. Hyg., I. Abt. Orig. Reihe C, 3:228-244.

Lewis, P. R., and D. P. Knight. 1977. Staining Methods for Sectioned Material. In Practical Methods in Electron Microscopy Edited by A. M. Glauert. North-Holland Pub., New York. p. 101.

Liu, Y, D. R. Boone, R. Sleat, and R. A. Mah. 1985. *Methanosarcina mazei* strain LYC, a new methanogenic isolate which produces a disaggregating enzyme. Appl. Environ. Microbiol. 49:608-613.

Mah, R. A. 1980. Isolation and characterization of *Methanococcus mazei*. Curr. Microbiol. 3:321-326.

Mah, R. A. 1981. The Methanogenic Bacteria, Their Ecology and Physiology. In Trends in the Biology of Fermentations for Fuels and Chemicals. Edited by A. Hollaender. Plenum Press, New York. pp. 357-374.

Mah, R. A., and D. A. Kuhn. 1984a. Transfer of the type species of the genus *Methanococcus* to the genus *Methanosarcina*, naming it *Methanosarcina mazei* (Barker 1936) comb. nov. et emend. and conservation of the genus *Methanococcus* (Approved lists 1980) with *Methanococcus vannielii* (Approved lists 1980) as the type species. Request for an opinion. Int. J. Syst. Bacteriol. 34:263-265.

Mah, R. A., and D. A. Kuhn. 1984b. Rejection of the type species *Mehanosarcina methanica* (Approved lists 1980, conservation of the genus *Methanosarcina* with *Methanosarcina barkeri* (Approved lists 1980) as the type species, and emendation of the genus *Methanosarcina*. Int. J. Syst. Bacteriol. 34:266-267.

Mah, R. A., and M. R. Smith. 1981. The methanogenic bacteria. In The Prokaryotes. M. P. Starr, H. Stolp, H. G. Truper, A Balows, and H. G. Schlegel (Eds.) Springer Verlag, New York.

Mah, R. A., M. R. Smith, and L. Baresi. 1978. Studies on an acetate-fermenting strain of *Methanosarcina*. Appl. Environ. Microbiol. 35:1174-1184.

Mah, R. A., D. M. Ward, L. Baresi, and T. L. Glass. 1977. Biogenesis of methane. Ann. Rev. of Microbiol. 31:309-341.

Marchant, R., and R. T. Moore. 1973. Lomasomes and plasmalemmasomes in fungi. Protoplasma 76:235-247.

Mazè, P. 1915. Ferment formenique. Fermentation formenique de l'acetone. Procede de culture simple du ferment formenique. C. R. Seances Soc. Biol. Ses Fil. 78:398-405.

Mollenhauer, H. H. 1964. Plastic embedding mixtures for use in electron microscopy. Stain Technol. 39:111.

Moreton, R. B. 1981. Electron-probe X-ray microanalysis: techniques and recent applications in biology. Biol. Rev. 56:409-461.

Mueller, M., N. Meister, and H. Moor. 1980. Freezing in a propane jet and its application in freeze-fracturing. Mikroskopie 36:129-140

Murray, P., J. Kemp, and S. H. Zinder. 1984. Polysaccharide accumulation in Methanosarcina strain TM-1. Nature 312:284-286.

Murray, R. G. E., and S. W. Watson. 1965. Structure of Nitrosocystis oceanus and comparison with Nitrosomonas and Nitrobacter. J. Bacteriol. 89:1594-1609.

Ollivier, B., A. Lombardo, and J. L. Garcia. 1984. Isolation and characterization of a new thermophilic Methanosarcina strain (strain MP). Ann. Microbio. (Inst. Pasteur) 135:187-198.

Palevitz, B. A., and E. H. Newcomb. 1970. A study of sieve element starch using sequential enzymatic digestion and electron microscopy. J. Cell Biol. 45:383-393.

Parkin, G. F., R. E. Speece, C. H. J. Yang, and W. M. Kocher. 1983. Response of methane fermentation systems to industrial toxicants. J. Water Pollut. Control Fed. 55:44-53.

Picket-Heaps, J. D. 1967. Preliminary attempts at ultrastructural polysaccharide localization in root tip cells. J. Histochem. Cytochem. 15:442-455.

Reynolds, E. S. 1963. The use of lead citrate at high pH as an electron opaque stain in electron microscopy. J. Cell Biol. 17:208-212.

Rieder, C. L. G. Rupp, and S. S. Bowser. 1985. Electron micrOscopy of semi-thick sections: advantages for biomedical research. J. Elect Microsc Techn. 2:11-28.

Rivard, C. J., J. M. Henson, M. V. Thomas, and P. H. Smith. 1983. Isolation and characterization of Methanomicrobium paynteri sp. nov., a mesophilic methanogen isolated from marine sediment. Appl. Environ. Microbiol. 46:484-490.

Rivard, C. J., and P. H. Smith. 1982. Isolation and characterization of a thermophilic marine methanogenic bacterium, *Methanogenium thermophilicum* sp. nov. Internat. J. System. Bacteriol. 32:430-436.

Robinson, R. W., D. Akin, R. A. Nordstedt, M. V. Thomas, and H. C. Aldrich. 1984. Light and electron microscopic examinations of methane-producing biofilms from anaerobic fixed-bed reactors. Appl. Environ. Microbiol. 48:127-136

Robinson, R. W., H. C. Aldrich, S. F. Hurst, and A. S. Bleiweis. 1985. Role of the cell surface of *Methanosarcina mazei* in cell aggregation. Appl. Environ. Microbiol. 49:321-327.

Robinson R. W., and C. R. Spotts. 1983. The ultrastructure of sporulation in *Sporosarcina ureae*. Can. J. Microbio. 29:807-814.

Romesser, J. A., R. S. Wolfe, F. Mayer, E. Spiess, and A. Walther-Mauruschat. 1979. *Methanogenium*, a new genus of marine methanogenic bacteria, and characterization of *Methanogenium cariaci* sp. nov., and *Methanogenium marisnigri* sp. nov. Arch. Microbiol. 121:147-153.

Roth, J., and M. Binder. 1978. Colloidal gold, ferritin and peroxidase as markers for electron microscopic double labeling lectin techniques. J. Histochem. Cytochem. 26:163-169.

Sauer, F. D., R. S. Bush, S. Mahadevan, and J. D. Erlfle. 1977. Methane production by cell-free particulate fraction of rumen bacteria. Biochem. Biophys. Res. Comm. 79:124-132.

Sauer, F. D., J. D. Erfle, and S. Mahadevan. 1980. Methane production by the membranous fraction of *Methanobacterium thermoautotrophicum*. Biochem. J. 190:177-182.

Scherer, P. A., and H. P. Bochem. 1983a. Ultrastructural investigation of 12 Methanosarcinae and related species grown on methanol for occurrence of polyphosphate-like bodies. Can. J. Microbiol. 29:1190-1199.

Scherer, P. A., and H. P. Bochem. 1983b. Energy dispersive X-ray microanalysis of the methanogen *Methanosarcina barkeri* "fusaro" grown on methanol and in the presence of heavy metals. Curr. Microbiol. 9:187-194.

Shively, J. M. 1974. Inclusion bodies of prokaryotes. Ann. Rev. Microbiol. 28:167-187.

Sleytr, U. B. 1978. Regular arrays of macromolecules on bacterial cell walls. Int. Rev. Cytol. 53:1-64.

Sleytr, U. B., and A. W. Robards. 1982. Understanding the artefact problem in freeze-fracture replication: a review. J. Microsc. 126:101-122.

Smit J. 1933. The biology of the fermenting sarcinae. J. Pathol. Bacteriol. 36:455-468.

Smith, U., and D. W. Ribbons. 1970a. Fine structure of Methanomonas methanooxidans. Arch. Mikrobiol. 74:110-122.

Smith, U., and D. W. Ribbons. 1970b. Fine structure of Methanococcus capsulatus. Tissue and Cell 4:513-520.

Soehngen, N. L. 1906. Het ontstaan en verdwijnen van waterstof en methaan onder den invoed van het organische leven, Thesis, Delft.

Sowers, K. R., S. F. Baron, and J. G. Ferry. 1984a. Methanosarcina acetivorans sp. nov., an acetotrophic methane-producing bacterium isolated from marine sediments. Appl. Environ. Microbiol. 47:971-978.

Sowers, K. R., and J. G. Ferry. 1983. Isolation and characterization of a methylotrophic marine methanogen, Methanococcoides methylutens gen. nov., sp. nov. appl. Environ. Microbiol. 45:684-690.

Sowers, K. R., J. L. Johnson, and J. G. Ferry. 1984b. Phylogenetic relationships among the methylotrophic methane-producing bacteria and the emendation of the family Methanosarcineae. Internat. J. System. Bacteriol. 34:444-450.

Spencer, R. W., L. Daniels, G. Fulton, and W. H. Orme-Johnson. 1980. Product isotope effects on in vivo methanogenesis by Methanobacterium thermoautotrophicum. Biochem. 19:3678-3683.

Sprott, G. D., L. C. Sowden, J. R. Covlin, and K. F. Jarrell. 1984. Methanogenesis in the absence of intracytoplasmic membranes. Can. J. Microbiol. 30:594-604.

Spurr, A. R. 1969. A low viscosity epoxy resin embedding medium for electron microscopy. J. Ultrastruct. Res. 26:31-43.

Stetter, K. O., M. Tomm, J. Winter, G. Wildgruber, H. Huber, W. Zellig, D. Jane-Covic, H. Konig, P. Palm, and S. Wunderl. 1981. Methanothermus fervidus, sp. nov., a novel extremely thermophilic methanogen isolated from an icelandic hot spring. Zentralb. Bakteriol. Parasitenkd. Infektionskr. Hyg., I. Orig. Reihe C, 2:166-178.

Stetter, K. O., and W. Zellig. 1980. The Sulfolobus-Calderiella group- taxanomy on the basis of the structure of DNA-dependent RNA-polymerase. Archiv. Microbiol. 125:259-269.

Steyn, P. L., H. J. van Tonder, D. J. J. Potgieter, Z. Apostolides, and C. H. van Aswegen. 1980. Endospore-like structures of methanogenic bacteria. Research Note. Phytophylactica 12:231-237.

Strohl, W. R., I. Geffers, and J. M. Larkin. 1981. Strucure of the sulfur inclusion envelopes from four Beggiatoas. Curr. Microbiol. 6:75-79.

Swift. J. A. 1973. The electron cytochemical demonstration of cystine disulfide bonds using silver-methenamine reagent. Histochemie 35:307-310.

Thornley, M. 1975. Cell envelopes with regularly arranged surface subunits in Acinetobacter and related bacteria. CRC Critical Rev. in Microbiol. 4:65-100.

Thornley, M. J., R. W. Horne, and A. M. Glauert. 1965. The fine structure of Micrococcus radiodurans. Arch. Mikrobiol. 51:267-289.

Tornabene, T. G., R. S. Wolfe, W. E. Balch, W. E. Holzer, G. Fox, and J. Oro. 1978. Phytanyl-glycerol ethers and squalenes in the archaebacterium Methanobacterium thermoautotrophicum. J. Mol. Evol. 11:259-266.

Touzel, J. P., and G. Albagnac. 1983. Isolation and characterization of Methanococcus mazei strain MC|3|. FEMS Microbiol Lett. 16:241-245.

Van Iterson, W. 1984. Inner Structures of Bacteria. Van Nostrand Reinhold Co., New York.

Voelz, H. V. Voelz, and O. R. Ortigoza. 1966. The "polyphosphate overplus" phenomenon in Myxococcus xanthus and its influence on the architectre of the cell. Arch. Mikrobiol. 53:371-388.

Walsby, A. E. 1972. Structure and function of gas vacuoles. Bacteriol. Rev. 36:1-32.

Webster, J. A., D. D. Fay, J. L. Costa, P. M. Jones, and R. Hugh. 1984. Elemental composition of bacterial metachromatic inclusions determined by electron microprobe X-ray analysis. J. Bacteriol. 158:441-446.

Wildgruber, G., M. Thomm, H. Koenig, K. Ober, T. Ricchiuto, and K. O. Stetter. 1982. Methanoplanus limicola, a plate-shaped methanogen representing a novel family, the Methanoplanaceae. Arch. Microbiol. 132:31-36.

Woese, C. R. 1977. A comment on the methanogenic bacteria and the primitive ecology. J. Mol. Evol. 9:369-371.

Woese, C. R. 1982. Archaebacteria and cellular origins: an overview. Zentralb. Bakteriol. Parasitenk. Infektionskr. Hyg. I. Abt. Orig. Reihe C, 3:1-17.

Woese, C. R., and G. E. Fox. 1977. Phylogenetic structure of the prokaryotic domain: The primary kingdoms. Proc. Nat. Acad. Sci. U.S.A. 74:5088-5090.

Woese, C. R., L. J. Magrum, and G. E. Fox. 1978. Archaebacteria. J. Mol. Evol. 11:245-252.

Wolfe, R. S. 1971. Microbial fermentation of methane. Adv. in Microb. Physiol. 6:107-146.

Zeikus J. G. 1977. The biology of methanogenic bacteria. Bacteriol Rev. 41:514-541.

Zeikus, J. G., and V. G. Bowen. 1974. Comparative ultrastructure of methanogenic bacteria. Can. J. Microbiol. 21:121-129.

Zeikus, J. G., and V. G. Bowen. 1975. Fine structure of Methanospirillum hungatii. J. Bacteriol. 121:373-380.

Zeikus, J. G., and R. S. Wolfe. 1973. Fine structure of *Methanobacterium thermoautotrophicum*: effect of growth temperature on morphology and ultrastructure. J. Bacteriol. 113:461-467.

Zhilina, T. N. 1971. The fine structure of *Methanosarcina*. Microbiol. 40:587-591.

Zhilina, T. N. 1972. Death of *Methanosarcina* in the air. Microbiol. 40:980-981.

Zhilina T. N. 1976. Biotypes of *Methanosarcina*. Microbiol. 45:414-421.

Zhilina T. N., and G. A. Zavarzin. 1979a. Mycoplasma in *Methanosarcina* cultures. Microbiol. 48:439-441.

Zhilina T. N., and G. A. Zavarzin. 1979b. Comparative cytology of *Methanosarcina* and description of *Methanosarcina vacuolata* sp. nova. Microbiol. 48:223-228.

Zhilina T. N., and G. A. Zavarzin. 1979c. Cyst formation by *Methanosarcina*. Microbiol. 48:349-354.

Zinder, S. H., and R. A. Mah. 1979. Isolation and characterization of a thermophilic strain of *Methanosarcina* unable to use H_2-CO_2 for methanogenesis. Appl. Environ. Microbiol. 38:996-1008.

BIOGRAPHICAL SKETCH

Ralph Robinson was born July 31, 1953, the third child of Verdia and Paul D. Robinson in Burbank, California. The Robinson family resided in the San Fernando Valley within the incorporated city limits of Los Angeles. After graduating from Birmingham High School in 1971, Ralph attended Pierce Jr. College in Woodland Hills, California. He later attended California State University Northridge where he obtained hid B.S. and M.S. degrees in biology. Ralph then moved to Gainesville, Florida, to obtain the Ph.D. in the Department of Microbiology and Cell Science.

I certify that I have read this study and that in my opinion it conforms to acceptable standards of scholarly presentation and is fully adequate, in scope and quality, as a dissertation for the degree of Doctor of Philosophy.

Henry C. Aldrich

Henry C. Aldrich, Chairman
Professor of Microbiology
and Cell Science

I certify that I have read this study and that in my opinion it conforms to acceptable standards of scholarly presentation and is fully adequate, in scope and quality, as a dissertation for the degree of Doctor of Philosophy.

Sylvia S. Coleman

Sylvia S. Coleman
Professor of Microbiology
and Cell Science

I certify that I have read this study and that in my opinion it conforms to acceptable standards of scholarly presentation and is fully adequate, in scope and quality, as a dissertation for the degree of Doctor of Philosophy.

Arnold S. Bleiweis

Arnold S. Bleiweis
Professor of Microbiology
and Cell Science

I certify that I have read this study and that in my opinion it conforms to acceptable standards of scholarly presentation and is fully adequate, in scope and quality, as a dissertation for the degree of Doctor of Philosophy.

Edward P. Previc

Edward P. Previc
Associate Professor of Microbiology
and Cell Science

I certify that I have read this study and that in my opinion it conforms to acceptable standards of scholarly presentation and is fully adequate, in scope and quality, as a dissertation for the degree of Doctor of Philosophy.

Carl M. Feldherr
Professor of Anatomy

This thesis was submitted to the Graduate Faculty of the College of Agriculture and to the Graduate School, and was accepted as partial fulfillment of the requirements for the degree of Doctor of Philosophy.

May, 1985

Jack L. Fry

Dean, College of Agriculture

Dean, Graduate School
and Research

UNIVERSITY OF FLORIDA
3 1262 08553 5424